

For Library

113

A PETROGRAPHIC AND DIAGENETIC STUDY  
OF THE WHIRLPOOL SANDSTONE  
FROM OUTCROPS IN THE  
HAMILTON AND NIAGARA GORGE AREAS

A PETROGRAPHIC AND DIAGENETIC STUDY  
OF THE WHIRLPOOL SANDSTONE  
FROM OUTCROPS IN THE  
HAMILTON AND NIAGARA GORGE AREAS

by

RUSSELL W. CALOW

A Thesis

Submitted to the Department of Geology  
in Partial Fulfillment of the Requirements  
for the Degree  
Honours Bachelor of Science

McMaster University

April, 1983

Honours Bachelor of Science  
[Geology]

McMaster University  
Hamilton, Ontario

TITLE:                   A Petrographic and Diagenetic Study  
                          of the Whirlpool Sandstone  
                          from outcrops in the  
                          Hamilton and Niagara Gorge Areas

AUTHOR:                 Russell W. Calow

SUPERVISOR:            Dr. Gerard V. Middleton

NUMBER OF PAGES:     xxi, 209

## A B S T R A C T

Four measured sections of the Whirlpool Sandstone were prepared from outcrops in the Niagara Gorge and Hamilton areas. Sedimentary structures and constituents present in the lower two-thirds of the unit are consistent with the sandy braided fluvial depositional model proposed by Salas [1983]. The upper one-third of the unit has been deposited in a near shore, shallow marine environment. All samples have been classified as Quartzarenites, or Sublitharenites after Folk [1974] and the source of the Whirlpool lies to the southeast in primarily pre-existing sediments, with some input from low grade metamorphic and hydrothermally veined terrains.

Cathodoluminescent microscopy has proven to be a safe, relatively inexpensive, easy to use method, that offers a great deal of new information. The technique's only drawback is the gradual destruction of thin sections by the electron beam. The CL study demonstrated that pressure solution was not the source of the massive, pore occluding, mesodiagenetic quartz cement. Since very low diagenetic temperatures have been calculated for the Whirlpool in the study area [ $36^{\circ}\text{C}$ ], the local generation of silica would be impossible. Instead, it has been

suggested that silica was carried in by saturated pore fluids that had migrated up-dip from source areas deep within the depositional basin to the southeast. Similarly, pyrite was precipitated as H<sub>2</sub>S bearing fluids migrated through the unit. These reducing fluids also produced the reduced zone at the top of the Queenston Formation. The H<sub>2</sub>S was produced during the maturation of hydrocarbons. Calcite cement is more abundant in the upper marine units of the Whirlpool. This suggests that the source of the calcite was local detrital carbonate in the upper marine units. Quartz cementation ceased when the porosity had been reduced sufficiently to inhibit the passage of the migrating pore fluids. Thus, the calcite cement precipitated from static pore fluids. The local detrital carbonate was dissolved by the acidic fluids that carried in the silica. This Ca<sup>+2</sup> rich fluid was prevented from mixing with the bulk porewater and calcite precipitation occurred due to an increase in CO<sub>2</sub> by the decay of organic detritus in the upper marine units. The major proportion of secondary porosity was formed during mesodiagenesis by the dissolution of calcite. The pore fluids became undersaturated with respect to calcite when local intershale water was released into the porewater. The formation of dolomite cement was in response to a decrease in the amount of available iron relative to magnesium due to

the precipitation of ferroan calcite. The zonation of the dolomite reflects rapid changes in porewater composition. Four morphologies of illite have been identified: two represent direct precipitation from alkaline,  $K^+$  rich solution; one may be detrital in origin, or it could represent illite that has been mechanically infiltrated down into the sand after deposition; and the fourth is a mixed layer assemblage that has been formed by the replacement of earlier clays by illite. The oil and gas found in the Whirlpool Sandstone in the Lake Erie area have probably migrated up-dip from source areas deep within the depositional basin to the southeast.

### ACKNOWLEDGEMENTS

The author wishes to express his sincere thanks to Dr. G.V. Middleton for his comments and criticism in supervision of this work. I would also like to thank Dr. H.D. Grundy for his assistance with the XRD and Dr. M.J. Risk for his identification of trace fossils. The help of Neil Hoey at Consumers' Gas was also appreciated.

Lastly I would like to extend my gratitude to Carlos Salas, my Whirlpool co-worker, for supplying information from his thesis and for providing a trying ground for new ideas.

## T A B L E O F C O N T E N T S

	Page	
Abstract	iii	
Acknowledgements	vi	
List of Figures	xi	
List of Plates	xiv	
List of Tables	xx	
Chapter		
1	Introduction	
	Unit and area of study	1
	Purpose of study	1
	General stratigraphy and age relationships	4
	Regional depositional framework	6
	Previous work	7
2	Facies Description and Depositional Environment	
	Introduction	10
	Facies A	11
	Subfacies Ag	18
	Facies C	18
	Subfacies Cv	23
	Facies D	26
	Facies E	27
	Facies F	28



	Facies G	28
	Facies H	30
	Facies I	30
	Facies M	31
	Facies J	31
	Facies K	33
	Interpretation	33
3	Petrography	
	Introduction	39
	Grain size	40
	Mineral composition	43
	Method	43
	Results	45
	Transmitted Light Microscopy	45
	Introduction	45
	Quartz	54
	Calcite and dolomite cements	
	Chert, phosphate and rock fragments	60
	Feldspar	69
	Heavy and opaque minerals	69
	Muscovite	77
	Clays	77
	Cathodoluminescent Microscopy	77
	Introduction	77
	Quartz	80
	Quartz Cement	94

	Feldspar	94
	Calcite and dolomite cements	95
	Minor constituents	98
	Grain contact study	98
	Classification, provenance and maturity	106
	Classification	106
	Provenance	109
	Maturity	118
	Porosity	118
	Weathering cavities	119
	Minus cement porosity	127
	Evaluation of Cathodoluminescent Microscopy as applied to sedimentological research	129
4	Clay Mineralogy	
	Introduction	131
	X-ray Diffraction	131
	Analysis	133
	Results	133
	Standard Clays	133
	Illite	133
	Kaolinite	135
	Chlorite	135
	Unknown samples	138
	Scanning Electron Microscopy	141
	Method	141
	Results	142

5	Diagenesis	
	Introduction	149
	Diagenetic theory and definitions	149
	Maximum diagenetic temperature	151
	Eodiagenesis	152
	Mechanical porosity reduction	153
	Early pore fluid composition	153
	Early clay diagenesis	154
	Formation of pyrite	155
	Hematite formation	158
	Eodiagenetic cements	158
	Mesodiagenesis	161
	Quartz cement	161
	Carbonatization	168
	Decarbonatization	171
	Illite formation	172
	Dolomitization	173
	Changes in pore fluid composition	174
	Mineral paragenesis	181
6	Conclusions	183
	Bibliography	191
	Appendix 1	201
	Appendix 2	204
	Appendix 3	208

## L I S T O F F I G U R E S

Figure		Page
1-1	Location of study area	2
1-2	Stratigraphic and age relationships of the units cropping out along the Niagara Escarpment	5
2-1	Legend for stratigraphic sections	12
2-2	Stratigraphic section of the Haul Road Cut	13
2-3	Stratigraphic section of the Art Park Outcrop	14
2-4	Stratigraphic section of the Jolley Cut	15
2-5	Stratigraphic section of the Sydenham Road Outcrop	16
3-1	Classification of the Whirlpool Sandstone after Folk [1978]	110
3-2	Quartz varieties [undulose, polycrystalline, etc.]	116
3-3	Constituent varieties [monocrystalline quartz, lithic fragments, etc.]	117
4-1	X-ray Diffraction Trace: Illite Standard	134
4-2	X-ray Diffraction Trace: Kaolinite Standard	136
4-3	X-ray Diffraction Trace: Chlorite Standard	137
4-4	X-ray Diffraction Trace: ART BASE sample	139
4-5	X-ray Diffraction Trace: SYD 4 sample	140
5-1	Eh vs. $pS^{-2}$ stability diagram for pyrite, pyrrhotite, hematite, magnetite and siderite	157

5-2	Textural stages of mesodiagenesis	162
5-3	Schematic representation of the major processes affecting porosity during mesodiagenesis	163
5-4	Log $[K^+/H^+]$ vs. log $[H_4SiO_4]$ stability diagram	164
5-5	Solubility vs. pH diagram for $CaCO_3$ and $SiO_2$	169
5-6	Log $[Mg^{+2}]/[H^+]^2$ vs. log $[K^+/H^+]$ stability diagram for Illite, Kaolinite, Chlorite and Microcline	178
5-7	Schematic representation of the paragenetic sequence of mineral formation during diagenesis	182

L I S T O F P L A T E S

Plate		Page
2-1a	Facies A/Ag/C and a small erosional channel at the base of Facies C	17
2-1b	Three dimensional view of large scale troughs near the base of Facies C	17
2-2a	Parallel laminated sandstone cutting large scale troughs and being cut laterally by large scale troughs, in Facies C	19
2-2b	Parting lineation found on the surface of the parallel laminated sandstone above	19
2-3a	Parallel laminated sandstone cutting large scale troughs and being cut by troughs above and laterally, in Facies C from the Art Park Outcrop	20
2-3b	Large grey-green, clay, rip-up clasts at the base of Facies C	20
2-4a	Superficial round weathering cavities at the base of Facies C	22
2-4b	Facies A/Ag/C and limonite staining at the base of Facies C. Photograph from the Sydenham Road Cut	22
2-5a	Parallel laminated sandstone in Facies Cv	24
2-5b	Facies C/Cv/E at Haul Road	24

2-6a	Facies Cv/D/E/I/M at the Jolley Cut	25
2-6b	Small scale trough cross-bedding in Facies F	25
2-7a	Facies G/H	29
2-7b	Oscillating current ripples with tuning fork bifurcations in Facies G	29
2-8a	Facies C/E/J at Sydenham Road	32
2-8b	Trace fossil <u>Chondrites</u> and casts of synaeresis mud cracks on the basal surface of Facies J at Sydenham Road	32
3-1a	Detrital quartz grains showing bubble trains as well as dust rims	55
3-1b	Polycrystalline quartz grain with more than 3 crystals, dolomite rhomb and a low grade MRF	55
3-2a	Primary quartz overgrowths on a detrital quartz grain, photomicrograph	56
3-2b	Primary, isolated quartz overgrowths growing into porosity, and secondary massive overgrowths occluding all porosity, photomicrograph	56
3-3a	Polycrystalline quartz grain, with less than 3 crystals, detrital zircon and a SRF	57
3-3b	Nonundulose, monocrystalline quartz grain with rutile inclusions	57
3-4a,b	Vermicular chlorite inclusions in a nonundulose monocrystalline quartz grain	59
3-5a	Ferroan and nonferroan calcite, dolomite and a phosphatized fossil fragment showing faint	

	internal lamination, and a very large SRF	61
3-5b	Ferroan calcite growing into nonferroan calcite	61
3-6a,b	Ferroan calcite replacing microcline	62
3-7a	Ferroan calcite replacing a detrital quartz grain	63
3-7b	Nonferroan calcite replacing a detrital quartz grain	63
3-8	An isolated dolomite rhomb, photomicrograph	64
3-9a	Cryptocrystalline and coarse crystalline chert grains	66
3-9b	Zoned chert grain	66
3-10a,b	Phosphatized echinoderm fragment	67
3-11	High grade MRF, schist fragment	68
3-12a	Detrital microcline grain and a low grade MRF	70
3-12b	Detrital microcline grain with a quartz overgrowth	70
3-13a	Euhedral zircon grain as an inclusion in a detrital quartz grain	71
3-13b	Detrital tourmaline grain	71
3-14	Hematite and illite rims around a detrital quartz grain	72
3-15a	Pyrite precipitated in ferroan calcite zone	74
3-15b	Framboidal pyrite, photomicrograph	74
3-16	Magnetite replacing calcite cement	75
3-17a,b	Unidentified mineral, possibly pyrite,	



	photomicrograph	76
3-18a	Detrital muscovite grain	78
3-18b	Detrital muscovite grain squeezed between quartz grains	78
3-19a,b	CL photograph showing blue and brown detrital quartz and a badly deformed feldspar grain	90
3-20a,b	CL photograph showing bluish-white feldspar grain and nonferroan calcite	91
3-21a,b	CL photograph showing feldspar being replaced by ferroan calcite	93
3-22a,b	CL photograph showing zonation of dolomite around a ferroan calcite core	96
3-23a,b	CL photograph showing zonation of dolomite grains associated with ferroan and nonferroan calcite	97
3-24a,b	CL photograph showing the differences in contact description between transmitted light and CL in a coarse grained sample	103
3-25a,b	CL potograph showing the differences in contact description between transmitted light and CL in a fine grained sample	104
3-26	Dissolution of microcline leading to the formation of secondary porosity	120
3-27a,b	Dissolution of feldspar leading to the formation of secondary porosity, photomicrograph	121

3-28a,b	Dissolution of calcite leading to the formation of secondary porosity, photomicrograph	122
3-29a	Dissolution of a SRF leading to the formation of secondary porosity	123
3-29b	Secondary porosity formed due to the entire dissolution of a grain	123
3-30a	Secondary, massive quartz cement, occluding all porosity, photomicrograph	124
3-30b	Occlusion of all remaining porosity by nonferroan calcite cement	124
3-31a,b	CL photograph showing a weathering cavity	125
3-32a	Weathering cavity displaying no grain rotation	126
3-32b	Dissolution of patchy calcite cement leading to the formation of a weathering cavity	126
4-1a,b	Pore lining illite laths, photomicrograph	143
4-2a	Pore lining, wispy laths of illite, photomicrograph	144
4-2b	Pore lining, short digitate flakes, with wispy lath like terminations, photomicrograph	144
4-3a	Pore bridging, spaghetti like laths of illite, photomicrograph	146
4-3b	"Mudcrack" type illite on the surface of a detrital quartz grain, photomicrograph	146
4-4a,b	Unidentified clay mineral displaying a flower like morphology, possibly chlorite, photomicro-	

	graph	148
5-1a	Primary and secondary massive quartz cements, photomicrograph	160
5-1b	Third generation, pore bridging quartz cement, photomicrograph	160

L I S T O F T A B L E S

Table		Page
3-1	Average grain size	42
3-2a,b	Point count results: Transmitted Light	46
	to Microscopy	to
3-5a,b		53
3-6	Various minerals and their CL colours	81
3-7a,b	Point count results: Cathodoluminescent	82
	to Microscopy	to
3-10a,b		89
3-11	Grain contact study: Transmitted Light	
	Microscopy	100
3-12	Grain contact study: Cathodoluminescent	
	Microscopy	101
3-13	Point count results: Quartz, feldspar and rock fragments	107
3-14	Point count results: Rock fragments and SRF components, Transmitted Light Microscopy	108
3-15	Monocrystalline, polycrystalline quartz: Transmitted Light Microscopy	112
3-16	Quartz, feldspar and lithic fragments	114
3-17	Monocrystalline quartz, feldspar and lithic fragments	115
3-18	Minus cement porosity	128

5-1 Formation water analysis of the Leep Frog  
Wildcat Well

175

to Pam

apart we are none

together we are one

A maxim to live by:

One will accomplish only what he desires,  
and he will desire only what he must work for.

## CHAPTER 1

### I N T R O D U C T I O N

#### UNIT AND AREA OF STUDY:

The Whirlpool Sandstone, the basal member of the Lower Silurian Medina Group, is a natural gas producer in northern New York State and southwestern Ontario. It is exposed in outcrop along the Niagara River Gorge and in road cuts and stream channels in the Hamilton area. The study area consists of these exposures and figure 1-1 displays the exact locations of the outcrops studied.

#### PURPOSE OF STUDY:

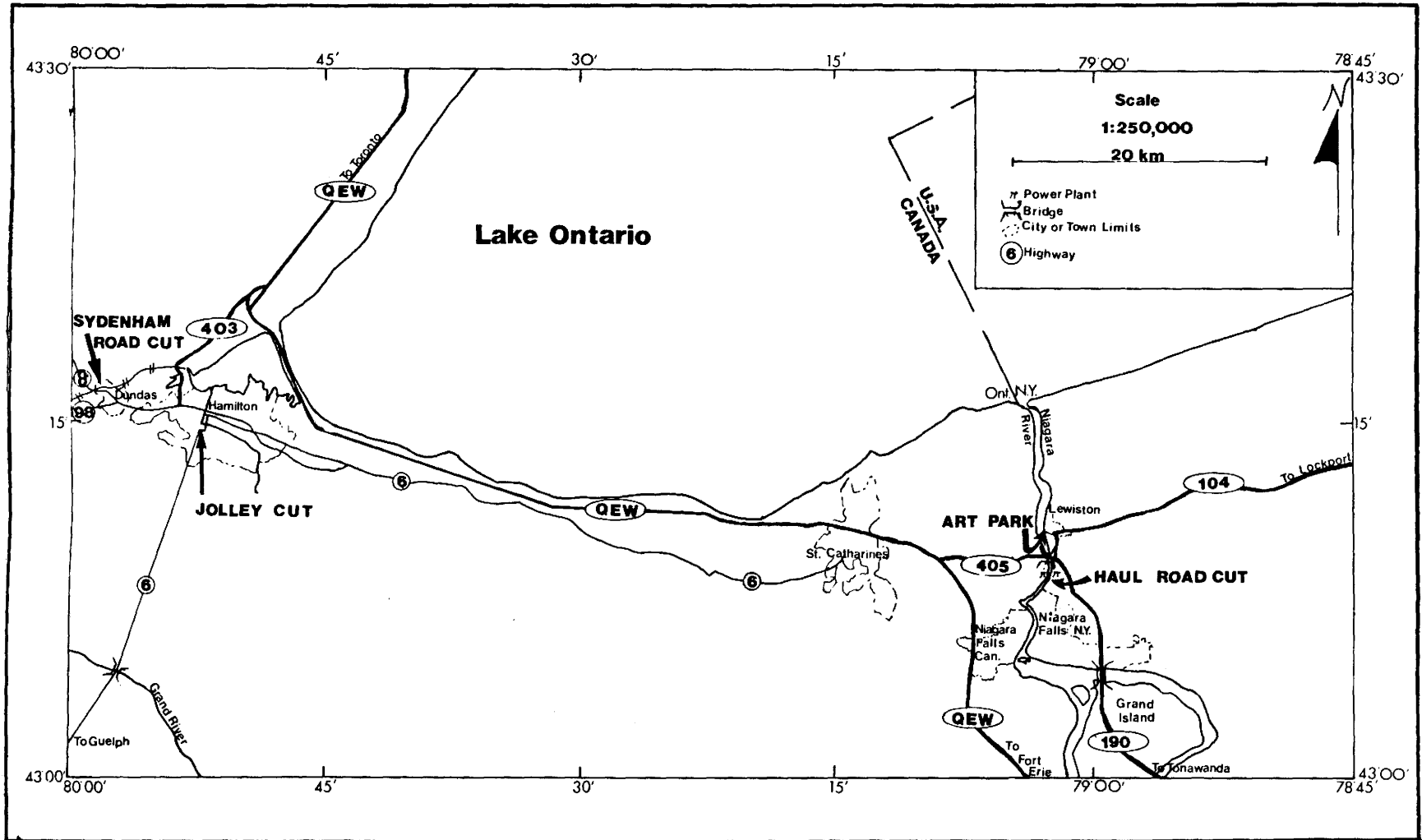
The purpose of this study was to prepare measured sections of four Whirlpool outcrops and to examine, in detail, the petrography of the Whirlpool Sandstone in the study area.

Field observations were then compared with the Sandy Braided Fluvial depositional model prepared by C.J. Salas from work done on a series of rock quarries in the Georgetown area, roughly 50 km north of Hamilton. From the detailed petrographic study a diagenetic history of the Whirlpool was prepared.

A secondary aspect of the study concerned the evaluation of Cathodoluminescent Microscopy as applied to



Figure 1-1: Location of the study area with respect to the cities of Hamilton and Niagara Falls Ontario.



Sedimentological research.

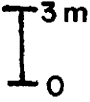
GENERAL STRATIGRAPHY AND AGE RELATIONSHIPS:

The Whirlpool Sandstone is recognizable in outcrop from the Nottawasaga River in the north [Bolton, 1957] to the town of Medina, New York State, in the south [Fisher, 1954]. The Whirlpool thins to the east and west, where the Grimsby Red Beds and the Manitoulin Dolomite, to the northwest, and the Cabot Head Shales, to the southwest, occur at the same stratigraphic position as the Whirlpool [Martini, 1965]. Seyler [1981] from subsurface studies in northern New York State, described the Whirlpool as "an extensive sheet like sand with variations in thickness...over relatively short distances."

The Lower Silurian Medina Group, of which the Whirlpool Sandstone is the basal member, is unconformably underlain by the Upper Ordovician Queenston Shale [Fisher, 1966] and is conformably overlain by the Silurian Clinton Group. Figure 1-2 displays the stratigraphic and age relationships of the units cropping out along the Niagara Escarpment [after Miller and Eames, 1982].

The lack of recognizable fauna in the lower Whirlpool, and the general poor correlation of fauna in the Medina Group with other lower Silurian groups elsewhere [Bolton, 1957; Fisher, 1954] has allowed only an indirect method of dating the Medina Group.

Figure 1-2: Stratigraphic and age relationships of the units cropping out along the Niagara Escarpment, [after Miller and Eames, 1982].

<b>System</b>	<b>Series</b>	<b>Stage</b>	<b>FORMATION</b>	Litho-Stratigraphy		
<b>Silurian</b>	<b>Llandovery</b>	<b>Idwian</b>	<b>CLINTON</b>	Post-Reynales Carbonates Reynales Ls. Neahga Shale Thorold Sst.		
		<b>Rhuddian</b>	<b>MEDINA</b>	Grimsby Sandstone  Cabot Head Shale  Manitoulin Dolomite NW / SE Power Glen Shale		
		<b>Ordo</b>	<b>Ashgill</b>			Whirlpool Sst.  Queenston Shale

Grabau [1913a,b] and Liberty and Bolton [1971] used stratigraphy to show that the Queenston Shale had a late Ashgill age. [see figure 1-2 for a breakdown of the Ordovician and Silurian Systems] Ziegler [in Rickard, 1975] used atrypcean brachiopod lineages to date the Reynales Limestone, a basal member of the Clinton Group, as Idwian in age. His work is supported by the conodont studies of Rexroad and Rickard [1965] and by acritarch study of Lister [1970] on the Neahga Shale in the Niagara Gorge. Lister showed that taxa, which Hill [1974] considered to define the base of the Idwian age, are present in the Neahga Shale, but not in the Medina Group directly below. Thus, a pre-Idwian age was suggested for the Medina Group.

Recently Gray and Boucott [1971] and Miller and Eames [1982] identified tetrad palynomorphs in the Medina Group, that Cramer and Diez de Cramer [1972] recognized as having world wide distribution during the Silurian Period.

#### REGIONAL DEPOSITIONAL FRAMEWORK:

During the Ordovician Period the "Queenston Delta" was growing westward from a land mass in the present position of the Appalachian Mountains. At the close of the Ordovician the area that is now Ontario became emergent, but was not substantially affected by the Taconic Orogeny, that severly folded, faulted and metamorphosed the present day area of eastern New York State.

Deposition in the Silurian was in response to subsidence and Ontario formed a hinge area between two major sedimentary basins, the Allegheny Basin to the south and the Michigan Basin to the west [Sanford, 1969]. During the Silurian, the Michigan Basin was a depocentre for carbonates and evaporites, while the Allegheny Basin was blanketed with clastics that thickened towards a terrigenous sediment source to the southeast.

PREVIOUS WORK:

Grabau [1913] first applied the name Whirlpool Sandstone. He thought that the Whirlpool Sand was eolian in origin and existed as a local formation cut off from any direct eastern source. Williams [1919] suggested that both wind and water produced the observed sedimentary structures, with the sediment derived from source beds to the east in the Appalachian region. Alling [1936] suggested that most of the quartz was derived from a pre-existing sandstone. Holstein [1936] concluded that since only the most stable detrital minerals were present "...wind and water were jointly responsible for the transportation of the constituent grains...". Also, the heavy minerals found were not typical of a Precambrian source, rather, the degree of sorting increased to the northwest, suggesting a source area to the southeast. Secondly, the restricted variety of heavy minerals present indicated a pre-existing

sedimentary source, possibly the Appalachian sediments and the rocks of Adirondacks. Geitz [1952] demonstrated, using size distribution curves from five localities, that the Whirlpool Sandstone displayed a definite fining trend to the north and west, placing its source to the southeast. He also found a vertical fining trend in the Hamilton area. Fisher [1954] envisioned a windswept surface, with eolian frosted sand grains being deposited in mud cracks. These eolian sands formed the basal units of the Whirlpool followed by a marine transgression that reworked the earlier sediments in a shallow marine environment. Bolton [1957] concluded that the Whirlpool sands consisted of "...marginal sediments derived from the east and laid down on the undulating and mud cracked Queenston surface by transgressing shallow marine seas under reducing conditions..." and that "wind possibly played only a minor role in the transportation of the clastic material from the Appalachian source region." Seyler [1981] reinterpreted the Whirlpool as a shallow marine barrier island, including barrier islands, eolian sand dunes, tidal channels, tidal inlets and shallow marine and lagoonal conditions.

Presently I.P. Martini, G.V. Middleton and C.J. Salas are in the process of reinterpreting the lower units of the Whirlpool as being Sandy Braided Fluvial in origin,



from evidence supplied by sedimentary structures and paleo-current directions and the presence of terrestrial nadospores.

## CHAPTER 2

### FACIES DESCRIPTION

#### AND

### DEPOSITIONAL ENVIRONMENT

#### INTRODUCTION:

A total of five outcrops were studied and measured sections were prepared from four of them. The outcrops are situated in two areas: the Sydenham Road and Jolley Cut outcrops are in the Hamilton area and the Art Park, Haul Road Cut and Whirlpool outcrops are in the Niagara Gorge [figure 1].

A detailed study of the Whirlpool exposure was not attempted, due to the fact that at the time the field work was completed the Niagara River was at its peak height. It was not until late October that the Niagara River was low enough to allow direct observation of the Whirlpool Sandstone from its base to the base of the Power Glen Formation. It was unfortunate that a measured section could not be prepared from this outcrop, for this location represents the best exposure of the Whirlpool in the study area. It offers the opportunity of viewing the Whirlpool along bedding planes, as well as in vertical section.

An attempt has been made to identify the facies present at the Whirlpool location and paleo-current data, as well as photographs from this outcrop have been included where appropriate.

As the main thrust of this thesis concerns the petrography and diagenetic history of the Whirlpool, a depositional model has not been prepared from field observations. Instead, these observations will be compared with the Sandy Braided Fluvial depositional model prepared by C.J. Salas from work done on a series of rock quarries in the Georgetown area, roughly 50 km north of Hamilton.

The sediments of the Whirlpool Sandstone in the Hamilton and Niagara Gorge areas have been divided into eleven facies and two subfacies. They can be differentiated on the basis of lithology, sedimentary structures and biogenic content.

Figures 2-2 and 2-5 are stratigraphic sections detailing the position of the facies and the locations at which samples were taken for thin sectioning. Figure 2-1 is a legend describing all symbols used.



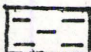
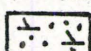
#### Facies A:

Facies A is better known as the Queenston Formation. Middleton [1982] described it as a "remarkably monotonous red shale, roughly 150 m thick in the Hamilton area and thickening rapidly to the southeast, with thin siltstone, fine sandstone and calcareous interbeds." He found it to be





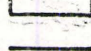
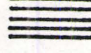

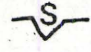
Figure 2-1: Legend for Stratigraphic Sections, figures  
2-2 to 2-5.

LEGEND





LITHOLOGIES

-  Sandstone
-  Grey Shale
-  Red Shale
-  Calcareous Sandstone

SEDIMENTARY STRUCTURES

-  Trough Cross-bedding
-  Undulating Contact
-  Oscillating Current Ripples
-  Variable Contact Zone Between Grey and Red Shales
-  Plane Parallel Lamination
-  Casts of Mud Cracks
-  Casts of Syneresis Cracks
-  -?- Covered Area

PALEO-CURRENT

-  LT Large Scale Trough Cross-bedding
-  MT Medium Scale Trough Cross-bedding
-  ST Small Scale Trough Cross-bedding
-  SR Small Scale Current Ripples

CONSTITUENTS





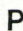

-  Mud Rip-up Clasts
-  Round Weathering Cavities
-  L Limonite Staining
-  G Galena Mineralization
-  P Pyrite Mineralization
-  Chondrites Trace Fossils

Figure 2-2: Stratigraphic Section of the Haul Road Cut.  
Refer to figure 1-1 for the location of the  
outcrop and figure 2-1 for a legend describing  
all symbols used.

# HAUL ROAD CUT

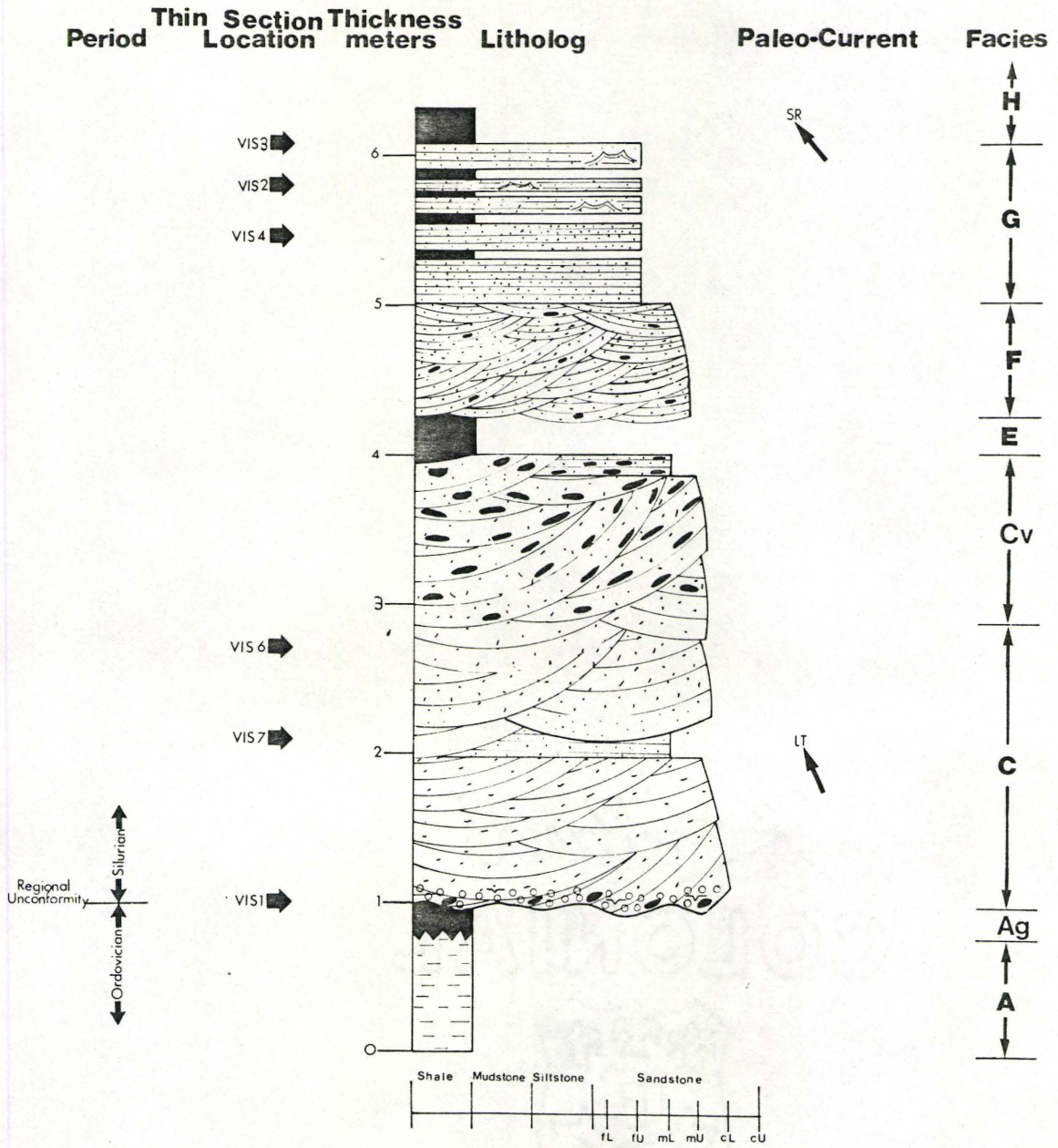


Figure 2-3: Stratigraphic Section of the Art Park outcrop.  
Refer to figure 1-1 for the location of the  
outcrop and figure 2-1 for a legend describing  
all symbols used.



# ART PARK

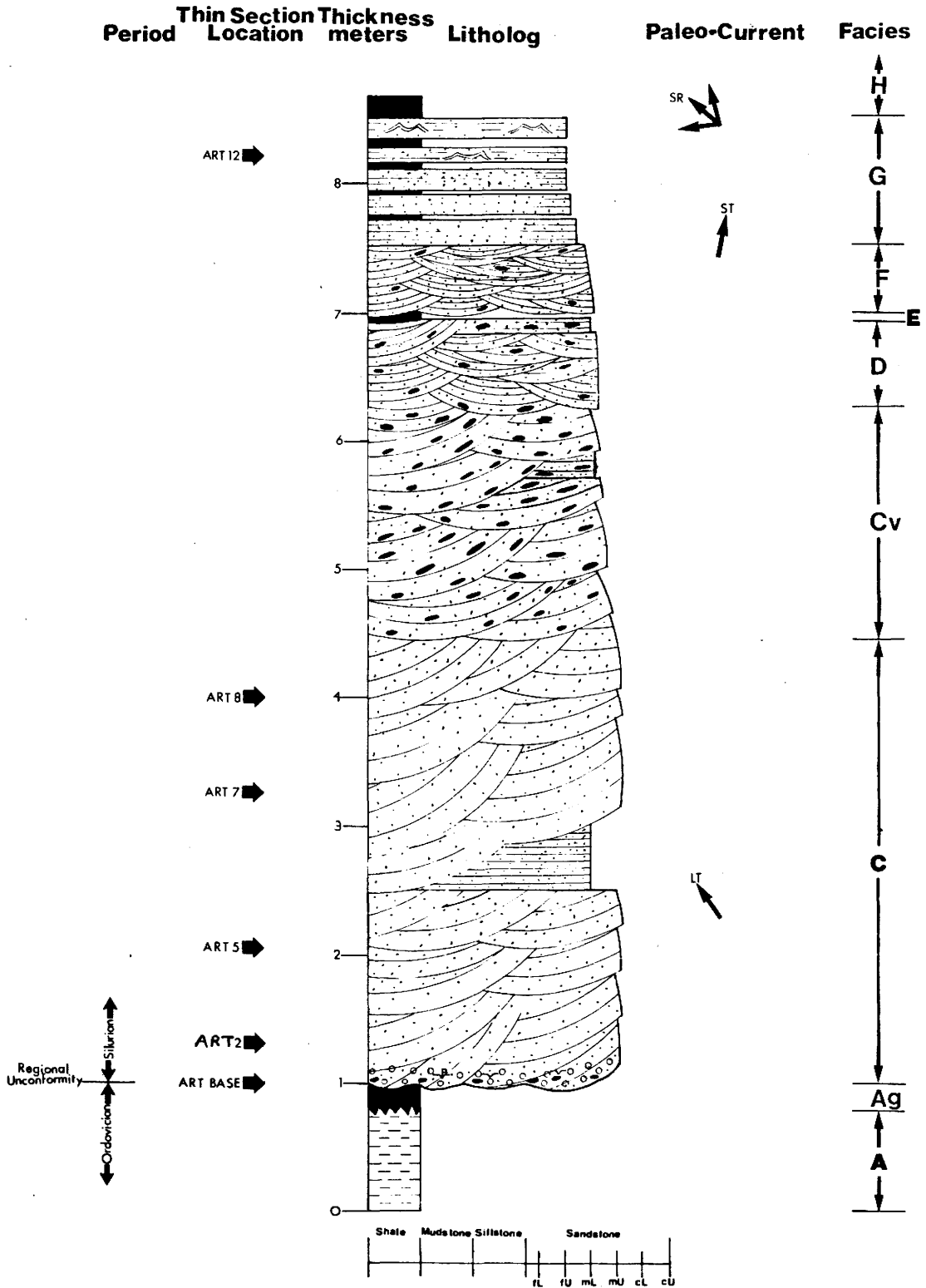


Figure 2-4: Stratigraphic Section of the Jolley Cut.

Refer to figure 1-1 for the location of the outcrop and figure 2-1 for a legend describing all symbols used.

# JOLLEY CUT

Thinsection Thickness  
 Period Location meters Litholog

Paleo-Current

Facies

Silurian ↑

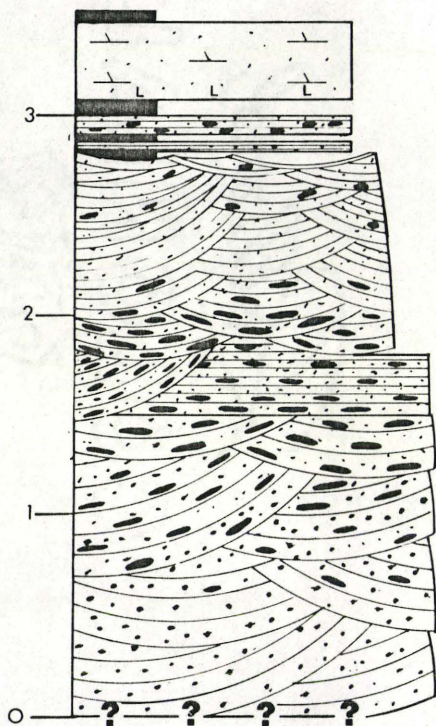
JOLL 1 →

JOLL 3 →

JOLL 4 →

JOLL 5 →

JOLL 6 →



MT →

MT →

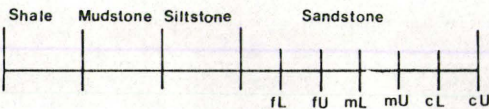


Figure 2-5: Stratigraphic Section of the Sydenham Road Cut. Refer to figure 1-1 for the location of the outcrop and figure 2-1 for a legend describing all symbols used.

# SYDENHAM ROAD CUT

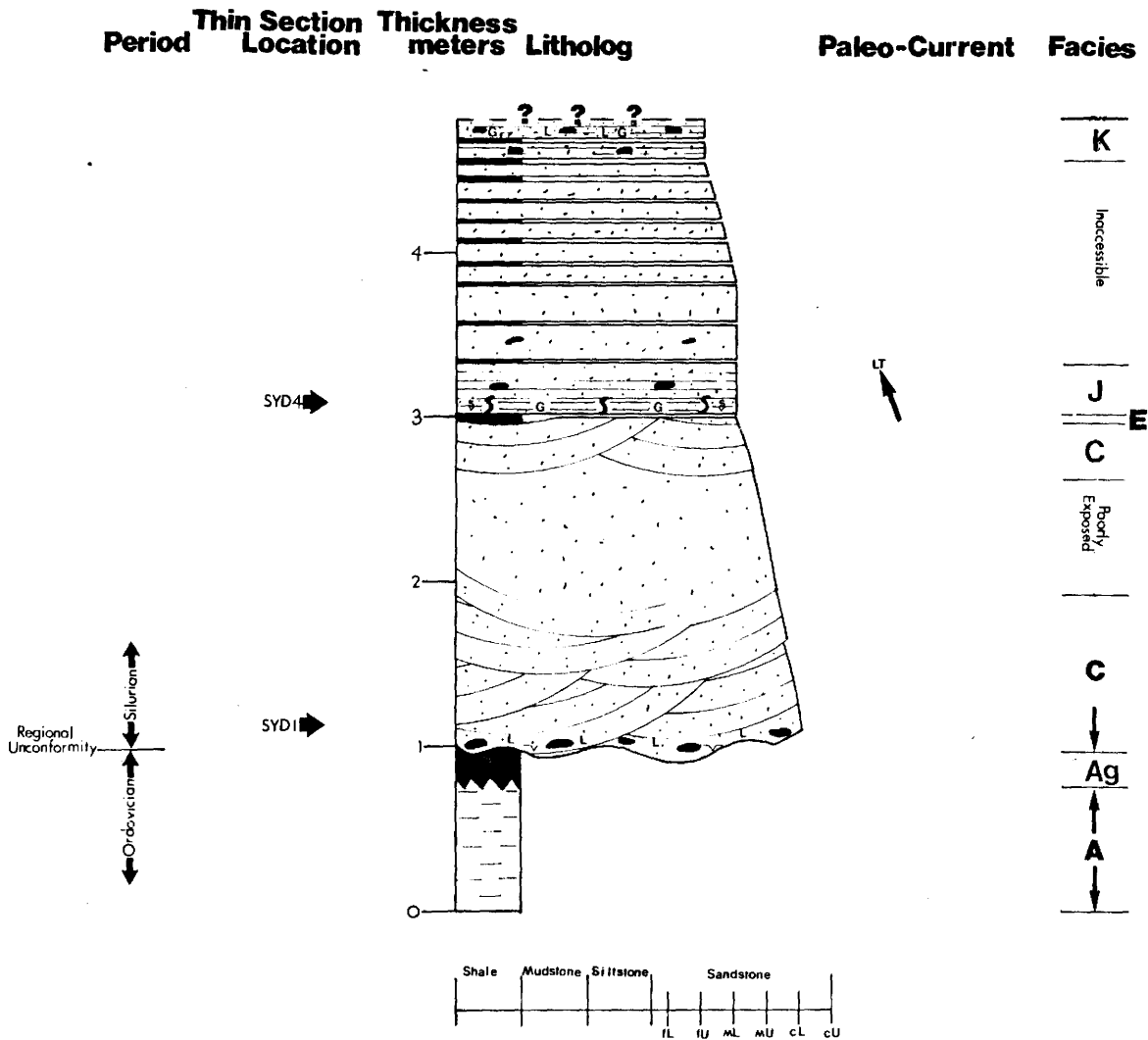


Plate 2-1a: Facies A/Ag/C and a small erosional channel at the base of Facies C. Note the protrusions of Facies Ag into Facies A. Photograph from the Whirlpool outcrop.

Plate 2-1b: Three dimensional view of large scale troughs near the base of Facies C. Photograph from the Whirlpool outcrop.



lacking in any type of fossils, including trace fossils. It is best exposed at the Art Park location. [see plates 2-1a and 2-4b]

Subfacies Ag:

Subfacies Ag consists of 20 to 30 cm of grey-green, fossil free shale. It is relatively constant in thickness and has been identified in deep cores from wells drilled in Chatoqua County, New York State [Seyler, 1981].

The lower contact with the Queenston Formation is variable. It comprises undulating surfaces, "fuzzy" boundaries, as well as "finger like" protrusions, a few cm in width and length, of the grey-green shale into the red shale of the Queenston Formation [see plates 2-1a and 2-4b].

The upper contact with the Whirlpool Sandstone is sharp. It is characterized by undulating surfaces, well defined casts of mud cracks and minor erosional features, i.e. the presence of small channels [see plate 2-1a].

Subfacies Ag is best exposed at the Art Park and Whirlpool outcrops.

Facies C:

Facies C consists of large scale trough cross-bedded sandstone, with relatively thin zones of parallel laminated sandstones, 50 to 20 cm thick, that cut troughs below and are cut by troughs above and laterally [see plates 2-1b,



Plate 2-2a: Parallel laminated sandstone cutting large scale troughs and being cut laterally by large scale troughs, in Facies C. Photograph from the Whirlpool outcrop.

Plate 2-2b: Parting lineations found on the surface of the parallel laminated sandstone pictured above. A paleo-current direction of  $300^{\circ}$  was measured from these lineations in Facies C, (courtesy of Dr. G.V. Middleton). Photograph from the Whirlpool outcrop.

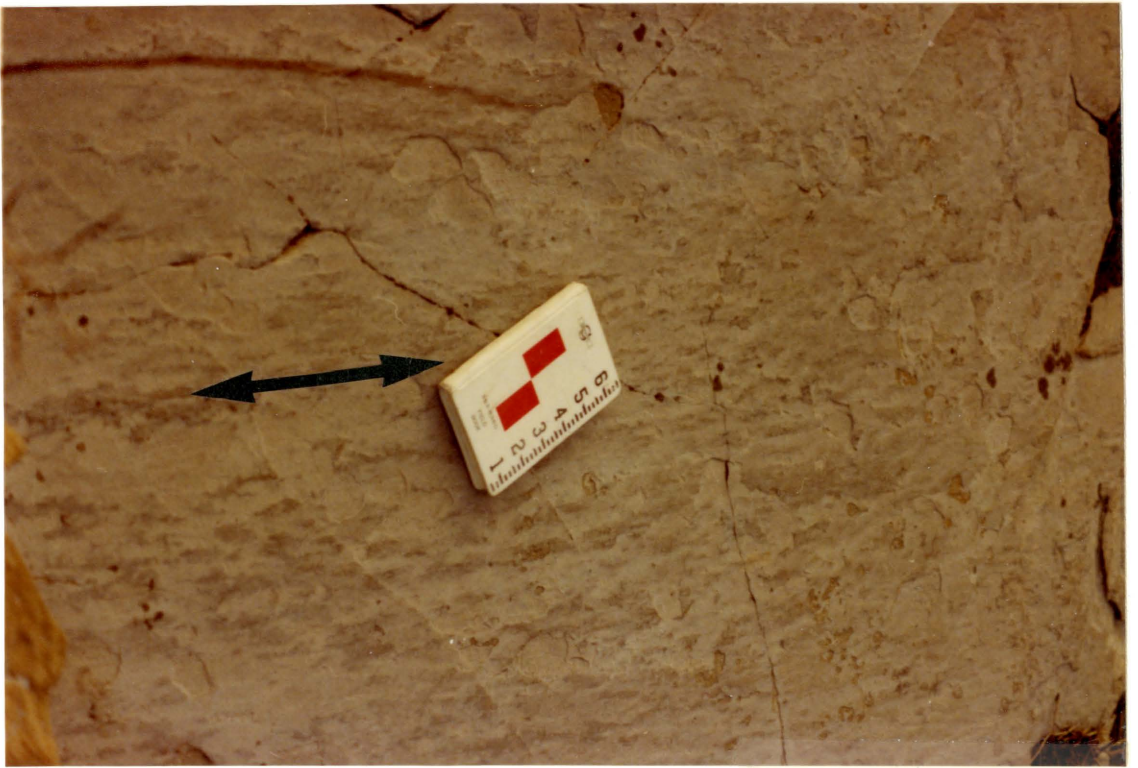
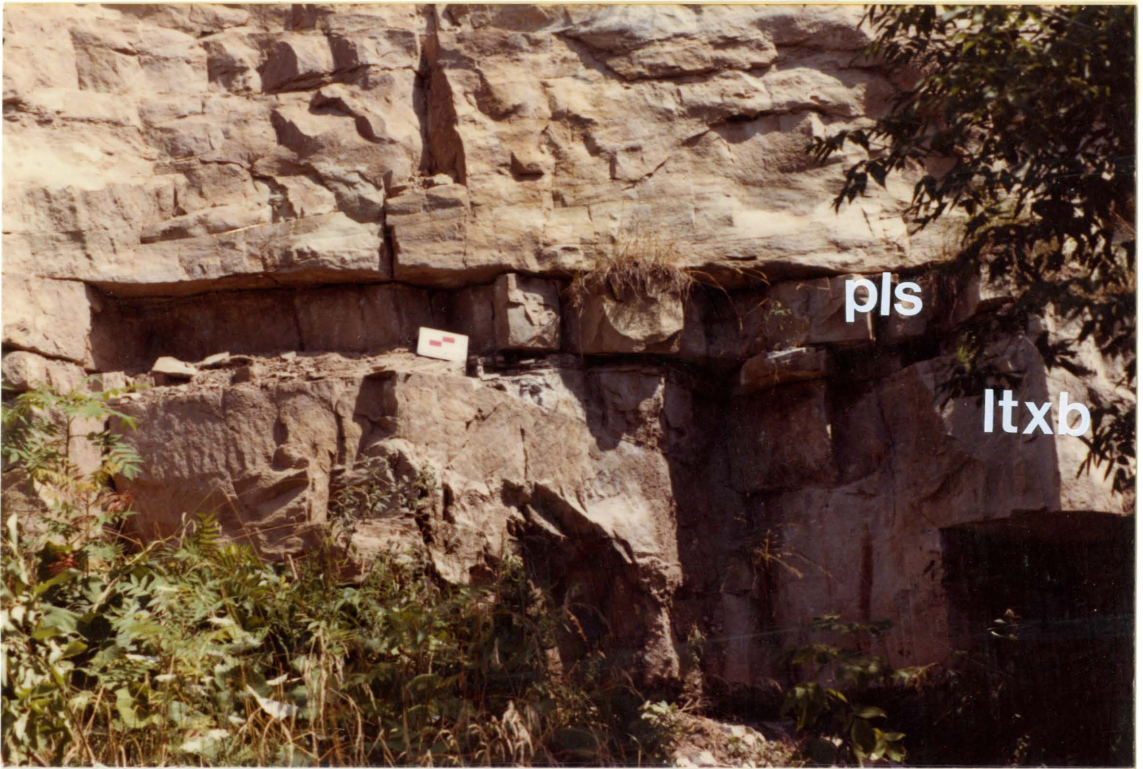


Plate 2-3a: Parallel laminated sandstone cutting large scale troughs and being cut by troughs above and laterally, in Facies C. Photograph from Art Park outcrop.

Plate 2-3b: Large grey-green, clay, rip-up clasts at the base of Facies C. Photograph from Whirlpool outcrop.



2-2a,b and 2-3a].

The unit is coarsest at the base and fines upward. Also, the troughs are coarsest at their bases and fine upwards to the base of the next trough where the trend is repeated. Facies C is found throughout the study area, but is best exposed at the Art Park and Whirlpool outcrops.

Facies C decreases in thickness to the northwest, ranging from 3m, at Art Park, to 1.5 m, at Sydenham Road. The grain size varies from 1.0-0.5  $\phi$  at the base, to 1.5-1.0  $\phi$ , at the top, with the parallel laminated sandstones displaying finer grain sizes of 2.0-1.5  $\phi$ .

Large, 15 to 1 cm, oval, grey-green, clay, rip-up clasts are found near the base and they appear to have been "plucked and rafted up" from the Queenston Formation below. There also appears to be small limonite stain rings around many of the clasts [see plate 2-3b].

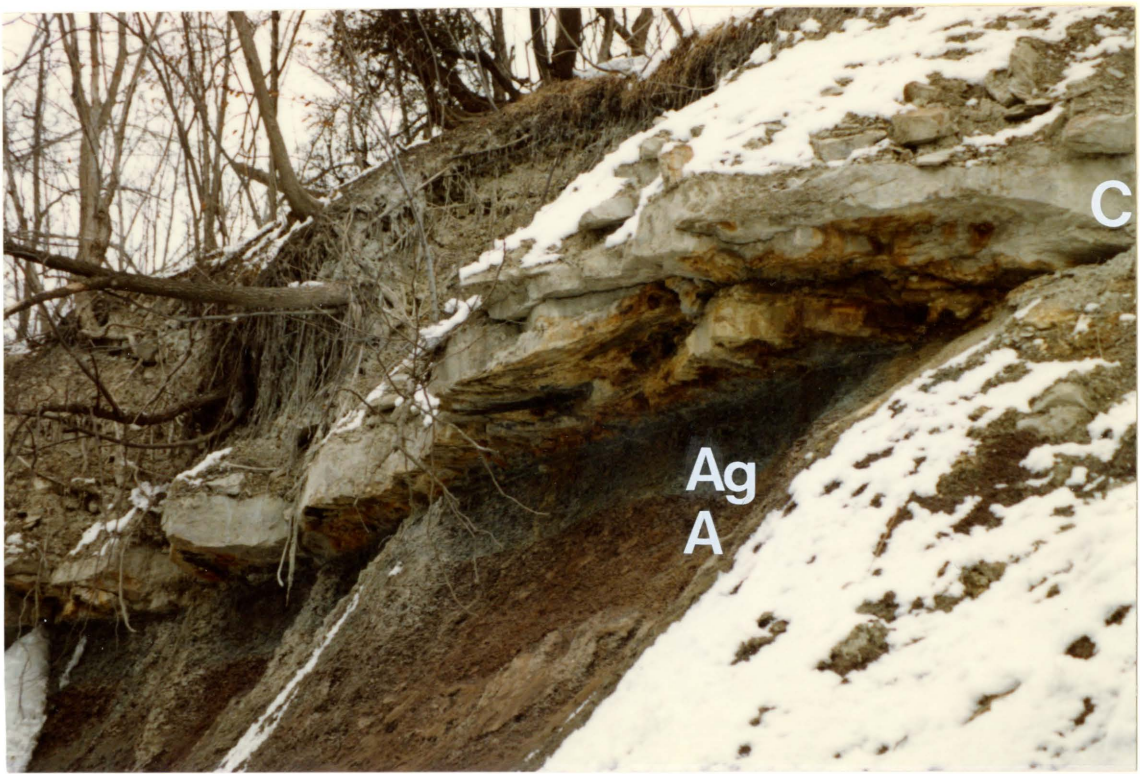
Near the base of Facies C, at the Niagara Gorge outcrops, there exists, in a narrow band roughly 30 cm wide, an accumulation of round, superficial, weathering cavities.

These cavities exist on the vertical and horizontal faces of the outcrops and range in diameter from 1.0 to 0.5 cm. When dilute HCl was applied to the cavities a vigorous reaction took place, signifying the presence of calcite [see plate 2-4a].

Well developed casts of mud cracks are found on the

Plate 2-4a: Superficial round weathering cavities at the base of Facies C. Photograph from the Art Park outcrop.

Plate 2-4b: Facies A/Ag/C and limonite staining at the base of Facies C. Photograph from the Sydenham Road Cut outcrop.



basal surface of the Haul Road Cut and Art Park outcrops and patchy pyrite cement is found in the casts at Art Park.

Red limonite staining has developed at the base of the Sydenham Road exposure, but due to inaccessibility and poor exposure, the source of the staining can only be inferred to be due to the weathering of sulphide minerals, which have been found higher up in the outcrop [see plate 2-4b].

The large scale trough cross-beds give paleo-current directions of  $300^{\circ}$  to  $340^{\circ}$  and parting lineations on the surface of a parallel laminated sandstone at the Whirlpool outcrop give an azimuth of  $300^{\circ}$  [courtesy of Dr. G.V. Middleton] [see plate 2-2a,b].

#### Subfacies Cv:

Subfacies Cv consists of imbricated, grey-green, clay, rip-up clasts, 3.0 to 0.5 cm long, oriented along the bedding planes of large scale trough cross-bedded and parallel laminated sandstones [see plates 2-5a,b and 2-6a].

The parallel laminated sandstones consist of relatively thin zones, 30 to 20 cm thick, that cut troughs below and are cut by troughs above and laterally.

Subfacies Cv is differentiated from Facies C by the presence of clay rip-up clasts. Troughs from Subfacies Cv are seen to cut into Facies C.



Plate 2-5a: Parallel laminated sandstone cutting large scale troughs and being cut by troughs above and laterally in Facies Cv. Note the orientation of the clay rip-up clasts along bedding planes. Photograph from the Jolley Cut outcrop.

Plate 2-5b: Facies C/Cv/E, photograph from the Haul Road Cut outcrop.



Plate 2-6a: Facies Cv/D/E/I/M, photograph from the Jolley  
Cut outcrop.

Plate 2-6b: Small scale trough cross-bedding in Facies F.  
Photograph from the Art Park outcrop.



Subfacies Cv is found at all outcrops in the study area except for the Sydenham Road Cut outcrop, and is best exposed at the Art Park and Jolley Cut outcrops. The absence of the unit at Sydenham Road may just be due to the poor exposure of the Whirlpool at this location.

The unit decreases in thickness to the northwest, from 2 m at Art Park to 1 m at the Jolley Cut. The large scale trough cross-bedding has an average grain size of 1.5-1.0  $\phi$ . Also, the troughs are coarsest at their bases and fine upwards to the base of the next trough, where the trend is repeated. The parallel laminated sandstones have a finer grain size of 2.0-1.5  $\phi$ .

At the Art Park and Jolley Cut outcrops, Subfacies Cv is cut from above by medium scale trough cross-bedded sandstone with imbricated clay rip-up clasts. At the Haul Road Cut a grey-green shale appears to rest conformably on the unit.

Paleo-current directions in Subfacies Cv appear to be consistent with Facies C, but due to lack of good bedding plane exposure, current directions could not be measured.

#### Facies D:

Facies D consists of medium scale trough cross-bedded sandstone, with imbricated, grey-green, rip-up clasts, 1.0 to 0.5 cm in length, oriented along bedding planes.

Facies D is present only at the Art Park and Jolley Cut locations [see figure 2-6a]. It is observed to cut down into Subfacies Cv and a grey-green shale appears to rest conformably on its top.

Facies D is relatively constant in thickness at 1 m. It has an average grain size of 2.0-1.5  $\phi$  and the troughs are coarsest at their bases and fine upwards to the base of the next trough, where the trend is repeated.

At the Art Park location, a thin zone 20 cm thick, of parallel laminated sandstone is present at the top of Facies D. It cuts the troughs below and is cut laterally by troughs. The parallel laminated sandstone has a grain size slightly finer than the medium trough cross-bedded sandstone below.

Paleo-current directions of 300° were measured from the troughs.

#### Facies E:

Facies E consists of grey-green shale. It is found at all locations and is variable in thickness, ranging from 30 cm at Haul Road, to 10 cm at Sydenham Road. It is best exposed at the Haul Road Cut [see plates 2-5b, 2-6a and 2-8a].

Facies E appears to rest conformably on Facies Cv at Haul Road, Facies C at Sydenham Road and Facies D at the Jolley Cut and Art Park outcrops. Facies E is cut

by Facies F at Haul Road and Art Park, by Facies I at Jolley Cut and by Facies J at the Sydenham Road location.

#### Facies F:

Facies F consists of small scale trough cross-bedded sandstone, with a scattering of imbricated, grey-green, clay rip-up clasts, 0.3 to 0.5 cm in length, oriented along bedding planes.

Facies F cuts into Facies E and is cut from above by a parallel laminated sandstone, Facies G. Facies F is found only at the Niagara Gorge outcrops [see plate 2-6b].

Facies F is relatively constant in thickness, roughly 0.5 m, and has an average grain size of 2.0-1.5  $\phi$ , with a slight fining towards the top.

The small scale trough cross-beds give paleo-current directions of  $10^{\circ}$  [courtesy of Dr. G.V. Middleton].

#### Facies G

Facies G consists of interbedded parallel laminated sandstones and grey-green shales. The sandstones have thicknesses on average of 20 cm, while the shales are on average 5 cm thick. The beds are in a 5:4 ratio, sandstone to shale. The bottom sandstone bed is seen to cut into Facies F and a grey-green shale, Facies H, rests conformably on top. Facies G is found only at the Niagara Gorge outcrops [see plate 2-7a].

Plate 2-7a: Facies G/H, photograph from the  
Art Park outcrop.

Plate 2-7b: Oscillating current ripples with tuning  
fork bifurcations in Facies G.





The sandstone has a grain size on average of 2.5-2.0  $\phi$ . At the top of the sandstone beds there exists oscillating current ripples with tuning fork bifurcations [see plate 2-7b]. Small scale current ripples displaying paleo-current direction of 265° to 345° [courtesy of Dr. G.V. Middleton] are also present in facies G. Bill Duke [personal communication] has reported the presence of Hummocky Cross-stratification on the top sandstone beds.

#### Facies H:

Facies H is better known as the Power Glen Shale. Middleton [1982] described it as a grey, fossiliferous, shale with dolomitic interbeds. The Power Glen is found only in the Niagara Gorge and the contact with the Whirlpool is sharp [see plate 2-7a].

The Power Glen Shale is progressively replaced to the northwest by the Manitoulin Dolomite and the transition is complete in the Hamilton area. Middleton [1982] suggests that the Power Glen Shale should be included with the Cabot Head Formation directly above.

#### Facies I:

Facies I consists of interbedded parallel laminated sandstones and grey-green shales in a 1:1 ratio. The sandstones are on average 20 cm thick and have a grain size of 3.0-2.5  $\phi$ . Scattered throughout the sandstones are grey-green, oval, clay, rip-up clasts, 1.0 to 0.3 cm in length,

oriented along bedding planes. The shales are on average 10 cm thick [see plate 2-6a].

The lower sandstone bed is observed to cut into the shale of Facies E and the top shale bed of Facies I appears to be cut by the calcareous sandstone of Facies M.

Facies I is found only at the Jolley Cut outcrop.

Facies M:

Facies M represents the transition from the Whirlpool Sandstone to the Manitoulin Dolomite. It is observed only at the Jolley Cut and consists of a calcareous sandstone, 40 cm thick, interbedded with 10 cm thick, grey-green, shales. The calcareous sandstone appears to be extensively bioturbated.

Middleton [1982] described the Manitoulin Dolomite as 3 to 4 m of thin bedded, buff weathering, fossiliferous, bioturbated, dolomite [see plate 2-6a].

The Manitoulin thickens and becomes less argillaceous towards the northwest and is replaced by the Power Glen Shale, to the southeast.

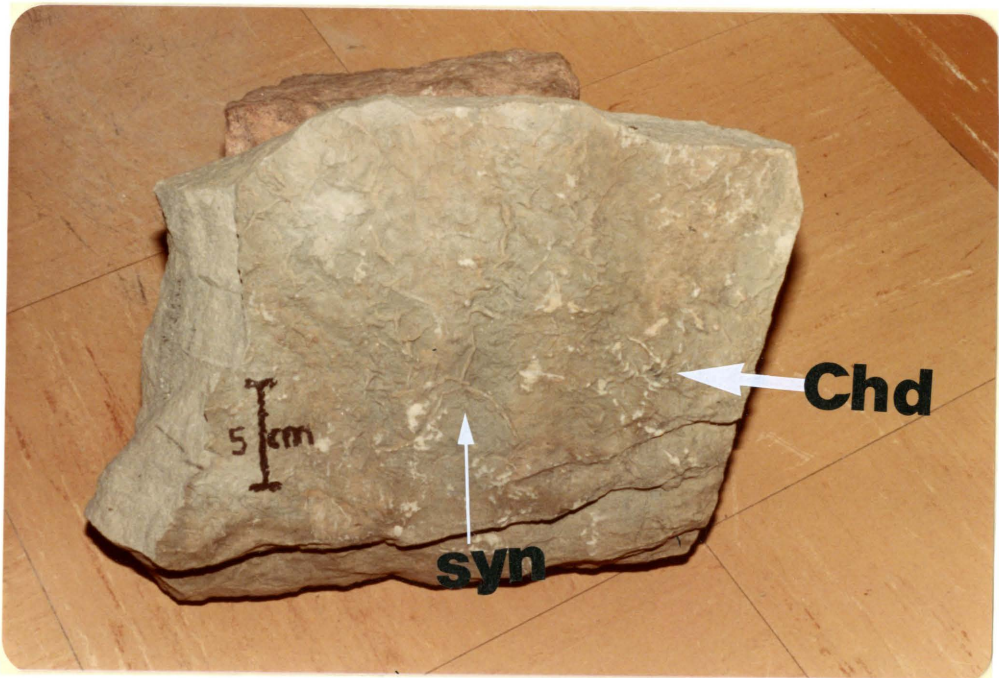
Facies J:

Facies J consists of a parallel laminated sandstone, 30 cm thick, displaying the trace fossil Chondrites at its base. Facies J is found only at the Sydenham Road outcrop [see plate 2-8a,b].

Galena mineralization and grey-green, oval, clay

Plate 2-8a: Facies C/E/J, photograph from the Sydenham Road outcrop.

Plate 2-8b: Trace fossil Chondrites and casts of synaeresis mud cracks on the basal surface of Facies J. Photograph from the Sydenham Road outcrop.



rip-up clasts, 1.0 to 0.5 cm in length, oriented along bedding planes are found within the unit. The sandstone has a grain size of 2.0-1.5  $\phi$  and the trace fossil Chondrites and casts of synaeresis mud cracks are displayed on the basal surface [Dr. M.S. Risk, personal communication].

Facies J is observed to cut into the shale of Facies E below, its vertical extent is not known, due to the inaccessibility of the upper regions of the outcrop.

#### Facies K:

Facies K consists of interbedded parallel laminated sandstones and grey-green shales in a 1:1 ratio. The sandstones are on average 20 cm thick and display galena mineralization and grey-green, oval, clay, rip-up clasts, oriented along bedding planes. The sandstones have a grain size of 2.0-1.5  $\phi$  and limonite staining, from the weathering of the sulphides, is present at the bases of the sandstones. The shales are on average 10 cm thick.

Facies K is found only at the Sydenham Road outcrop. Its vertical extent is not known, due to the fact that only 60 cm of the unit is exposed.

#### Interpretation:

The scarcity of fossils and red colour, high oxidized iron content, prompted Grabau [1913b] to associate the Queenston Formation with a terrestrial deltaic environment of deposition. Middleton [1982] raised a serious

criticism of this interpretation by questioning the ability of a delta to deposit a very thick, non-marine shale, without any channel deposits, or marine intercolations. Thus, no accepted depositional environment for the Queenston Formation presently exists.

The relative constancy of thickness and the "finger like" protrusions of the grey-green shale into the Upper Red Queenston, tends to suggest that the grey-green shale represents a reduced and leached form of the Queenston, due to percolating water in a reducing environment. Sandford [1969] interpreted this zone as a region of reduction of ferric iron to ferrous iron during diagenesis. Seyler [1981] interpreted the presence of large grey-green, clay, rip-up clasts at the base of the Whirlpool in outcrop and deep core as signifying the leaching of the Upper Queenston before deposition of the Whirlpool Sand. It seems more likely, however, that the rip-up clasts were originally of oxidized clay and then, like the 30 cm of Upper Red Queenston Shale, became reduced during diagenesis. The presence of patchy pyrite cement in the very base of the Whirlpool tends to suggest that the reduction of the oxidized clays took place in an environment that was only able to reprecipitate very small amounts of reduced iron, as pyrite, locally.

Salas [1983] concluded from his work on the

Whirlpool Sandstone in the Georgetown area that any depositional model prepared for the Whirlpool must first explain the seven characteristics outlined by Bolton [1957]:

- 1] the gradation of white or grey sandstone eastward into red, coarser grained sandstone;
- 2] the easterly increase of impurities combined with a decrease in sorting;
- 3] the presence of lutite clasts and grey lutite lenses along the inclined foresets and horizontal bedding planes;
- 4] the limited size of the crossbedding, suggestive of an aqueous, rather than an eolian, origin;
- 5] the presence of both well rounded, frosted and subangular, clear quartz grains;
- 6] the predominance of only the most stable heavy minerals [Holstein, 1936];
- 7] the reasonable constancy of thickness along the Niagara escarpment with westward thinning;

and also it must take into account:

- i] the lack of marine body fossils in the lower two thirds of the formation [Fisher, 1954];
- ii] the presence of non-marine microfossils in the lower two thirds of the formation;
- iii] the absence of bioturbation in the lower two thirds of the formation;



- iv] the abrupt change from a high energy, non-bioturbated, non-fossiliferous lower facies, into a low energy, bioturbated, fossiliferous transition zone, with no gradation;
- v] the regionally consistent paleo-flow towards the northwest, which is in accordance with the Whirlpool's southern correlative, the Tuscorora Formation.

Salas has concluded that the origin of the Whirlpool Sandstone is consistent with a sandy braided fluvial system of low sinuosity and flashy discharge, with a transgression into a near-shore shallow marine environment.

If we apply the sandy braided fluvial model to the Whirlpool Sandstone in the study area, then the lower, trough crossbedded facies, C and D, may represent in-channel deposits. The plane beds associated with the troughs represent in-channel deposits as well, but due to a decrease in grain size, the flow has moved out of the dune field and into the upper plane bed regime [Blatt et al., p. 141]. The presence of only in-channel deposits is probably due to the constant switching of channels, which would destroy any bar deposits [C.J. Salas, personal communication].

The transition zone is marked by the appearance of Facies E, a layer of grey shale, separating the fluvial,

trough crossbedded sandstones from the upper, marine sandstones.

The marine sandstones consist of facies F and G in the Niagara Gorge, I at the Jolley Cut and J and K at the Sydenham Road outcrop. These beds are near shore deposits, as they display marine fossils and trace fossils as well as oscillation ripples. There is indication that there may also exist storm deposits [C.J. Salas, personal communication].

In the Niagara Gorge the transition of the Whirlpool into the Cabot Head shales is represented by facies H. Middleton [1982] interprets the Cabot Head as being fully marine, offshore deposits, and states that the transition upwards to shale from the Manitoulin Dolomite reflects an increase in the input of terrigenous mud from the southeast, due to progradation. Thus, the Cabot Head Shales in the Hamilton and Niagara Gorge areas could be described as prodeltaic [ibid.].

Facies M at the Jolley Cut represents the transition from the Whirlpool Sandstone to the Manitoulin Colomite. Middleton [1982] interprets the Manitoulin as being originally deposited as a bioclastic sand in relatively deep marine waters.

The sedimentary structures and constituents observed in the lower units of the Whirlpool Sandstone in the

study area appear to fit the sandy braided fluvial depositional model developed by C.J. Salas [1983], but detailed field work is required in order to confirm this.

## CHAPTER 3

### P E T R O G R A P H Y

#### Introduction:

Twenty thin sections were prepared from samples collected at five locations in the study area. Nineteen were cut from samples taken at the four outcrops that were studied in detail, Art Park, Haul Road Cut, Jolley Cut and the Sydenham Road location. One thin section was prepared from a sample taken at the very base of the Whirlpool outcrop. All thin sections were cut perpendicular to bedding and ten were impregnated with blue epoxy in order to determine true porosity. The sections were prepared slightly thicker, lightly polished on the bottom side and left uncovered in order to be analyzed by Cathodoluminescent Microscopy [see Appendix 1 for description of technique].

All thin sections were stained for: 1] ferroan/nonferroan calcite and dolomite using a method developed by Lindholm and Finkelman [1971]. 2] plagioclase and K-feldspar, using a method developed by Houghton [1980] [see Appendix 2 for description of staining techniques].

The results obtained from the calcite staining were excellent, dolomite as well as ferroan and nonferroan

calcite have been identified [see plate 3-5a,b]. The feldspar staining was inconclusive. The stain did not take, even after repeated treatments. Thus, all feldspar identification has had to be done using Cathodoluminescent Microscopy and the presence of twinning.

After the Cathodoluminescent study and staining had been completed, the cover slips were fixed on the thin sections so that they could be analyzed under transmitted light.

Most of the thin sections were prepared from samples taken in the lower, coarser facies, i.e. Facies C and D, in order to carefully study the fluvial beds of the Whirlpool. Six thin sections were prepared from samples taken in Facies G, I and J in order to contrast the upper, shallow marine beds with the lower fluvial beds.

#### Grain Size:

The Shadowmaster<sub>TM</sub> was used to determine the greatest, natural diameter, i.e. excluding quartz overgrowths, of twenty of the largest grains per slide. These diameters were then averaged and accepted as the average grain size for that slide.

According to Blatt et al. [1980, p.66-68] a section cut across a population of uniform spheres, randomly arranged in space, will not yield a uniform size distribution. Only the maximum size observed corresponds to the true size

of the parent population. Also, nonspherical particles will show anisotropic dimensional fabrics, and thus the results of measuring the section size will depend on the direction in which the section is cut relative to the grain fabric. Since the direction of grain orientations is generally unknown, thin sections should be cut parallel to bedding. Blatt et al. [1980] have recognized that the problem of inferring the three dimensional parent size from two dimensional observations is theoretically unsolvable. They suggest, instead, that a standardized method of measurement of grain size in thin section be developed.

The method used in this study has taken into account the non-uniform size distribution of grain in a thin section, but no consideration has been given to grain fabric orientation. Neglecting grain fabric orientation will introduce a small negative error. Since the thin sections were not oriented with respect to paleo flow, the size of the error will vary. But, since the error will be small, the average grain size data in Table 3-1 should still be valid for recognizing general size trends in the study area.

Table 3-1 contains a listing of the thin sections prepared, the location, stratigraphic position, the facies from which they were obtained and the average grain size.

TABLE 3-1

## AVERAGE GRAIN SIZE

LOCATION	SAMPLE NUMBER	HEIGHT ABOVE BASE (meters)	FACIES	AVERAGE GRAIN SIZE (mm)
HAUL ROAD CUT	VIS 1	base	C	0.6
	VIS 7	1.1	C	0.2
	VIS 6	1.9	C	0.4
	VIS 4	5.5	G	0.3
	VIS 2	5.8	G	0.2
	VIS 3	6.05	G	0.3
ART PARK	ART BASE	base	C	0.3
	ART 2	1.3	C	0.5
	ART 5	2.05	C	0.4
	ART 7	3.25	C	0.5
	ART 8	4.0	C	0.6
	ART 12	8.2	G	0.3
WHIRLPOOL	WHIRL 1	base	C	0.3
JOLLEY CUT	JOLL 6	base*	C	0.4
	JOLL 5	2.4	D	0.3
	JOLL 4	2.7	D	0.2
	JOLL 3	2.9	Dm	0.3
	JOLL 1	3.0	I	0.3
SYDENHAM ROAD CUT	SYD 1	base	C	0.2
	SYD 4	3.05	J	0.2

n= 20 largest grains per slide, measured on the Shadowmaster<sup>TM</sup>

\*= stratigraphic base of Whirlpool is not exposed at Jolley Cut

It is evident from studying the table that the decrease in grain size from bottom to top of the Whirlpool, reported by Gietz [1952] is well developed within the study area.

In general the Whirlpool is coarsest at the very base, ranging from values of 0.6 to 0.5 mm, and rapidly fines upwards to values of 0.3 to 0.2 mm. In the lower regions of the outcrops, specifically in Facies C and D, a local grain size decrease to 0.2 mm is observed. This reflects the grain size decrease found in the parallel laminated sandstone zones.

The lateral fining trend to the northwest reported by Gietz [1952] also appears to be developed, but the lack of basal exposure at the Jolley Cut hinders the definite recognition of this trend.

#### Mineral Composition:

#### Method:

Point counting was completed using both Transmitted light and Cathodoluminescent Microscopy.

Point counting completed using transmitted light can be separated into four steps:

- i] twenty thin sections were point counted for general mineralogy, 300 point counts per slide.
- ii] twenty thin sections were point counted for types of rock fragments, 100 point counts per slide.



iii] twenty thin sections were point counted to determine the abundance of four possible quartz types [Basu et al., 1975]:

- a] monocrystalline quartz with less than 5° of undulosity.
- b] monocrystalline quartz with greater than 5° of undulosity.
- c] polycrystalline quartz with 2-3 crystal per grain.
- d] polycrystalline quartz with greater than 3 crystals per grain.

100 point counts per slide.

iv] eleven thin sections were point counted for a grain contact study. Six sections were taken from the Haul Road Cut outcrop and five sections were taken from the Jolley Cut outcrop. Grains were counted in a method after Fuchtbauer [1974]. All of the contacts per grain in a given field of view were counted and categorized after Taylor [1950] until one hundred grains had been counted.

Point counting completed using Cathodoluminescent Microscopy can be separated into two steps

i] twenty thin sections were point counted for general mineralogy, 300 point counts per slide.

ii] eleven thin sections were point counted for a grain contact study. Six sections were taken from the Haul Road Cut outcrop and five were taken from the Jolley Cut outcrop. Grains were counted in a method after Fuchtbauer [1974]. All of the contacts per grain in a given field of view were counted and categorized after Taylor [1952] until 100 grains had been counted.

#### Results:

The minerals and constituents found in the Whirlpool Sandstone in the study area are: quartz, present as detrital grains and authigenic overgrowths; feldspar; opaque and heavy minerals, opaques present as authigenic and secondary precipitate minerals; chert, phosphatized fossil fragments and rock fragments; ferroan and nonferroan calcite and dolomite cements; authigenic clays, identified on the SEM and XRD, and detrital muscovite.

All samples are classified as Quartzarenites or Sublitharenites after Folk [1974] [see figure 3-1].

#### Transmitted Light Microscopy:

##### Introduction:

Tables 3-2a,b to 3-5a,b indicate point count results obtained from the analysis of the twenty thin sections under transmitted light at 250X magnification.

TABLE 3-2a

## POINT COUNT RESULTS: TRANSMITTED LIGHT MICROSCOPY

LOCATION	SAMPLE NUMBER	QUARTZ	QUARTZ CEMENT	FELDSPAR	PHOSPHATE	OPAQUES AND HEAVIES	CHERT AND ROCK FRAGS.
	VIS 1	86.7	12.5	0.8	t	t	t
	VIS 7	83.0	14.5	t	1.0	t	0.3
HAUL ROAD CUT	VIS 6	77.8	15.7	t	0.7	1.0	2.0
	VIS 4	70.6	20.7	t	0.3	t	t
	VIS 2	72.5	10.0	t	1.0	1.0	t
	VIS 3	78.4	12.1	0.3	0.3	1.0	1.0

n = 300 point counts per slide, corrected for grain loss during thinsection preparation

t = mineral present, but not counted

- = mineral not present in slide

N.I.E. = slide not impregnated with blue epoxy, unable to determine true porosity

Table 3-2b

SAMPLE NUMBER	FERROAN CALCITE CEMENT	NONFERROAN CALCITE CEMENT	DOLOMITE CEMENT	VERMICULAR CHLORITE	CLAYS	MUSCOVITE	POROSITY	TOTAL %
VIS 1	t	-	-	0.3	-	-	N.I.E.	100.3
VIS 7	t	1.0	-	t	t	t	N.I.E.	99.8
VIS 6	t	1.7	-	t	1.7	-	N.I.E.	99.3
VIS 4	8.0	-	0.3	t	-	-	N.I.E.	99.9
VIS 2	13.7	1.0	t	t	-	-	N.I.E.	99.9
VIS 3	3.7	2.0	1.3	t	-	-	N.I.E.	100.4

TABLE 3-3a

## POINT COUNT RESULTS: TRANSMITTED LIGHT MICROSCOPY

LOCATION	SAMPLE	QUARTZ	QUARTZ CEMENT	FELDSPAR	PHOSPHATE	OPAQUES AND HEAVIES	CHERT AND ROCK FRAGS.
	ART BASE	68.0	22.3	0.3	0.7	0.3	1.7
	ART 2	70.7	15.3	t	0.7	0.7	2.7
	ART 5	81.2	14.1	t	1.0	t	3.4
ART PARK	ART 7	85.1	13.5	t	0.3	t	1.0
	ART 8	84.1	15.0	t	t	t	0.3
	ART 12	69.1	24.5	0.7	t	t	5.2

n = 300 point counts per slide, corrected for grain loss during thinsection preparation

t = mineral present, but not counted

- = mineral not present in slide

N.I.E. = slide not impregnated with blue epoxy, unable to determine true porosity

Table 3-3b

SAMPLE	FERROAN CALCITE CEMENT	NONFERROAN CALCITE CEMENT	DOLOMITE CEMENT	VERMICULAR CHLORITE	CLAYS	MUSCOVITE	POROSITY	TOTAL %
ART BASE	2.7	-	-	t	-	-	4.0	100.0
ART 2	0.3	-	t	0.3	-	-	9.3	99.9
ART 5	0.3	-	-	t	-	t	N.I.E.	100.0
ART 7	t	-	-	t	-	-	N.I.E.	99.9
ART 8	0.3	0.3	-	t	-	-	N.I.E.	100.0
ART 12	t	-	-	t	0.3	t	N.I.E.	99.8

TABLE 3-4a

## POINT COUNT RESULTS: TRANSMITTED LIGHT MICROSCOPY

LOCATION	SAMPLE NUMBER	QUARTZ	QUARTZ CEMENT	FELDSPAR	PHOSPHATE	OPAQUES AND HEAVIES	CHERT AND ROCK FRAGS.
JOLLEY CUT	JOLL 6	74.3	14.3	0.7	t	1.0	3.7
	JOLL 5	75.7	15.3	0.3	t	0.3	1.3
	JOLL 4	78.0	14.7	t	t	t	1.0
	JOLL 3	68.7	21.7	0.3	t	t	2.0
	JOLL 1	64.7	24.0	0.3	0.7	2.6	1.6

n = 300 point counts per slide, corrected for grain loss during thinsection preparation

t = mineral present, but not counted

- = mineral not present in slide

N.I.E. = slide not impregnated with blue epoxy, unable to determine true porosity

Table 3-4b

SAMPLE NUMBER	FERROAN CALCITE CEMENT	NONFERROAN CALCITE CEMENT	DOLOMITE CEMENT	VERMICULAR CHLORITE	CLAYS	MUSCOVITE	POROSITY	TOTAL %
JOLL 6	0.7	0.7	0.3	t	-	-	4.3	100.0
JOLL 5	-	t	-	0.3	-	-	7.0	100.2
JOLL 4	-	-	-	t	-	-	6.3	100.0
JOLL 3	0.3	7.0	-	t	-	-	t	100.0
JOLL 1	1.0	1.3	1.3	t	-	-	3.7	99.9



TABLE 3-5a

## POINT COUNT RESULTS: TRANSMITTED LIGHT MICROSCOPY

LOCATION	SAMPLE NUMBER	QUARTZ	QUARTZ CEMENT	FELDSPAR	PHOSPHATE	OPAQUES AND HEAVIES	CHERT AND ROCK FRAGS.
SYDENHAM ROAD CUT	SYD 1	71.3	13.7	0.7	1.3	2.3	0.3
	SYD 4	76.0	11.3	1.0	2.3	0.3	t
WHIRLPOOL NIAGARA RIVER	WHIRL 1	70.6	19.3	0.3	0.3	t	2.0

n = 300 point counts per slide, corrected for grain loss during thinsection preparation

t = mineral present, but not counted

- = mineral not present in slide

N.I.E. = slide not impregnated with blue epoxy, unable to determine true porosity

Table 3-5b

SAMPLE	FERROAN CALCITE CEMENT	NONFERROAN CALCITE CEMENT	DOLOMITE CEMENT	VERMICULAR CHLORITE	CLAYS	MUSCOVITE	POROSITY	TOTAL %
SYD 1	t	3.0	-	-	-	-	7.3	99.9
SYD 4	-	t	-	t	-	-	9.0	100.2
WHIRL 1	0.7	t	t	t	0.3	-	6.3	99.8

## Quartz

The detrital quartz grain population consists of: nonundulose and undulose monocrystalline quartz, comprising roughly 75% and 15% of the total population respectively; polycrystalline quartz with more than 3 crystals per grain, comprising roughly 8% of the total population; and polycrystalline quartz with fewer than 3 crystals per grain, comprising roughly 2% of the total population [see table 3-15].

All grains are surrounded by well developed syntaxial overgrowths of silica cement. The overgrowths are in general easy to recognize, due to the presence of bubble trains in the original grain and dust rims consisting of hematite and illite clay as well as unknowns [see plate 3-18] around the rim of the detrital grain [see plates 3-1a,b, 3-2a,b and 3-3a]. Dust rims are formed by the creation of void space between the overgrowth and the nucleus during cementation [Pittman, 1972]. When nucleation is initiated at a number of sites on the surface of a quartz grain, and as competitive crystal growth proceeds, a small number of nuclei will grow together forming the overgrowth [Hutcheon, 1982]. The voids represent the interstices between the original nuclei, which later became filled with "dust".

The monocrystalline detrital quartz grains appear to be subrounded to rounded, while the polycrystalline detrital

Plate 3-1a: Detrital quartz grain showing bubble trains as well as a dust rim, note the near total occlusion of all porosity by quartz overgrowths. Sample ART 12, 160X magnification, XN.

Plate 3-1b: Polycrystalline quartz grain with more than 3 crystals [center], dolomite rhomb, [arrow], and a low grade MRF, [arrow]. Note the orientation of crystals within the MRF and the lack of any deformation, even though the grain is between two quartz grains. Sample VIS 4, 160X magnification, XN.

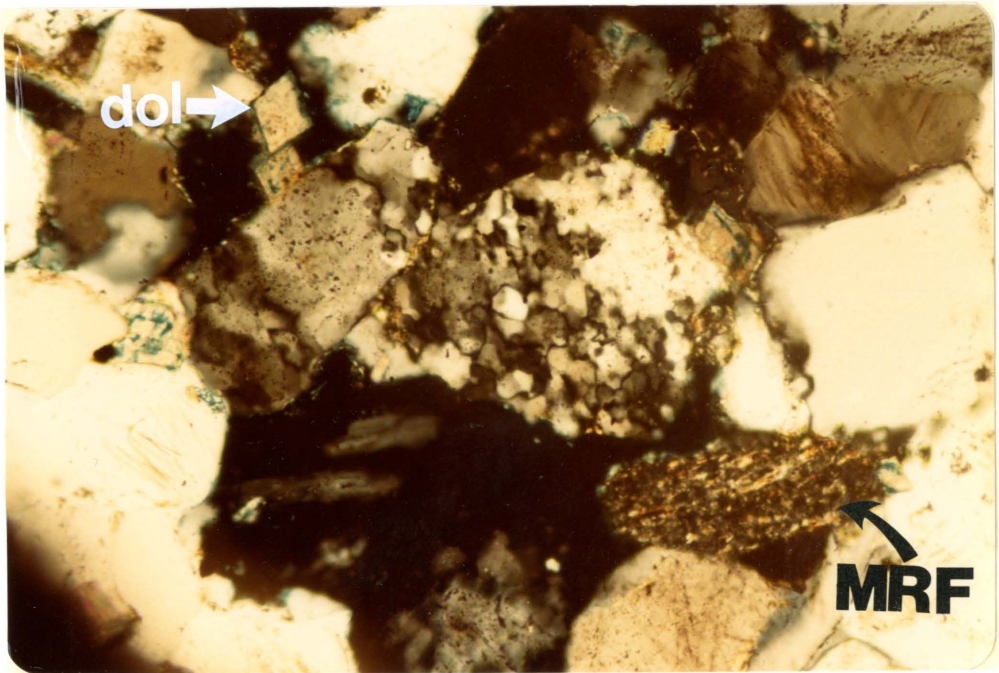
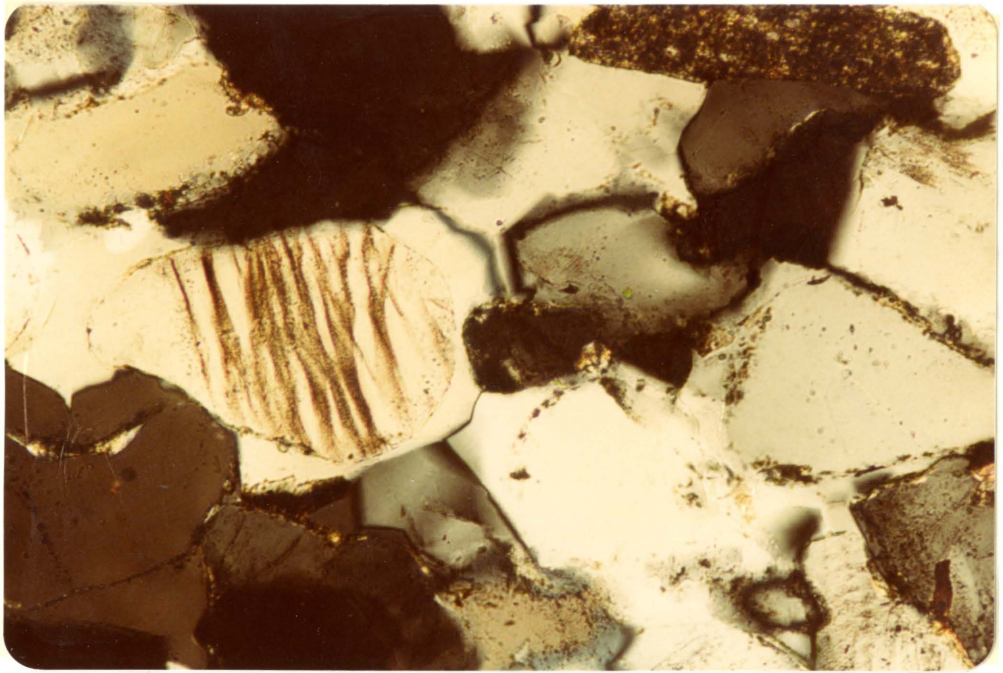


Plate 3-2a: Primary quartz overgrowths on detrital quartz grain. Scale bar divisions equal 10 microns.  
ART BASE.

Plate 3-2b: Primary, isolated quartz overgrowths growing into porosity, and secondary massive overgrowths occluding all porosity. Scale bar divisions equal 10 microns. WHIRL 1

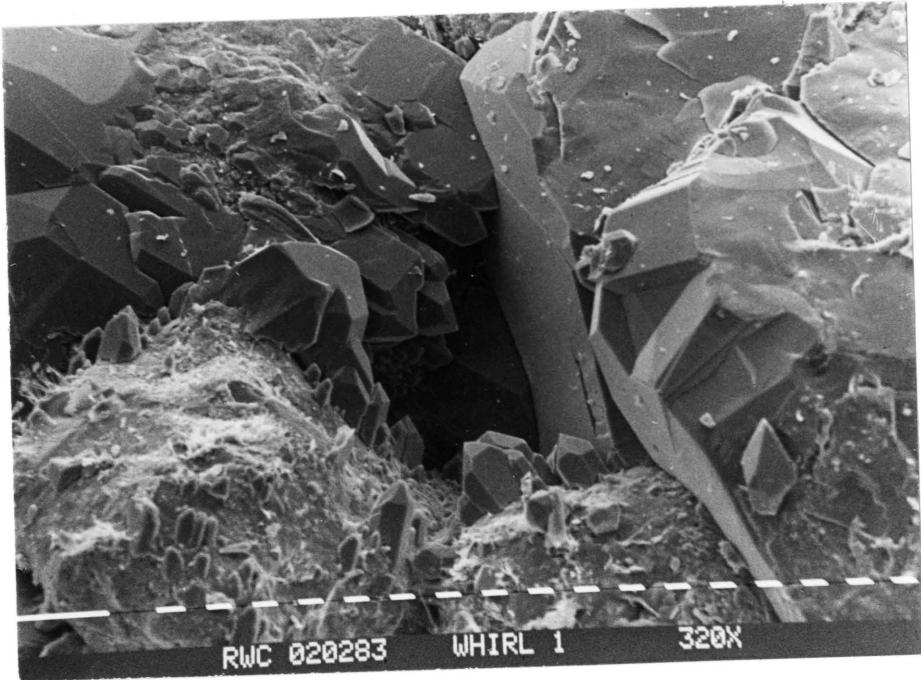
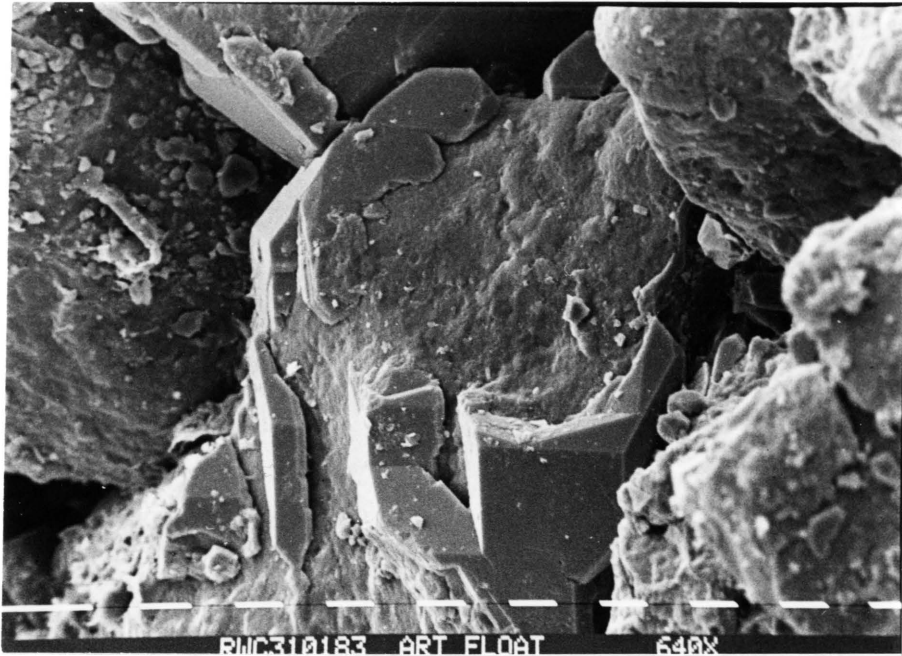
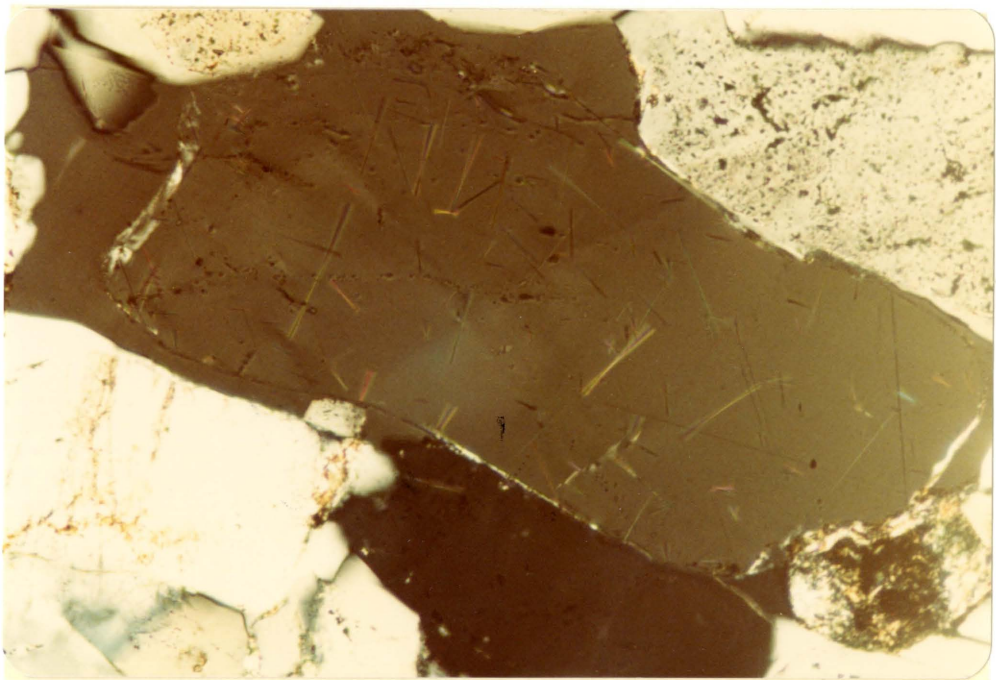
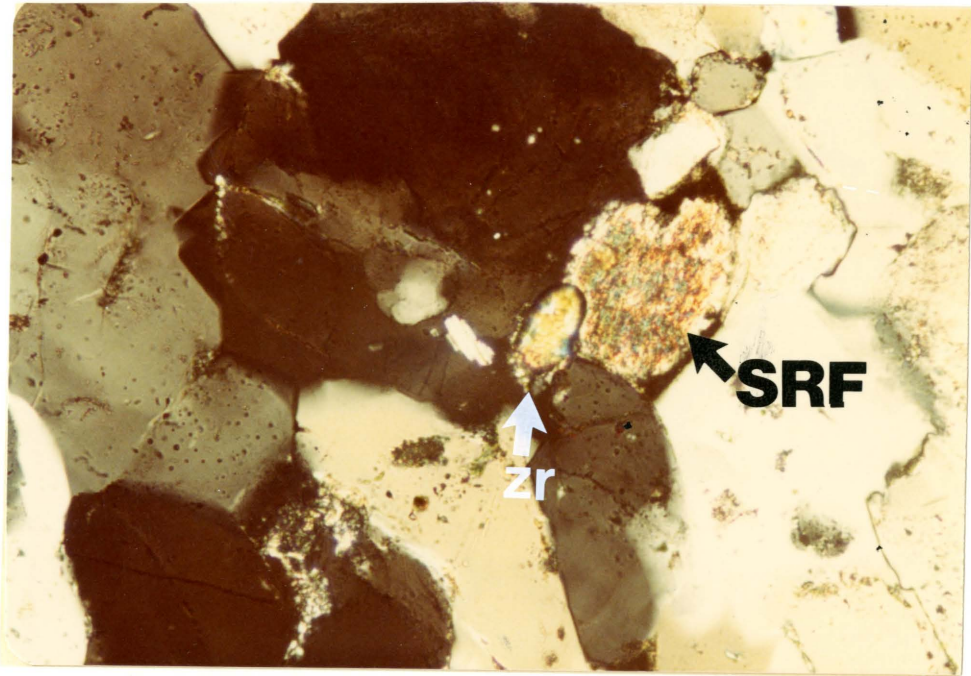


Plate 3-3a: Polycrystalline quartz grain, with less than 3 crystals [center], detrital zircon, [arrow], and SRF, [arrow]. Note the homogeneous internal structure and embayments by the surrounding quartz grains into the SRF. Sample VIS 6, magnification 160x, XN.

Plate 3-3b: Nonundulose, monocrystalline quartz grain with rutile inclusions. Sample VIS 6, magnification 160x, XN.





grains are highly rounded. The greater degree of rounding probably reflects the poorer stability of the polycrystalline grains rather than distance of transport.

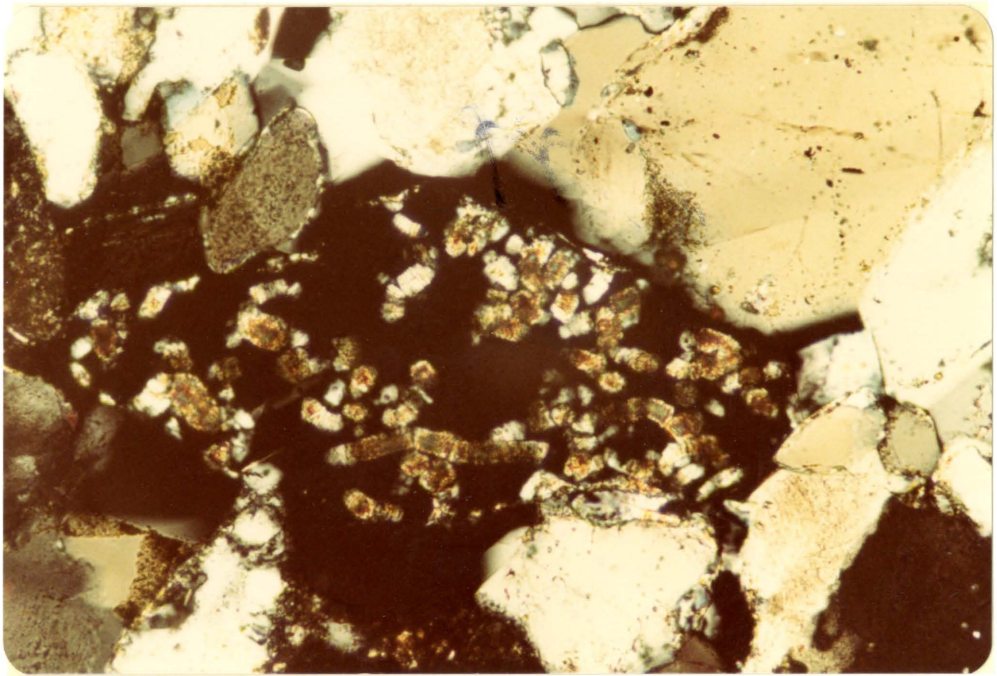
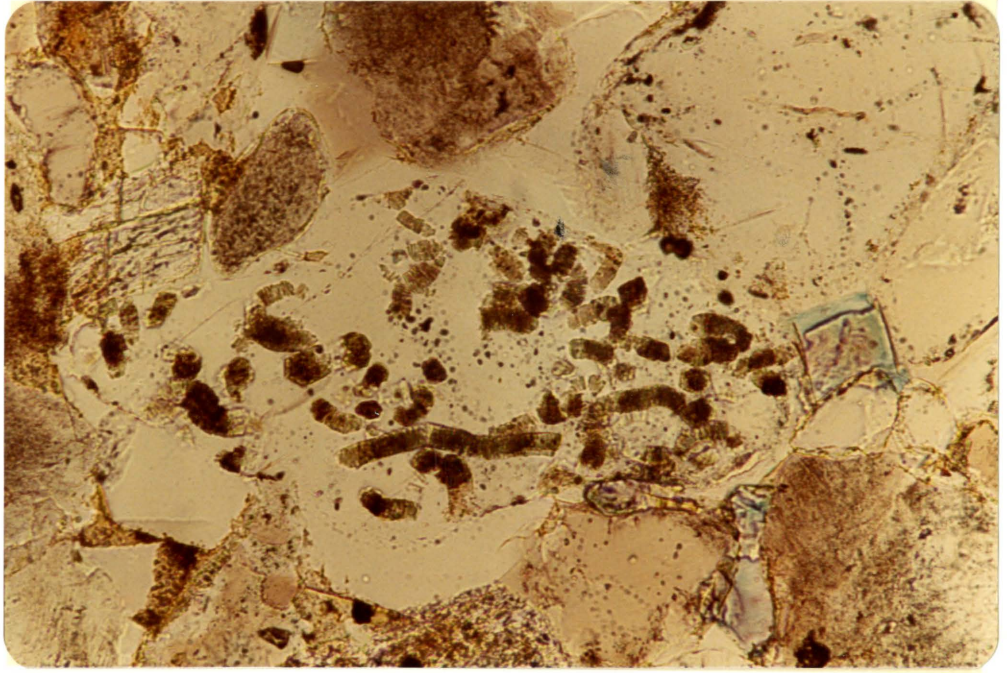
The overgrowths exhibit euhedral crystal shapes and are so well developed that virtually all primary porosity has been occluded [see plate 3-31]. At least two generations of quartz cement have been observed [see plates 3-1a, 5-1a,b and 5-2a]. The primary quartz cement observed occurs as small isolated euhedral crystals growing from the surface of the detrital grains. The younger generations of cement are massive, and it is this cement that occludes most of the porosity [see plate 5-1a].

Nonundulose monocrystalline quartz grains commonly show rutile and vermicular chlorite inclusions as well as liquid filled vacuoles [see plates 3-2b and 3-4a,b]. The vermicular chlorite inclusions and the abundance of liquid filled vacuoles in some of the quartz grains suggests that they are derived from a hydrothermal vein source [Blatt et al., 1980, p. 290; Scholle, 1979]. The rutile inclusions suggest a plutonic source for these grains [Blatt et al., 1980, p. 292]. The polycrystalline and highly strained quartz grains are typical of quartz found in metamorphic terrains.

#### Calcite and Dolomite Cements

Calcite is present as ferroan and nonferroan

Plates 3-4a,b: Vermicular chlorite inclusions in a nonundulose monocrystalline quartz grain. Note the booklet nature of the chlorite. Sample VIS 6, magnification 160X, top PPL, bottom XN.



authigenic poikilotopic cement. In general it is most abundant in the upper marine facies, i.e. Facies G spore, I spore, and J, and a general increase in calcite cement in all facies is observed to the northwest [refer to Tables 3-2a,b to 3-5a,b] [see plate 3-5a,b].

The ferroan calcite appears to have formed after the nonferroan calcite cement and both cements are post-dated by a second, or third generation of silica cement [see plates 3-5a,b and 3-7a,b].

In general the ferroan calcite is most abundant, but in one case, sample JOLL 3, nonferroan calcite comprises virtually all of the calcite cement and is so well developed that it has occluded all porosity [see plate 3-31b].

Both calcite cements are observed to replace microcline and in a few cases actual monocrystalline quartz grains [see plates 3-6a,b and 3-7a].

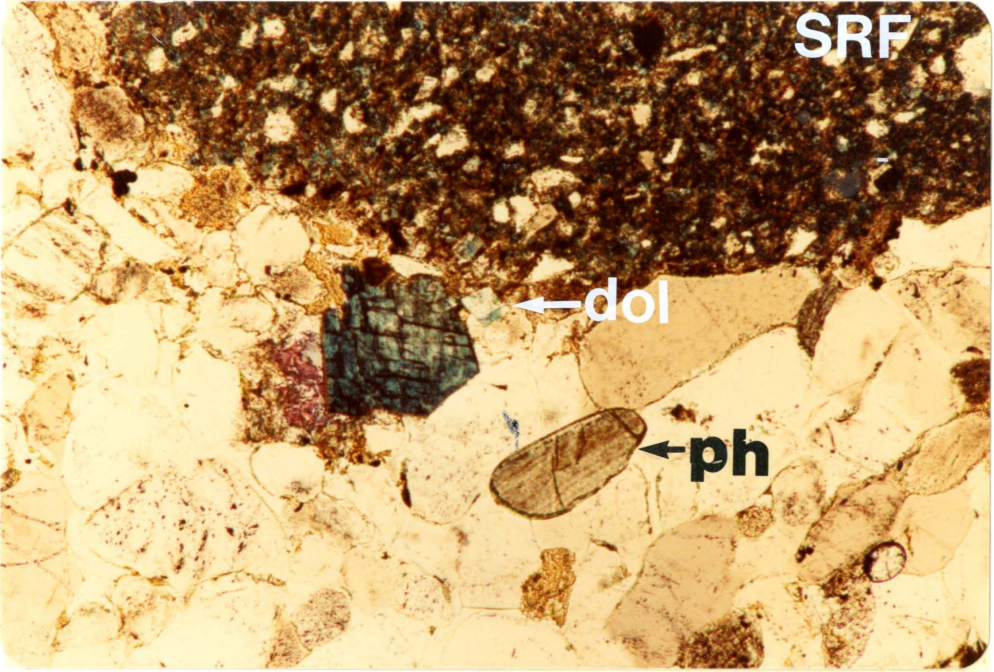
Dolomite rhombs are seen in isolation and replacing ferroan calcite cement [see plates 3-5a,b, 3-8, 3-23a,b and 3-24,b]. It is thought that the dolomite formation is late stage.

#### Chert, Phosphate and Rock Fragments

Well rounded chert grains are present in all samples, but decrease in abundance to the northwest [see Table 3-14]. Coarse crystalline chert is the most abundant, although several grains of cryptocrystalline chert have been observed

Plate 3-5a: Ferroan and nonferroan calcite [blue and red masses near center], dolomite rhomb [arrow], phosphatized fossil fragment showing faint internal lamination [arrow], and a very large SRF [top]. Sample VIS 6, 63X magnification, PPL.

Plate 3-5b: Ferroan calcite growing into nonferroan calcite. Sample VIS 2, 160X magnification, PPL.



Plates 3-6a,b: Ferroan calcite replacing microcline.  
Sample ART BASE, 160X magnification,  
top PPL, bottom XN.



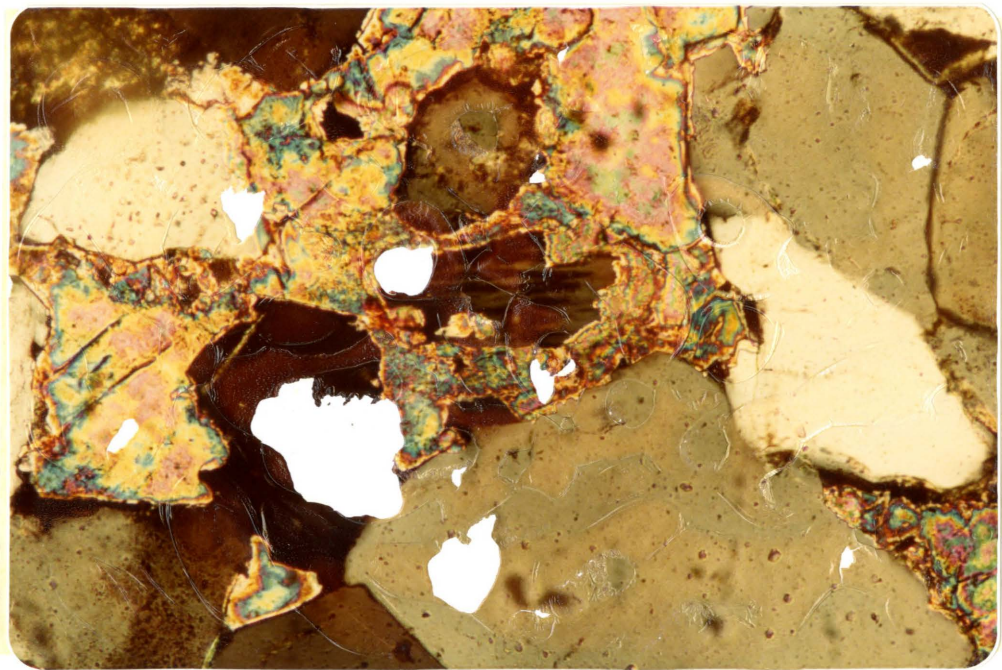
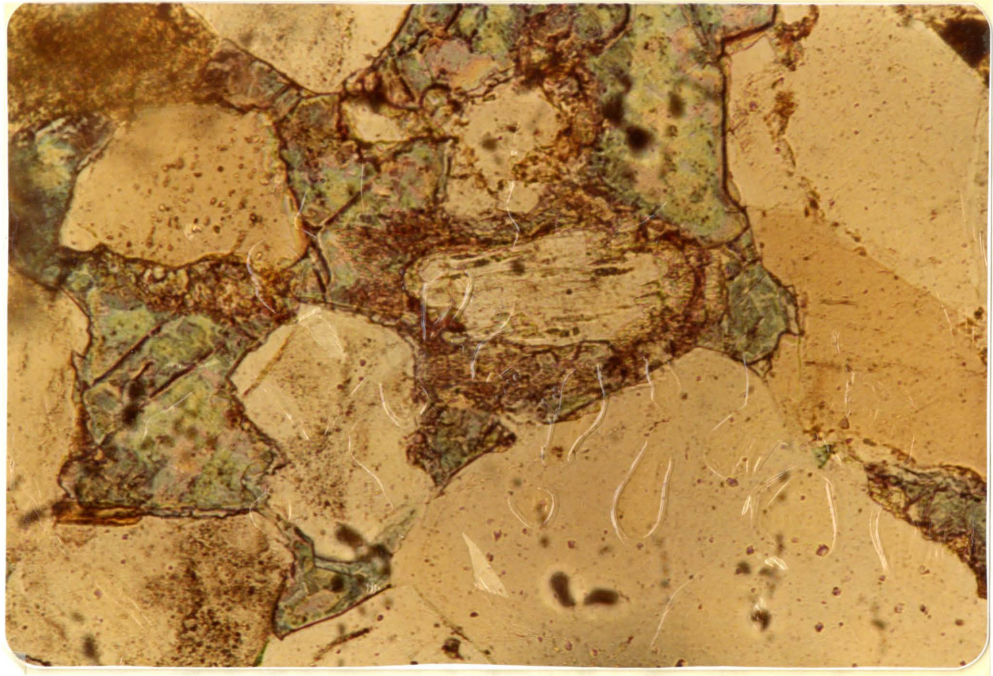


Plate 3-7a: Ferroan calcite replacing a nonundulose monocrystalline detrital quartz grain. Note that the calcite is surrounded by a quartz overgrowth. Sample JOLL 1, 250X magnification, XN.

Plate 3-7b: Nonferroan calcite replacing a detrital quartz grain. Sample JOLL 3, 63X magnification, XN.

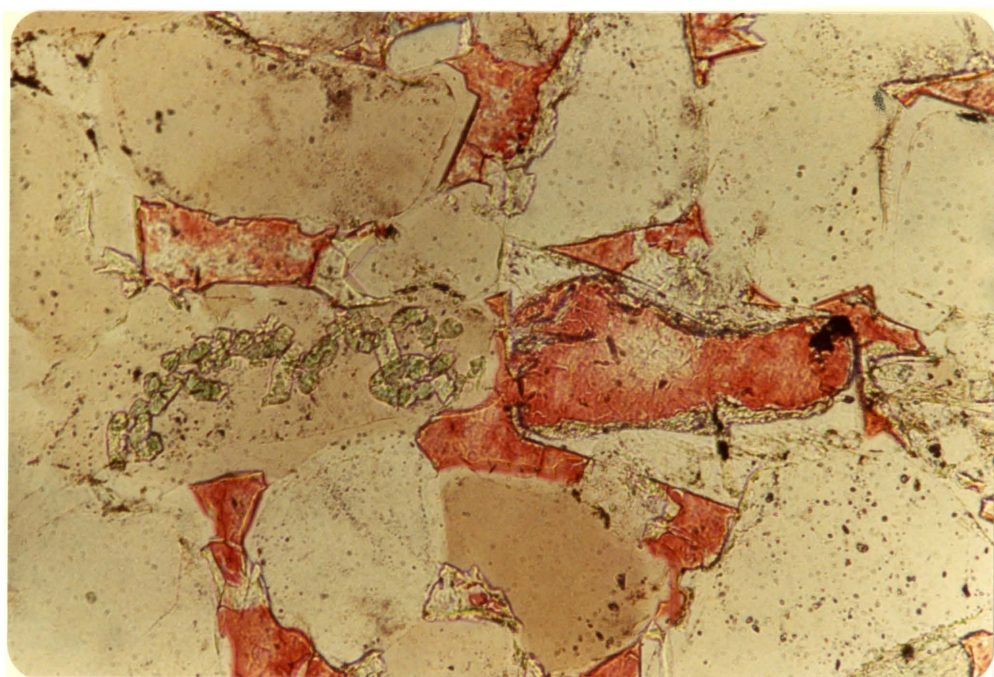
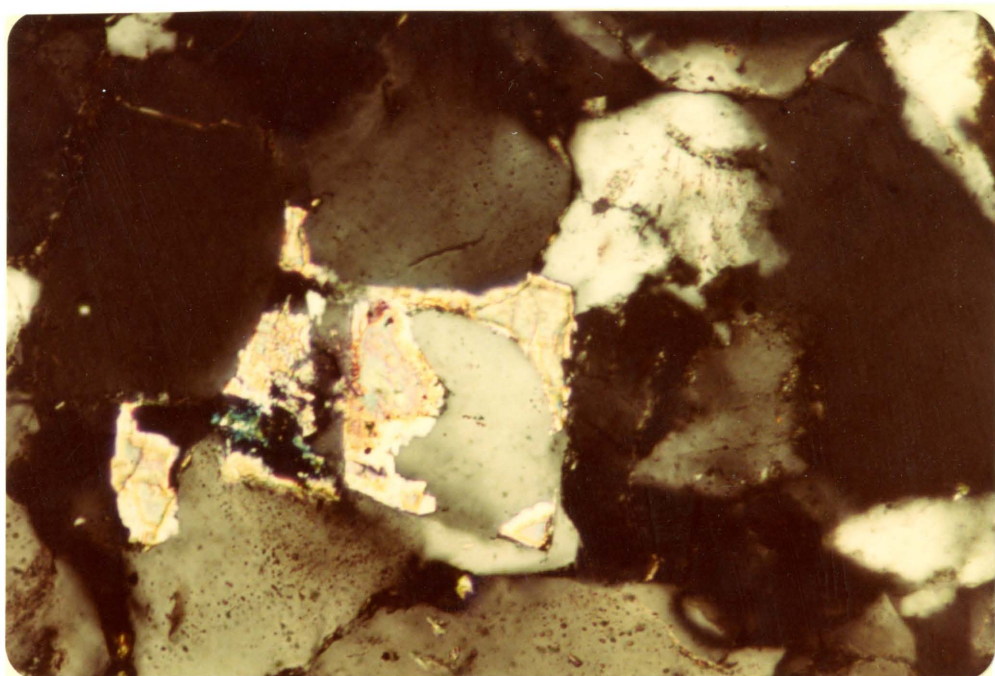
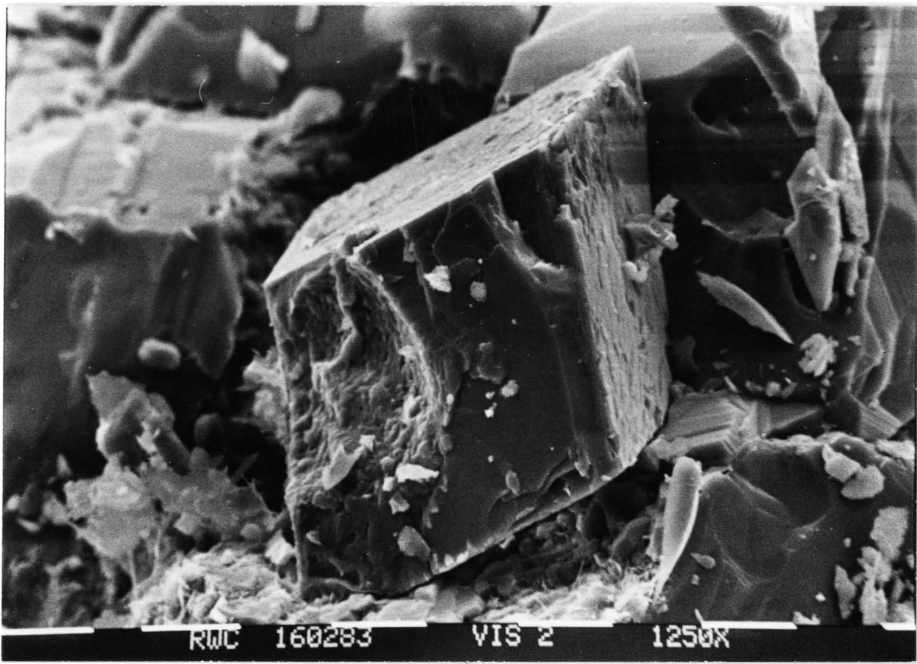


Plate 3-8: Isolated dolomite rhomb. Scale bar divisions  
equal 10 microns. VIS 2



[see plate 3-9a]. A chert grain in sample ART 2, showed a peculiar zoning around what appeared to be a clay fragment that was partially replaced by an opaque mineral [see plate 3-9b].

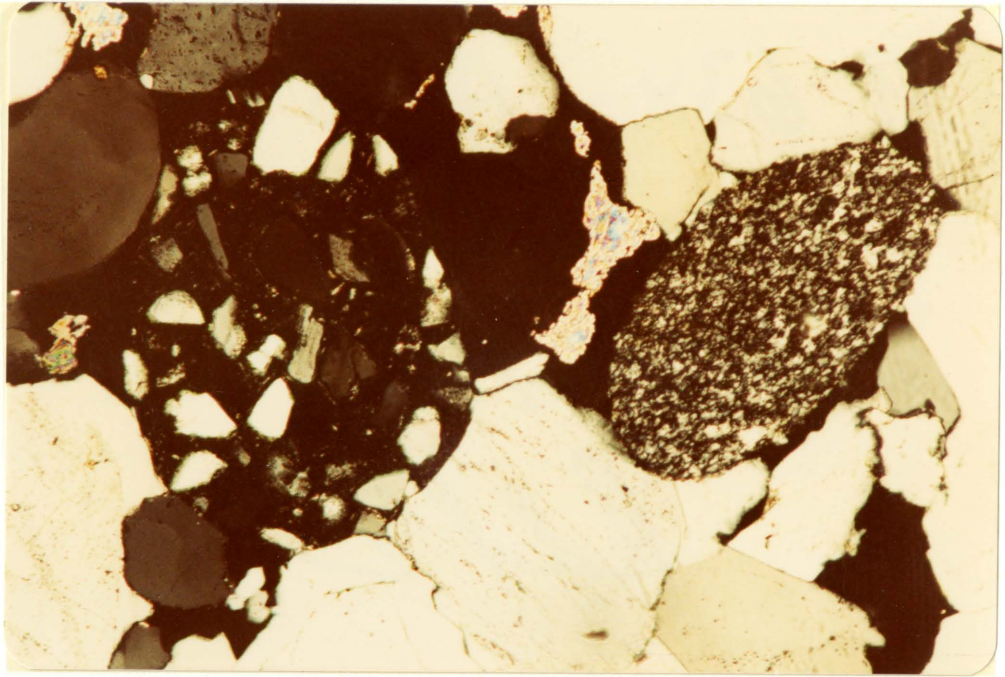
Phosphate is present as phosphatized fossil fragments [see plate 3-10a,b]. It is found in all samples, but decreases in abundance to the northwest [see Table 3-14].

Plate 3-10 is a photograph of a phosphatized echinoderm fragment from sample VIS 2, near the top of Facies G at the Haul Road Cut outcrop. Phosphatization is not complete as a calcitic core still remains. This fossil fragment was the only identifiable fragment seen: most phosphate grains had little discernable internal structure [see plate 3-5a].

Well rounded high and low grade metamorphic rock fragments are present in all samples, but in general decrease in abundance to the northwest [see Table 3-12]. It is very easy to recognize high grade fragments [see plate 3-11], but it is very difficult to tell the difference between low grade MRF's and sedimentary rock fragments, especially clay fragments. Identification was based on two criteria: 1] low grade MRF's show preferred orientation of crystals [see plate 3-1a], while SRF's have a homogeneous internal structure [see plate 3-3a]. 2] Many SRF's are very soft and are deformed or embayed by adjacent harder

Plate 3-9a: Crypocrystalline and coarse crystalline  
chert grains. Sample ART 8, 63X magnification  
XN.

Plate 3-9b: Zoned chert grain. Note clay fragment core  
partially replaced by an opaque mineral.  
Sample ART 2, 160X magnification, XN.





Plates 3-10a,b: Phosphatized echinoderm fragment.  
Note the calcitic core. Sample VIS  
2, 63x magnification, top PPL, bottom  
XN.

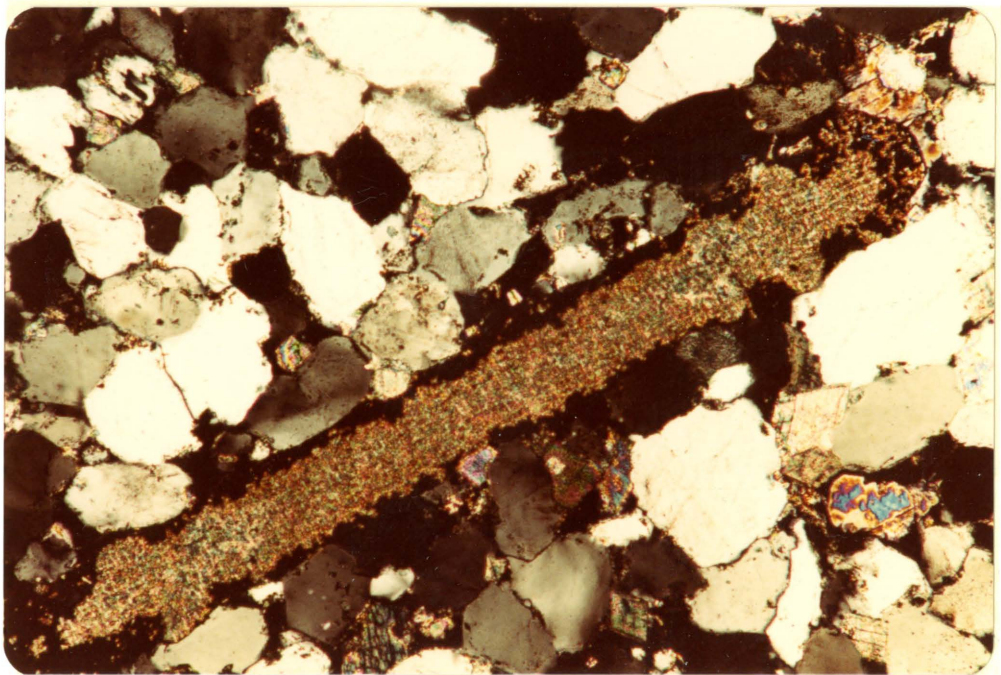
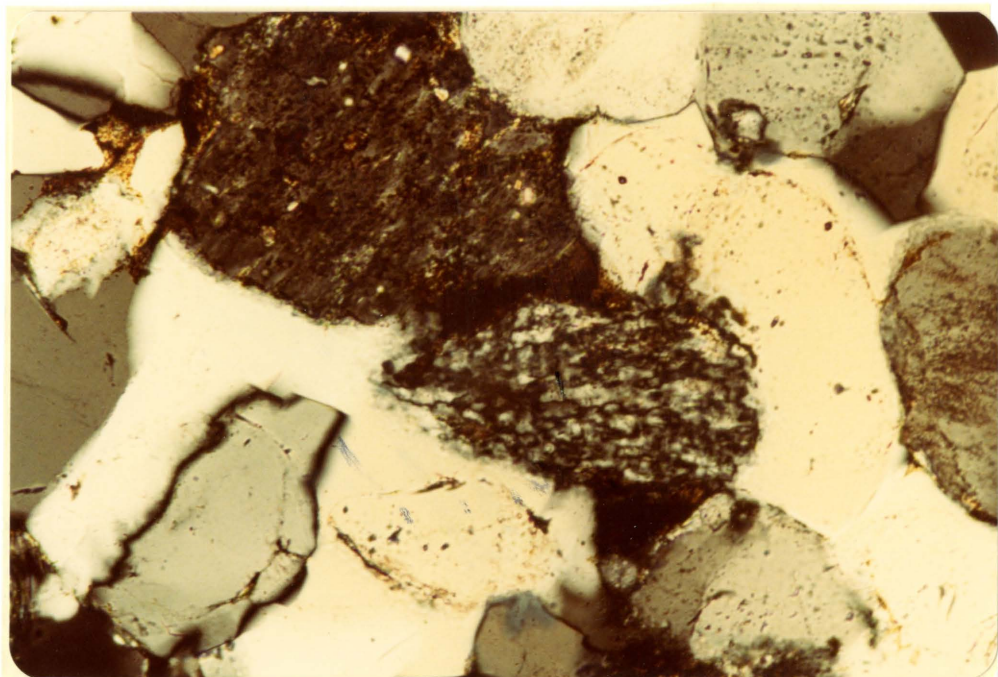


plate 3-11: High grade MRF, schist fragment [center].  
Sample VIS 2, 63X magnification, XN.



grains [see plate 3-3a], whereas MRF's are not [Scholle, 1979].

Deformed and embayed SRF's are found in all samples. No trends in distribution are observed.

#### Feldspar

The most abundant feldspar is microcline, displaying polysynthetic twinning [see plate 3-12a]. In a few cases microcline was observed to be surrounded by quartz cement, but in general the feldspar grains display dissolution features leading to the development of secondary porosity [see plates 3-6a,b, 3-27a, 3-28a,b and 5-3a,b].

Trace amounts of plagioclase displaying albite twinning were also found. These grains were badly deformed and can be hard to recognize.

Feldspar was present in all samples and no general distribution trends were observed.

#### Heavy and Opaque Minerals

The most common heavy mineral observed was zircon. Tourmaline was also observed. Euhedral zircons were present as inclusions in monocrystalline quartz grains [see plate 3-13a] while rounded zircons and badly deformed tourmaline grains appeared as detrital constituents [see plates 3-3a and 3-13 a,b].

Hematite, present as rims around detrital grains and minor cement is found in a few samples [see plate 3-14].

Plate 3-12a: Detrital microcline displaying combined albite and pericline twinning, low grade MRF, note the orientation of crystals. Sample VIS 4, 400X magnification, XN.

Plate 3-12b: Detrital microcline showing combined albite and pericline twinning, and a quartz overgrowth. Sample JOLL 1, 250X magnification, XN.

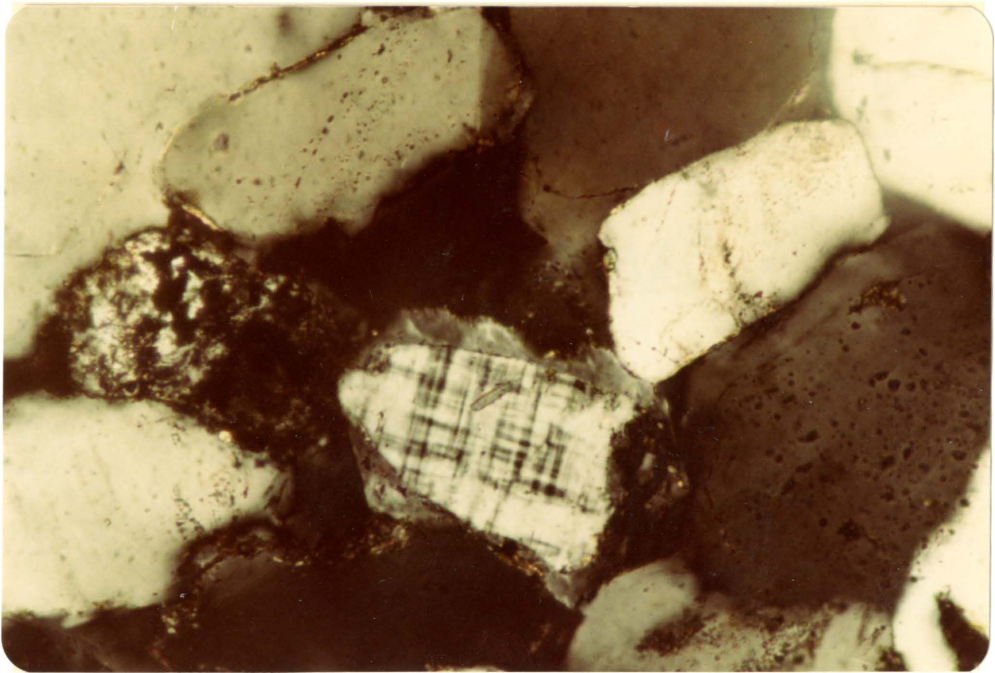
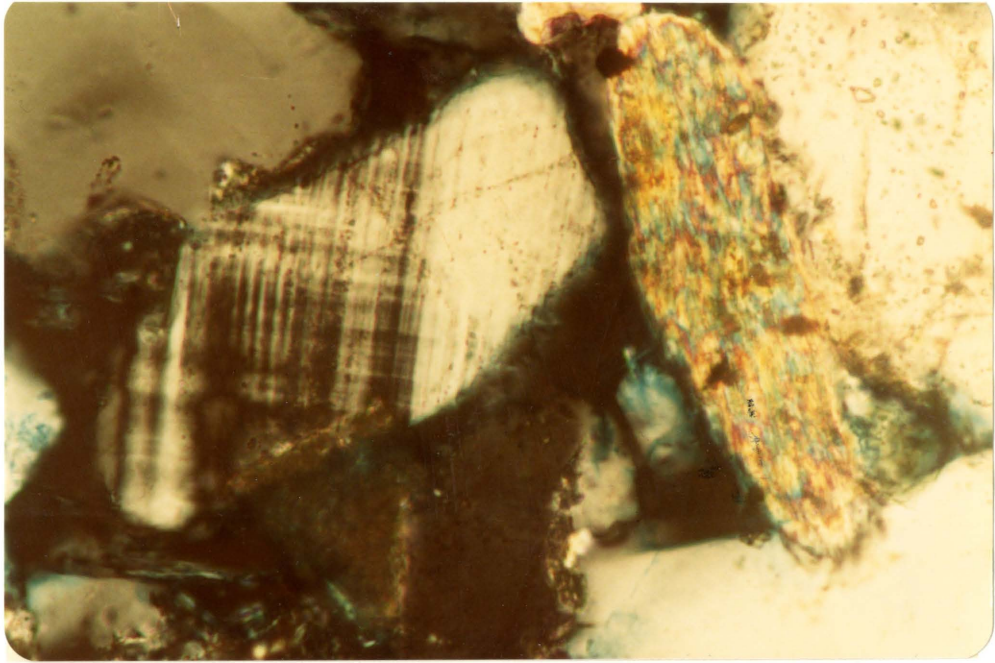


Plate 3-13a: Euhedral zircon grain as an inclusion in  
detrital quartz grain. Sample ART 2,  
250X magnification, XN.

Plate 3-13b: Detrital tourmaline grain. Sample  
VIS 3, 160 magnification, XN.



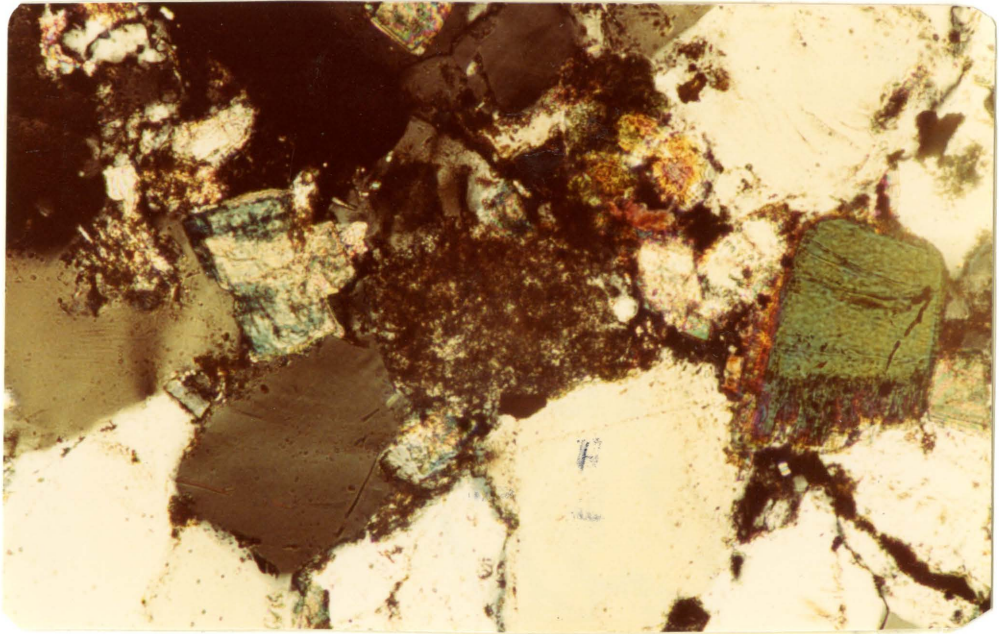
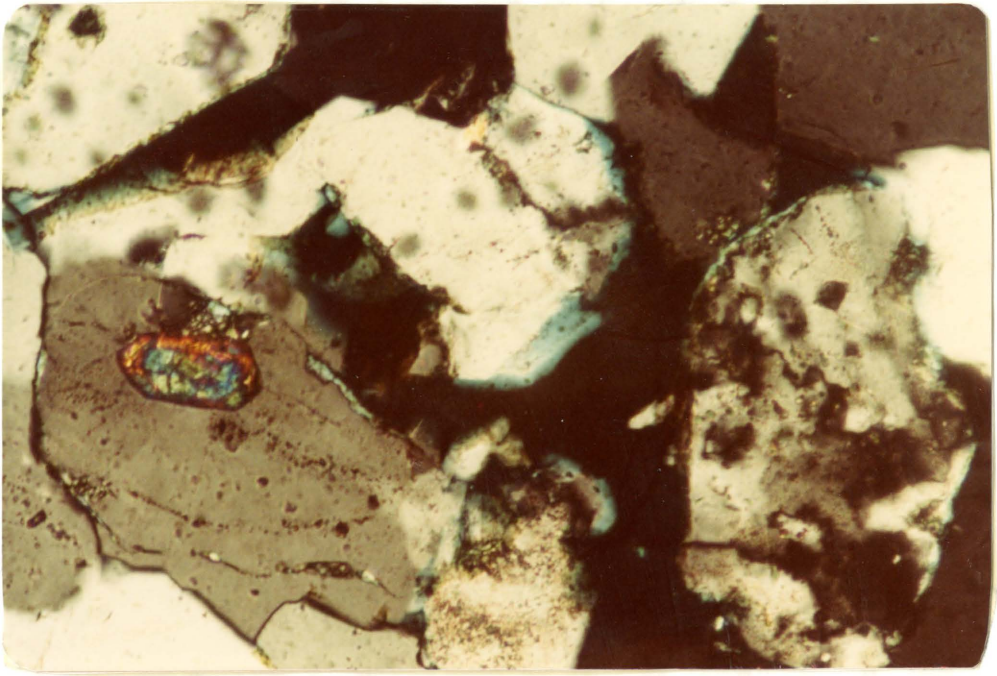
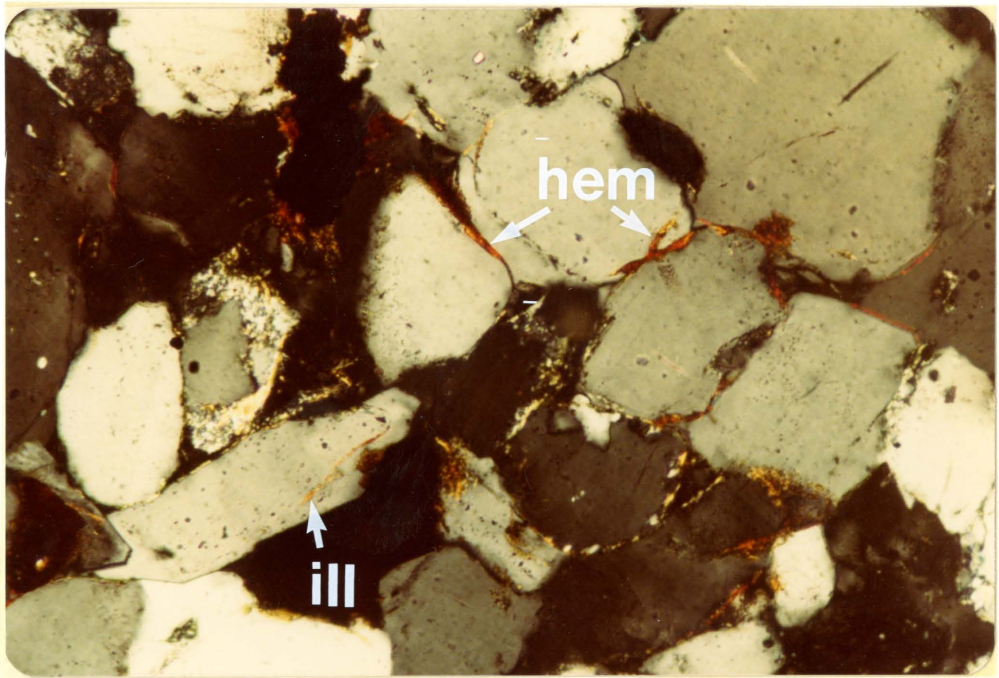


Plate 3-14: Hematite [arrow], and highly birefringent illite rims [arrow], around detrital quartz grains. Sample JOLL 1, 160X magnification, XN.



The hematite rims on the detrital quartz grains are not continuous since overgrowth formation has not been impeded [Scholle, 1979]. Seyler [1981] believes that the hematite might be detrital and authigenic in nature, but no clear cut evidence exists, suggesting detrital origin has been observed. It is possible that the hematite rims around the detrital quartz grains might represent detrital hematite, but it is more likely that they represent primary diagenetic formation, or secondary infilling of void space.

The opaque minerals found are pyrite, magnetite and leucoxene. The pyrite occurs as subhedral to euhedral crystals and is often associated with ferroan calcite. This may suggest that the pyrite has been precipitated at a late stage in response to the basic environment associated with the areas of calcite [see plate 3-15a]. Framboidal pyrite was observed under the SEM [see plate 3-15b]. Framboidal pyrite is typically present as micron size aggregates of euhedral pyrite crystals that form as authigenic replacements [Scholle, 1970].

Magnetite was observed replacing calcite cement in sample JOLL 1 [see plate 3-16].

Leucoxene was found only in trace amounts as an alteration product associated with hematite and pyrite. Seyler [1981] reports the presence of detrital leucoxene

plate 3-15a: Pyrite precipitated in ferroan calcite zone. Sample VIS 3, 63X magnification, XN.

plate 3-15b: Framboidal pyrite. Scale bar divisions equal 10 microns. VIS 1

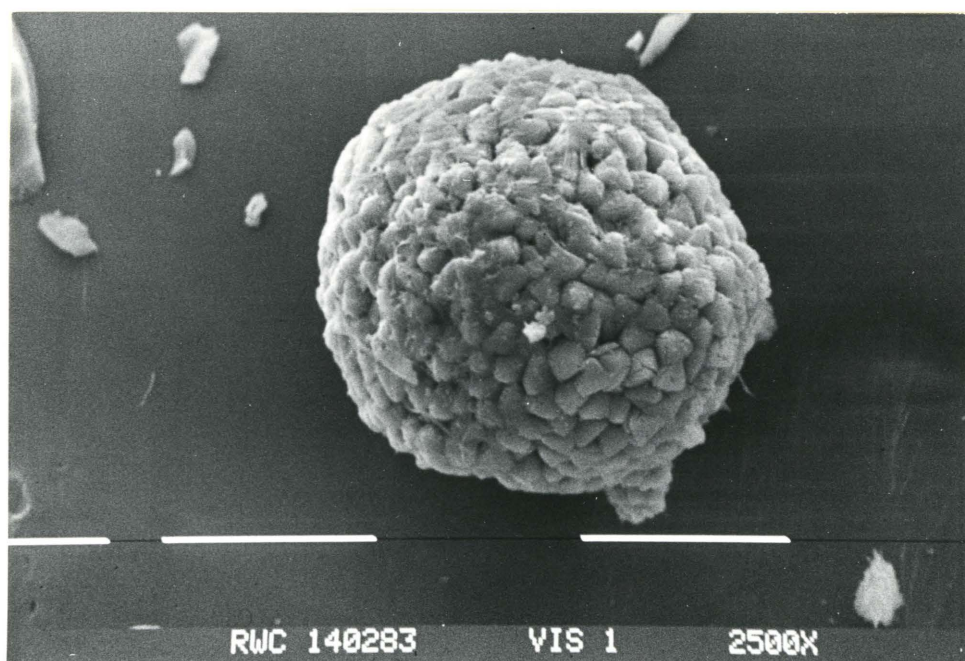
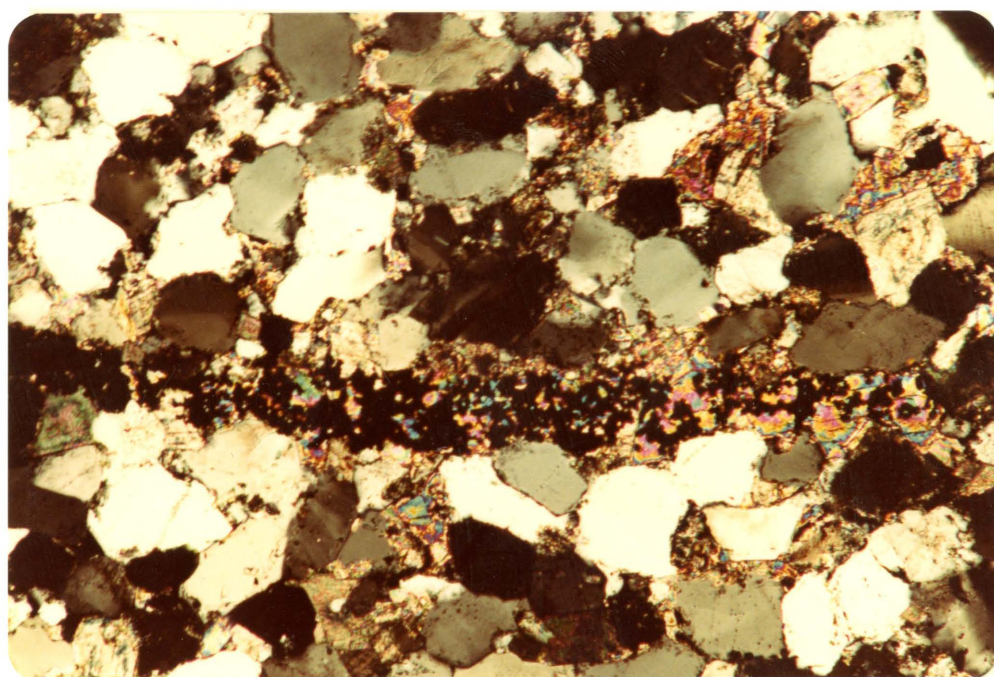


Plate 3-16: Magnetite replacing calcite cement.

Sample Joll 1, 250X magnification, XN.

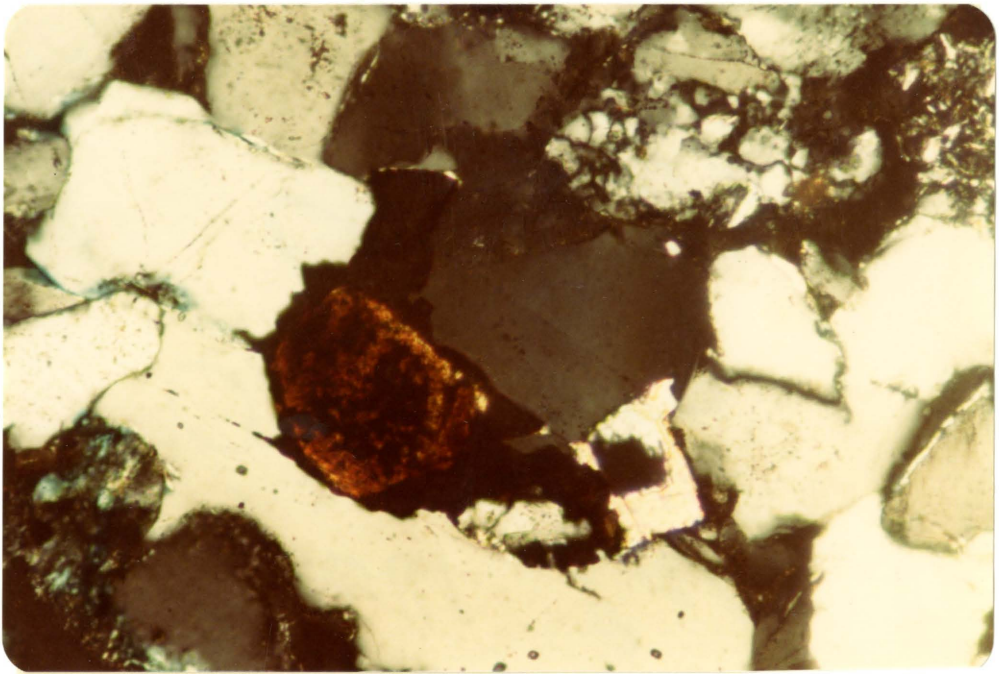
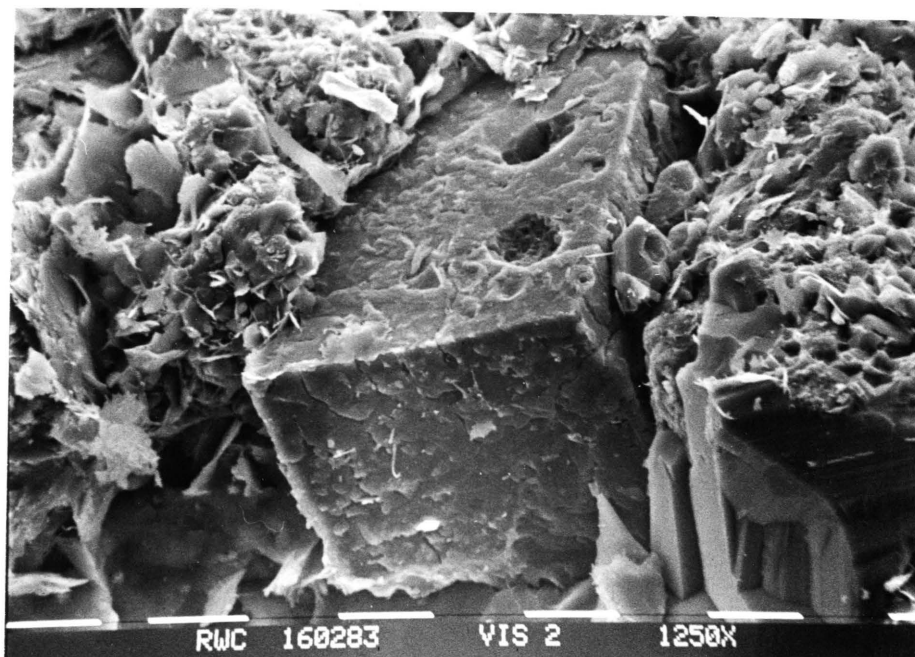
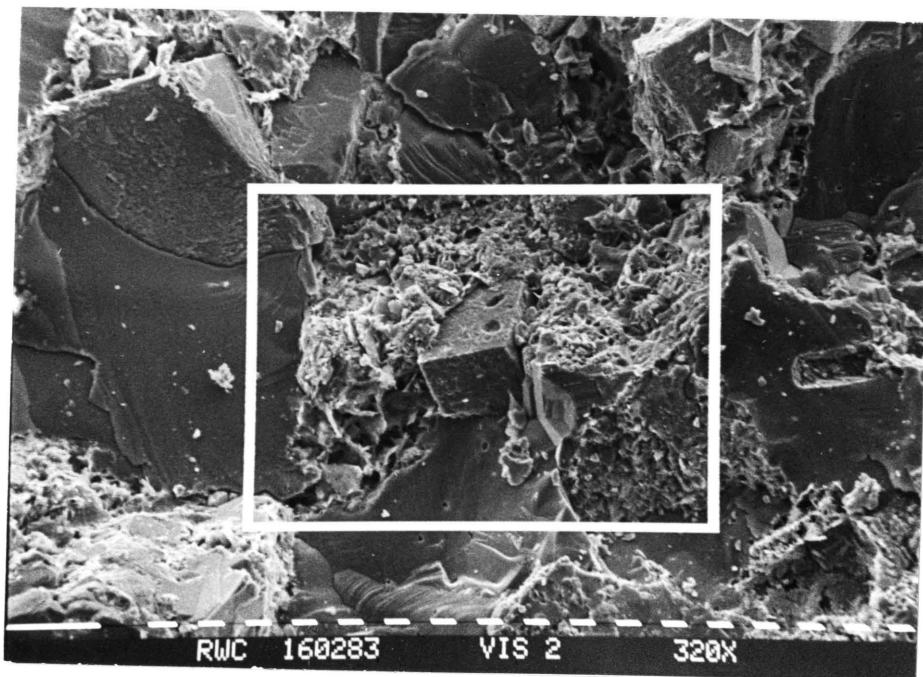




Plate 3-17a,b: Unidentified mineral found using the  
the SEM; possibly pyrite. Sample VIS  
2, scale bar divisions equal 10 microns.



and concludes that the grains are most likely alteration products of rutile, ilmenite and sphene from an igneous and metamorphic source terrain.

#### Muscovite

Muscovite grains were found in two samples, SYD 1 and ART 3 [see plate 3-18a,b]. They were badly deformed and squeezed between quartz grains.

#### Clays

Illite clay was observed to be present as highly birefringent rims around detrital quartz grains [see plate 3-14]. These rims must not be continuous because, if they were the overgrowths could not nucleate [Scholle, 1979]. The clays also appear to be associated with hematite in a few instances.

#### Cathodoluminescent Microscopy:

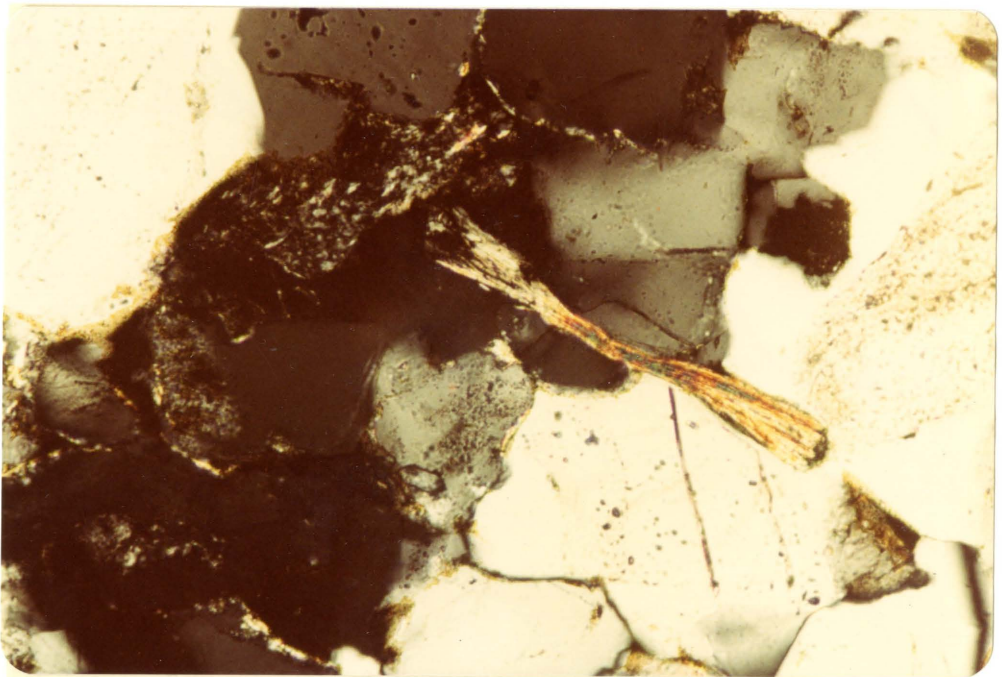
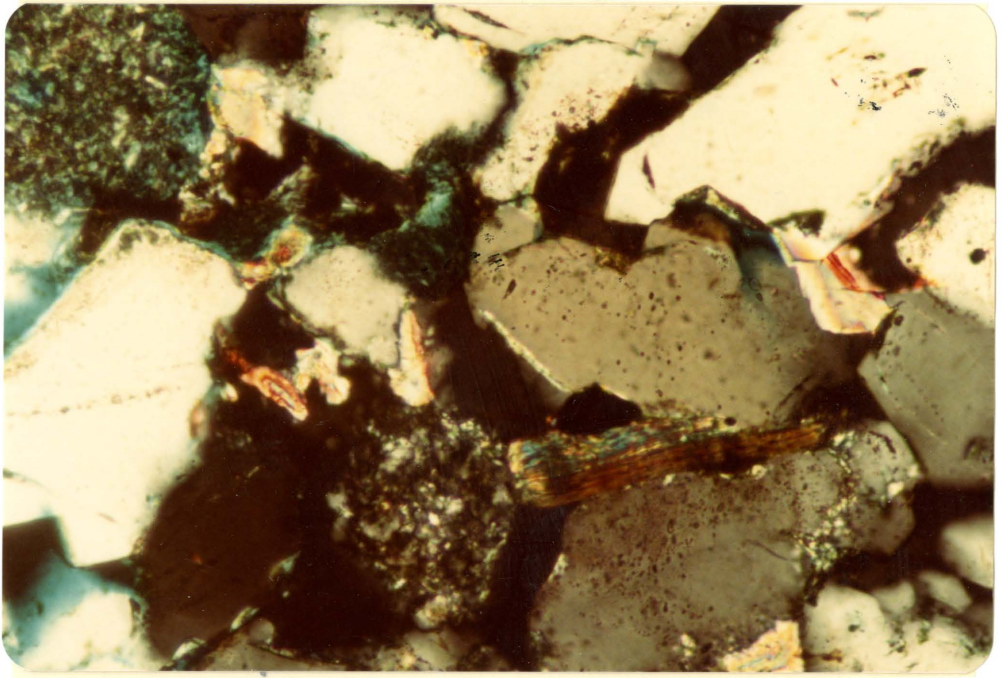
##### Introduction:

Cathodoluminescent is visible light emitted by a crystalline substance when it is bombarded with electrons.

The process of luminescence, of which CL is a form, involves: the excitation of molecular electrons to quantum mechanically allowed energy states by a transfer of energy between the molecular electrons and accelerated electrons; storage of the excitation energy by electrons in excited energy states having finite life times; de-excitation to the groundstate by the emission of radiation having

Plate 3-18a: Detrital muscovite grain. Sample  
SYD 1, 250X magnification, XN.

Plate 3-18b: Detrital muscovite grain squeezed between  
quartz grains. Sample ART 3, 250X  
magnification, XN.



wavelengths characteristics of the substance.

In a luminoscope, an electron beam is generated by applying a potential across a cold cathode in a partially evacuated tube. Electrons emitted from the cathode ionize any remaining gases in the tube and the positive ions produced are accelerated towards the cathode, producing more electrons upon impact. This eventually leads to a stable discharge, which is then focussed by magnets onto the sample [Kopp, 1981].

The intensities and colour of CL from crystalline substances is dependant on several complexly related and interacting factors [ibid.]. Some of the factors are intrinsic, such as the nature of the host rock and the kinds and amounts of activators and quenchers, present as impurities in the crystal lattice. Other factors are extrinsic, like the degree of penetration of the electron beam, which is related to the polish on the surface of the sample, the voltage across the cathode, etc. [ibid.].

Activators are substances, like unusual ionized atoms, e.g.  $Mn^{2+}$ , present in the crystal lattice, that are easily excited and emit radiation having wavelengths in the visible region. Quenchers are substances, like iron, that when excited emit radiation outside of the visible region, thereby quenching the luminescence. Thus, the concentration of the quenchers and activators in a mineral will define the colour

and the intensity at which the mineral luminesces. It is this characteristic that allows the use of CL in sedimentological research.

Table 3-6 consists of various minerals and their reported CL colours [after Nickel, 1978].

Tables 3-7a,b to 3-10a,b indicate point count results obtained from the analysis of the twenty thin sections by Cathodoluminescent Microscopy at 63X magnification.

### Quartz

At least three different general CL colours have been observed from the detrital quartz grains, blue, brown and red [see plate 3-20a,b]. These colour differences are due to varying amounts of activating and quenching substances, i.e.  $Mn^{2+}$  or  $Fe^{2+}$ , etc, in the quartz that were fixed at the time of crystallization. Thus, the Whirlpool Sandstone comprises quartz grains from at least three different sources. If plate 3-20a,b is studied, it can be observed that there exists many different shades of the general colours, i.e. blue-purple, light brown, dark brown, etc. These different shades may reflect different source beds or more likely they represent slight differences in the concentration of impurities on a local scale. It is not reasonable to assume that quartz grains derived from the extremities of a large pluton will have the identical concentrations and types of impurities as quartz

TABLE 3-6

## VARIOUS MINERALS AND THEIR CL COLOURS

Mineral	Luminescence Colour
<u>Quartz-synthetic</u>	red
Verrucano Sst. North Italy	red violet to light brown
detrital	dull blue, or dull red
secondary overgrowth	red, blue, or no colour
<u>Microcline</u>	
perthite, Finland	light blue
perthite, Plawen Kristallin, N. Italy	light blue to light brown
<u>Albite</u>	
vein in K rich microcline host	dark blue
pegmatite, Rutherford Mine, Va. USA	yellowish green
<u>Calcite</u>	
Low-Mg	bright orange
High-Mg	dull red
natural	brightly orange-red
<u>Dolomite</u>	
natural, N. Italy	dark red core, light red rim
Fe-dolomite	dark red-brown
	bright red

after Nickel, 1978



TABLE 3-7a

POINT COUNT RESULTS: CATHODOLUMINESCENT MICROSCOPY

LOCATION	SAMPLE NUMBER	QUARTZ ONE	QUARTZ TWO	QUARTZ THREE	TOTAL QUARTZ	QUARTZ CEMENT	FELDSPAR	PHOSPHATE
	VIS 1	53.4	22.7	-	77.3	20.4	t	1.1
	VIS 7	55.5	14.8	t	70.3	23.3	2.8	0.7
HAUL ROAD CUT	VIS 6	47.0	21.7	t	68.7	26.9	2.2	0.7
	VIS 4	45.4	12.1	t	57.5	17.2	1.0	2.0
	VIS 2	51.5	15.5	t	67.0	20.6	1.0	1.0
	VIS 3	49.1	15.3	-	64.4	14.3	2.0	1.0

n= 300 point counts per slide, corrected for grain loss during thinsection preparation

t= mineral present, but not counted

-= mineral not present in slide

N.I.E.= slide not impregnated with blue epoxy, unable to determine true porosity

TABLE 3-7b

SAMPLE NUMBER	CARBONATE CEMENT	DOLOMITE CEMENT	OPAQUES AND HEAVIES	CHERT AND ROCK FRAGS.	VERMICULAR CHLORITE	POROSITY	TOTAL %
VIS 1	2.3	t	t	t	t	N.I.E.	99.9
VIS 7	2.8	t	t	t	t	N.I.E.	100.0
VIS 6	1.5	t	t	t	t	N.I.E.	100.0
VIS 4	19.2	3.0	t	t	t	N.I.E.	99.9
VIS 2	8.2	2.1	t	t	t	N.I.E.	99.9
VIS 3	12.2	5.1	1.0	t	t	N.I.E.	100.0

TABLE 3-8a

## POINT COUNT RESULTS: CATHODOLUMINESCENT MICROSCOPY

LOCATION	SAMPLE NUMBER	QUARTZ ONE	QUARTZ TWO	QUARTZ THREE	TOTAL QUARTZ	QUARTZ CEMENT	FELDSPAR	PHOSPHATE
	ART 1 BASE	45.0	24.0	0.3	69.3	20.0	0.3	0.3
	ART 2	46.0	21.0	t	67.0	22.0	0.3	0.7
ART PARK	ART 5	50.0	21.0	t	71.0	25.0	0.7	1.3
	ART 7	52.4	24.7	-	77.1	21.6	t	1.3
	ART 8	49.5	25.8	-	75.3	21.6	t	1.8
	ART 12	54.4	16.0	t	70.4	25.6	2.9	0.3

n= 300 point counts per slide, corrected for grain loss during thinsection preparation

t= mineral present, but not counted

-- mineral not present in slide

N.I.E.= slide not impregnated with blue epoxy, unable to determine true porosity

TABLE 3-8b

SAMPLE	CARBONATE CEMENT	DOLOMITE CEMENT	OPAQUES AND HEAVIES	CHERT AND ROCK FRAGS.	VERMICULAR CHLORITE	POROSITY	TOTAL %
ART BASE	3.3	t	t	1.3	t	5.7	100.2
ART 2	3.3	t	0.3	0.3	t	6.5	100.4
ART 5	t	t	t	t	t	N.I.E.	99.7
ART 7	0.3	t	t	t	t	N.I.E.	100.3
ART 8	1.0	t	t	0.3	t	N.I.E.	100.0
ART 12	t	t	t	0.3	-	N.I.E.	99.5

TABLE 3-9a

POINT COUNT RESULTS: CATHODOLUMINESCENT MICROSCOPY

LOCATION	SAMPLE NUMBER	QUARTZ ONE	QUARTZ TWO	QUARTZ THREE	TOTAL QUARTZ	QUARTZ CEMENT	FELDSPAR	PHOSPHATE
	JOLL 6	51.3	18.7	0.3	70.3	15.3	2.3	0.7
	JOLL 5	42.7	23.3	t	66.0	18.3	0.3	1.0
JOLLEY CUT	JOLL 4	57.7	14.0	t	71.7	13.3	3.7	t
	JOLL 3	58.0	10.3	t	68.3	8.3	0.7	0.7
	JOLL 1	46.0	16.0	t	62.0	17.0	3.0	0.7

n= 300 point counts per slide, corrected for grain loss during thinsection preparation

t= mineral present, but not counted

-= mineral not present in slide

N.I.E.= slide not impregnated with blue epoxy, unable to determine true porosity

TABLE 3-9b

SAMPLE NUMBER	CARBONATE CEMENT	DOLOMITE CEMENT	OPAQUES AND HEAVIES	CHERT AND ROCK FRAGS.	VERMICULAR CHLORITE	POROSITY	TOTAL %
JOLL 6	0.7	0.7	t	t	t	10.0	100.0
JOLL 5	t	t	t	t	t	14.0	99.6
JOLL 4	t	-	t	t	t	11.3	100.0
JOLL 3	22.3	-	t	t	t	t	100.3
JOLL 1	16.0	t	t	t	t	1.3	100.0

TABLE 3-10a

POINT COUNT RESULTS: CATHODOLUMINESCENT MICROSCOPY

LOCATION	SAMPLE NUMBER	QUARTZ ONE	QUARTZ TWO	QUARTZ THREE	TOTAL QUARTZ	QUARTZ CEMENT	FELDSPAR	PHOSPHATE
SYDENHAM ROAD	SYD 1	48.0	13.0	t	61.0	13.0	4.3	0.7
CUT	SYD 4	52.0	14.0	t	66.0	15.0	4.3	0.3
WHIRLPOOL NIAGARA RIVER	WHIRL 1	52.0	15.0	0.3	67.3	20.0	2.0	0.7

n= 300 point counts per slide, corrected for grain loss during thinsection preparation

t= mineral present, but not counted

-= mineral present in slide

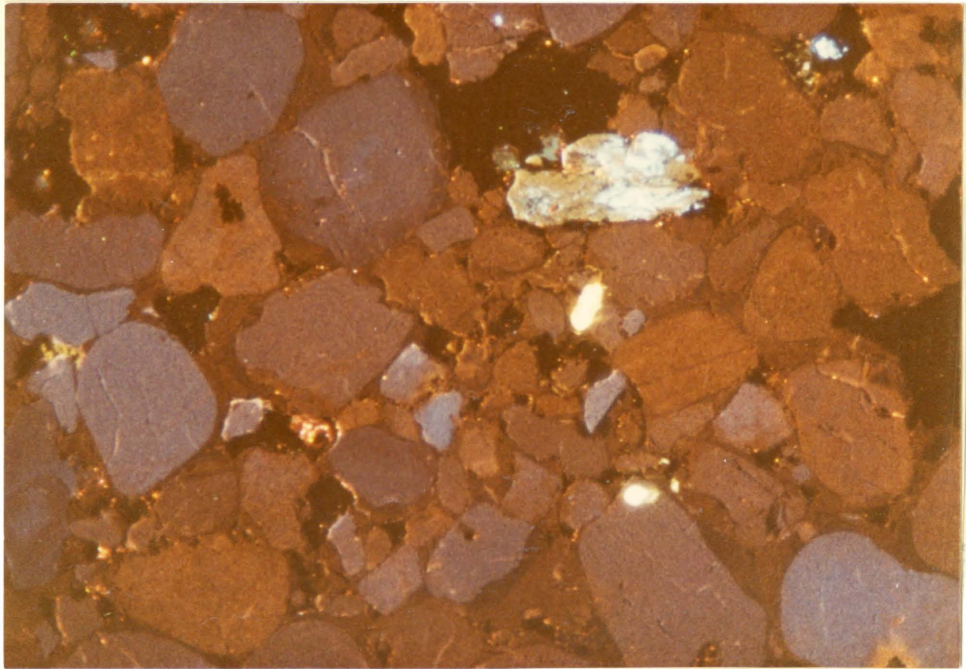
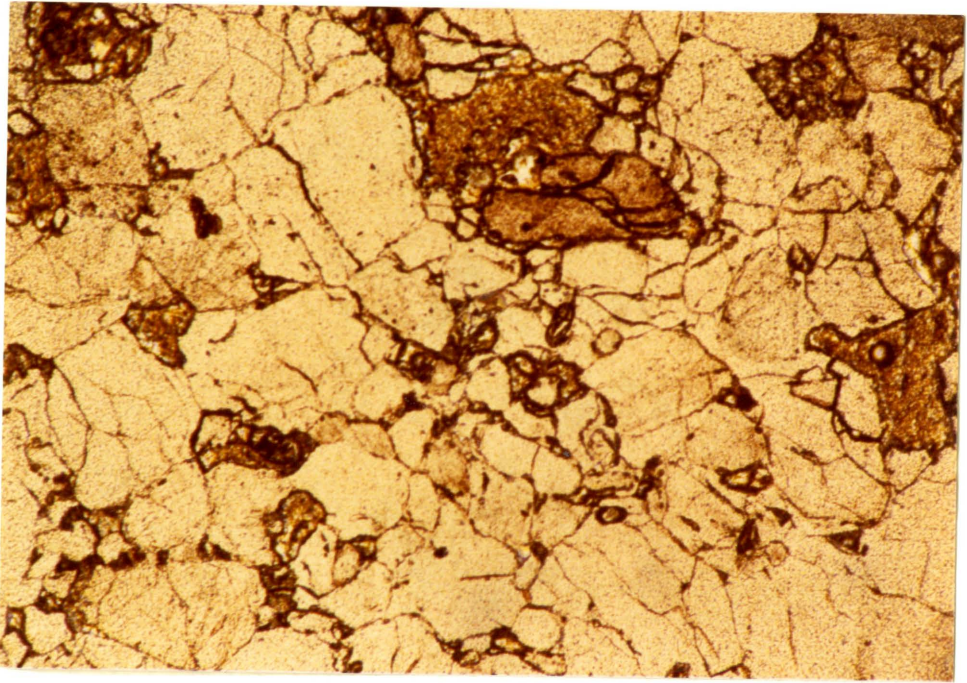
N.I.E.= slide not impregnated with blue epoxy, unable to determine true porosity

TABLE 3-10b

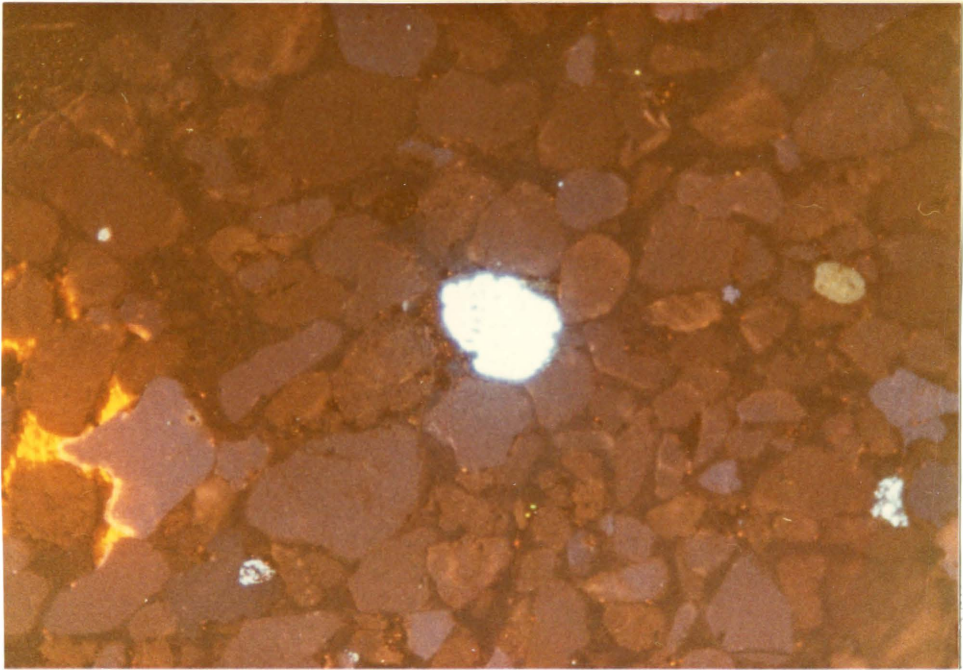
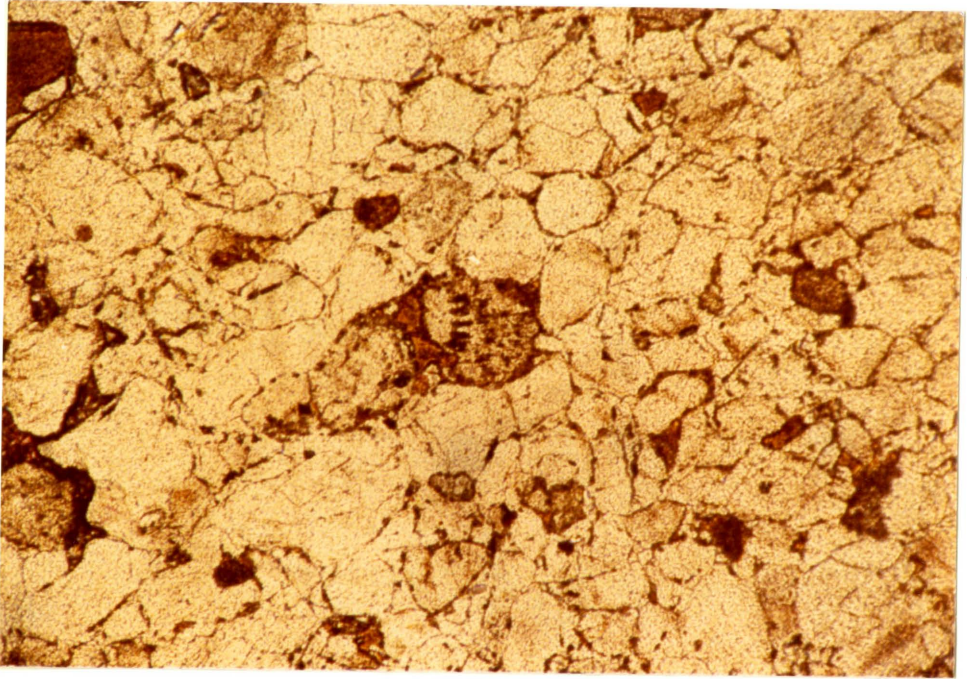
SAMPLE	CARBONATE CEMENT	DOLOMITE CEMENT	OPAQUES AND HEAVIES	CHERT AND ROCK FRAGS.	VERMICULAR CHLORITE	POROSITY	TOTAL %
SYD 1	8.0	t	1.0	0.3	-	12.0	100.3
SYD 4	2.0	t	t	t	t	12.0	99.6
WHIRL 1	3.0	t	t	1.0	t	6.3	100.3



Plate 3-19a,b: CL photograph showing blue and brown detrital quartz grains, suggesting multiple source terrains. Note that the blue quartz consists of the large well rounded monocrystalline grains, while the brown quartz consists of the smaller more angular grains. Note the badly deformed feldspar in the upper area of the photograph and the zircon grains showing bright white colour. Sample VIS 1, 63X magnification, top PPL, bottom CL.



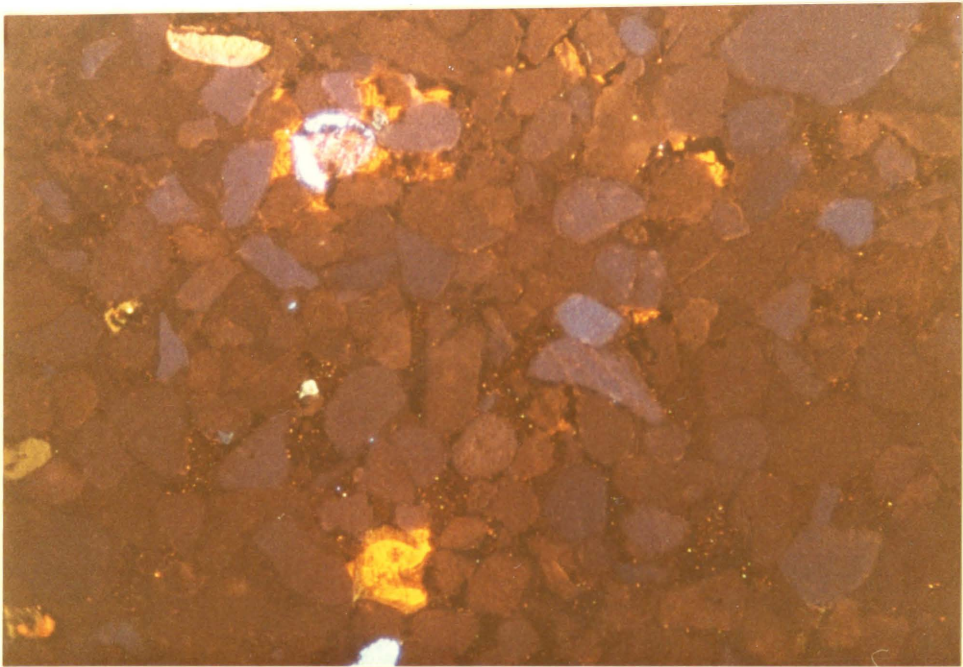
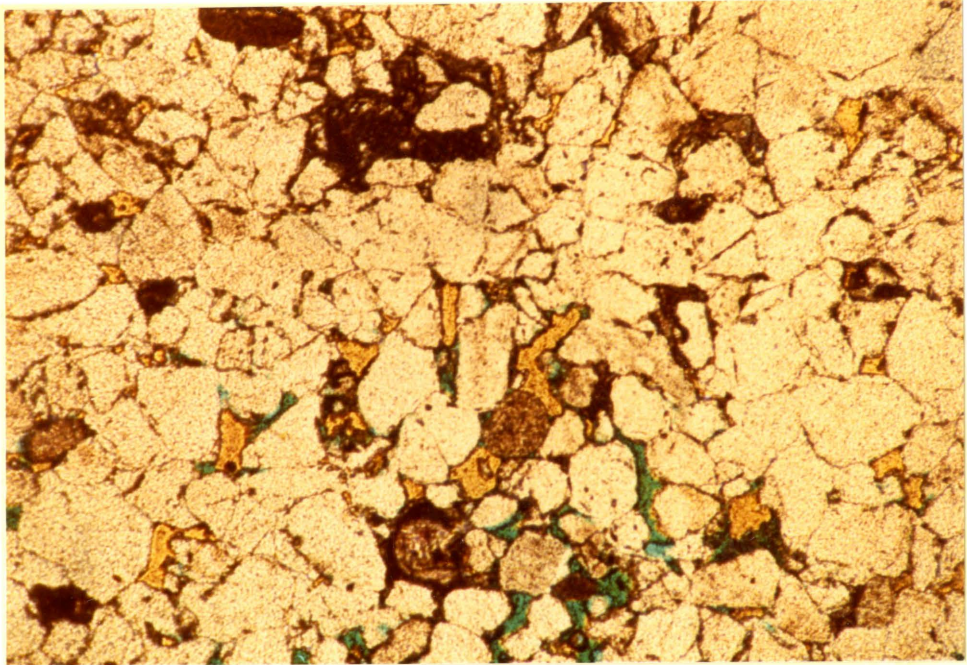
plates 3-20a,b: CL photograph showing bluish-white  
feldspar grain and nonferroan calcite  
[left hand side]. Sample VIS 6, 63X  
magnification, top PPL, bottom CL.



grains derived from the center of a pluton. What we would expect is a general similarity between the grains, and thus should see the same general CL colours. This effect might be more pronounced in metamorphic grains as local variability would be increased depending on the immediate environment, i.e. quartz grains recrystallizing in areas containing large amounts of free iron, due to the dissolution of magnetite, will display different CL colours than grains out of the iron rich area.

The "brown" quartz is the most abundant, comprising roughly 70% of the detrital quartz, while the "red" quartz is found only in trace amounts. Probably the "brown" quartz represents in general, quartz grains derived from metamorphic terrains, while the "blue" quartz is plutonic in origin. This hypothesis is consistent with the provenance plot, prepared after Basu et al, [1975] [see figure 3-2], which suggests that the source beds of the sediments from which the Whirlpool Sand was derived, were medium to high grade metamorphics with some plutonic character. This is substantiated by studying plates 3-19a,b to 3-21a,b. It can be observed that the "blue" quartz in general comprises the larger better rounded detrital grains, reflecting the greater stability of the plutonic grains. The "brown" quartz contains polycrystalline and highly strained grains and in general is composed of smaller, more angular grains.

Plates 3-21a,b: CL photograph showing feldspar  
being replaced by ferroan calcite  
cement. Sample ART BASE, 63X  
magnification, top PPL, bottom CL.



The size and shape of these grains reflects the poor stability of metamorphic derived quartz.

There appears to be no lateral or vertical distribution trends in the abundance of quartz types in the study area.

#### Quartz Cement

Quartz cement comprises roughly 20% of the samples and its CL colours are light brown to no colour. The less intense CL colour reflects the inability of the quartz lattice to accommodate impurities at low diagenetic temperatures.

The quartz overgrowths are observed to increase the size of most grains by roughly 5%. Generally, the amount of quartz cement appears to decrease to the northwest [see Tables 3-7a,b to 3-10a,b]. This could reflect different diagenetic temperatures in the two areas, i.e. the sediment in the Hamilton area would not have been buried as deeply as the sediment in the Niagara area, and would thus have had a lower maximum diagenetic temperature. Since quartz cementation occurs most likely at the maximum depth of burial [Dr. G.V. Middleton, personal communication] this trend could very well be linked to lateral movement away from the center of the depositional basin [see chapter 5].

#### Feldspar

Feldspars were observed to have bright blue CL colours, but have been reproduced on film as bluish-white



[see plates 3-19a,b to 3-21a,b]. All the feldspar grains observed appeared to be badly corroded, suggesting dissolution and the creation of secondary porosity. In several cases the feldspar was observed to be replaced by calcite cement, while under plain light the grain was not recognizable [see plate 3-21a,b].

The CL technique proved very useful for identifying feldspar as staining was not successful, and twinning and general appearance were not always reliable. No general distribution trends were observed.

#### Calcite and Dolomite Cements

Ferroan and nonferroan calcite cements were observed to have similar CL colours, orange-red. The ferroan calcite cement had more of a yellow shade, that proved difficult to recognize [see plates 3-21a,b to 3-23a,b].

Dolomite appears as brick red, pseudo rhombs under CL and displays well developed zonation [see plates 3-22a,b and 3-23a,b]. This feature has been reported by Amieux, from sediments in France [1982].

The zoned dolomite in plate 3-23a,b is typical of the dolomites found by Amieux. He described the zonation as arising from rapid changes in the composition of the dolomitizing fluids, i.e. first generation dolomite Fe poor fluids creates a zone that has bright red CL colour, followed by a rapid increase in the concentration of Fe in the

Plate 3-22a,b: CL photograph showing the zonation of dolomite around a ferroan calcite core. Note the pseudo rhomb and the phosphate grain to the right. Sample ART 2, 63X magnification, top PPL, bottom CL.

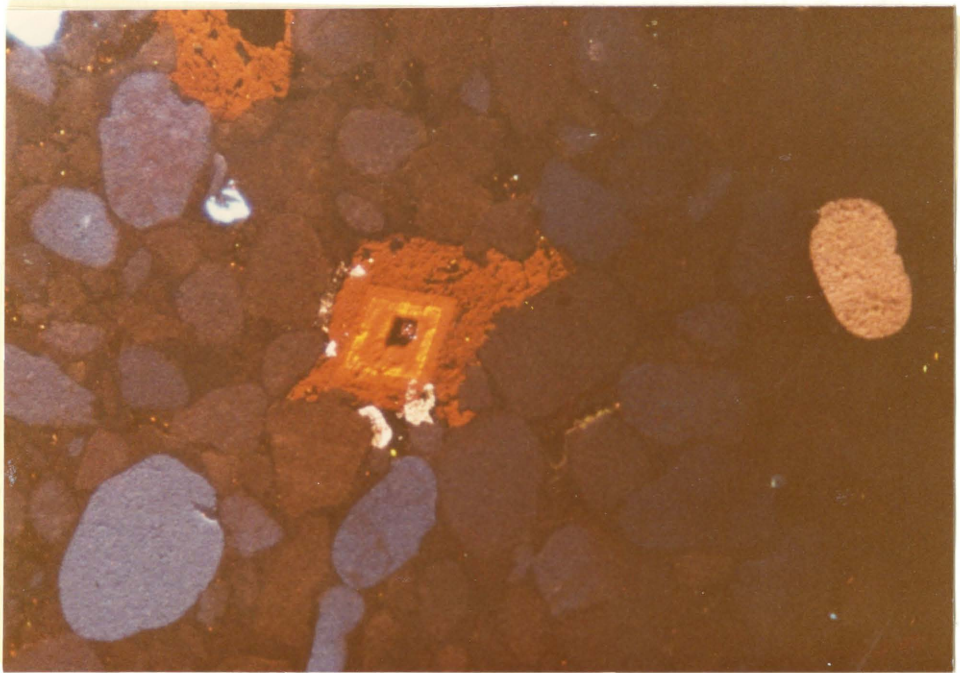
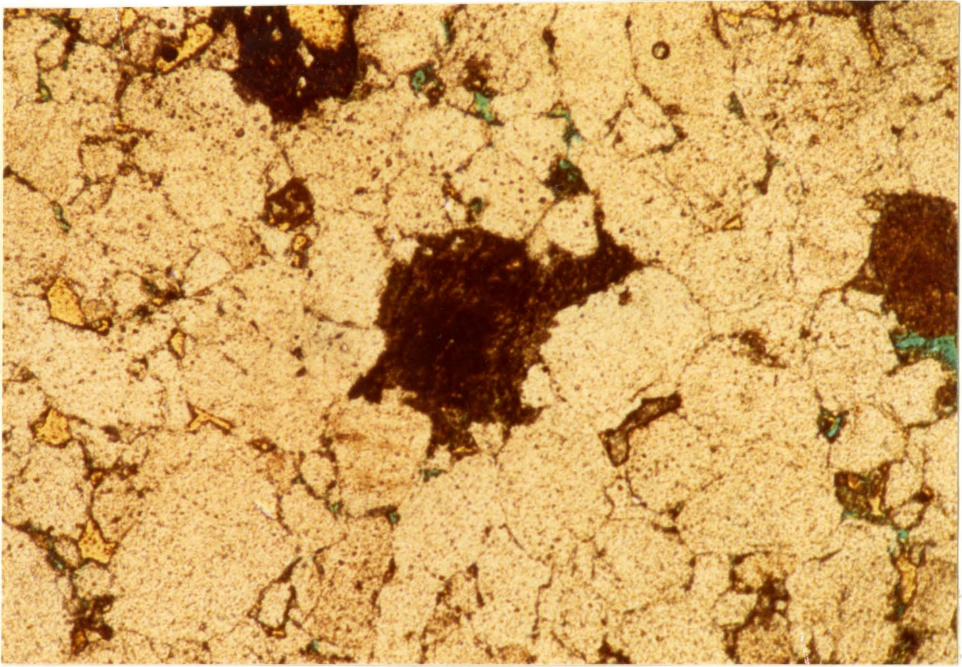
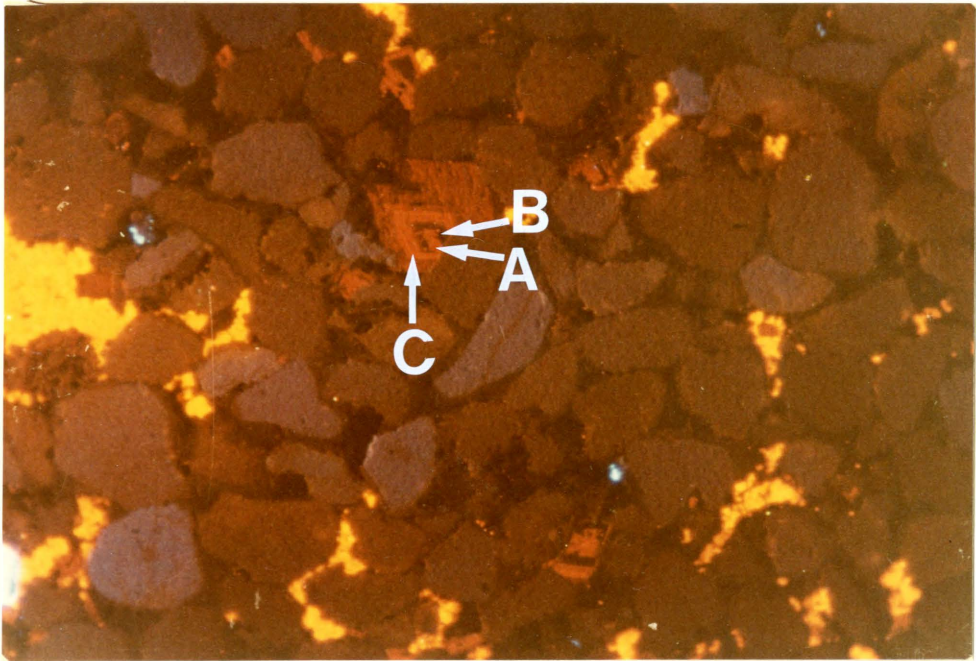


Plate 3-23a,b: CL photograph showing zonation of dolomite and ferroan and nonferroan calcite. Zones A and C represent dolomites rich in  $Mn^{2+}$ , zone B represents dolomite rich in Fe and zones D and E represent dolomites with smaller concentrations of  $Mn^{2+}$ . Sample VIS 2, 63X magnification, top PPL, bottom CL.



fluid which creates a zone of dolomite with no CL colour [Zone B] etc. It is not known how much change is needed in the fluids to bring about this behaviour [see chapter 5].

A second form of zonation is displayed in plate 3-21a,b. It consists of dolomite zoned around a core of ferroan calcite. This probably reflects the progressive dolomitization of the pre-existing calcite cement [see chapter 5].

The amount of calcite and dolomite cement appears to increase to the northwest [see Tables 3-7a,b to 3-10a,b]. This may reflect the lower maximum diagenetic temperatures obtained in the Hamilton area, i.e. during mesodiagenesis the sediment in the Hamilton area may not have been in the decarbonization "window" as long as the sediment in the Niagara area [see chapter 5].

#### Minor Constituents

Phosphatized fossil fragments were observed to have a mauve CL colour [see plate 3-22a,b]. Zircon grains were observed to have a very intense white CL colour [see plate 3-19a,b].

#### Grain Contact Study:

The porosity and permeability of a sandstone is greatly affected by the types of contacts between grains. Grain contacts, as they appear in the plane of a random thin section, have been classified by Taylor [1950] as

tangential, longitudinal, concavo-convex and sutured. Taylor goes on to suggest that tangential contacts are the result of original packing, longitudinal contacts are the result of original packing, pressure, or precipitated cement and concavo-convex and sutured contacts are generally the result of pressure. These contact types have been used in the literature as criterion for pressure solution [Sippel, 1968].

Eleven thin sections, six from the Haul Road outcrop and five from the Jolley Cut outcrop, were point counted using both transmitted light and CL, by a method after Fuchtbauer [1974]. All of the contacts per grain in a given field of view were counted and categorized after Taylor [1950] until one hundred grains had been counted. The formula:

$$\frac{1a + 2b + 3c + 4d}{a + b + c + d}$$

where: a= tangential contacts  
b= longitudinal contacts  
c= concavo-convex contacts  
and d= sutured contacts

then renders a measure of the contact strength.

Tables 3-11 and 3-12 results from the grain contact study.

If the tables are studied, it is observed that the

TABLE 3-11

GRAIN CONTACT STUDY: LIGHT MICROSCOPY

LOCATION	SAMPLE NUMBER	TANGENTIAL	CONCAVO -CONVEX	SUTURE	LONGITUDINAL	FLOAT	TOTAL %	CONTACT STRENGTH	AVERAGE CONTACTS per GRAIN
HAUL ROAD CUT	VIS 1	22.0	66.0	12.0	-	-	100.0	2.1	6.2
	VIS 7	43.0	46.0	11.0	-	-	100.0	2.2	4.8
	VIS 6	42.0	48.0	10.0	-	-	100.0	2.3	5.1
	VIS 4	50.0	38.0	12.0	-	-	100.0	2.1	5.1
	VIS 2	36.0	49.0	15.0	-	-	100.0	2.4	5.0
	VIS 3	40.0	46.0	14.0	-	-	100.0	2.3	6.2
								ave. 2.3	ave. 5.3
JOLLEY CUT	JOLL 6	55.0	42.0	3.0	-	-	100.0	1.9	4.5
	JOLL 5	65.0	32.0	3.0	-	-	100.0	1.7	4.4
	JOLL 4	59.0	37.0	4.0	-	-	100.0	1.9	4.4
	JOLL 3	48.0	39.0	13.0	-	-	100.0	2.2	4.3
	JOLL 1	48.0	43.0	9.0	-	-	100.0	2.1	5.2
							ave. 2.0	ave. 4.5	

n= 100 counts per grain

100



TABLE 3-12

GRAIN CONTACT STUDY: CATHODOLUMINESCENT MICROSCOPY

LOCATION	SAMPLE NUMBER	TANGENTIAL	CONCAVO -CONVEX	SUTURE	LONGITUDINAL	FLOAT	TOTAL %	CONTACT STRENGTH	AVERAGE CONTACTS PER GRAIN
HAUL ROAD CUT	VIS 1	85.0	14.0	1.0	-	-	100.0	1.3	4.5
	VIS 7	72.0	24.0	4.0	-	-	100.0	1.6	5.0
	VIS 6	61.0	32.0	7.0	-	-	100.0	1.8	3.5
	VIS 4	66.0	34.0	-	-	-	100.0	1.7	4.3
	VIS 2	82.0	17.0	1.0	-	-	100.0	1.4	3.2
	VIS 3	66.0	32.0	2.0	-	-	100.0	1.7	3.6
								ave. 1.6	ave. 4.0
JOLLEY CUT	JOLL 6	89.0	11.0	-	-	-	100.0	1.2	3.6
	JOLL 5	91.0	9.0	-	-	-	100.0	1.2	3.4
	JOLL 4	92.0	8.0	-	-	-	100.0	1.1	3.3
	JOLL 3	91.0	9.0	-	-	-	100.0	1.2	2.9
	JOLL 1	88.0	12.0	-	-	-	100.0	1.2	4.3
								ave. 1.2	ave. 3.5

101

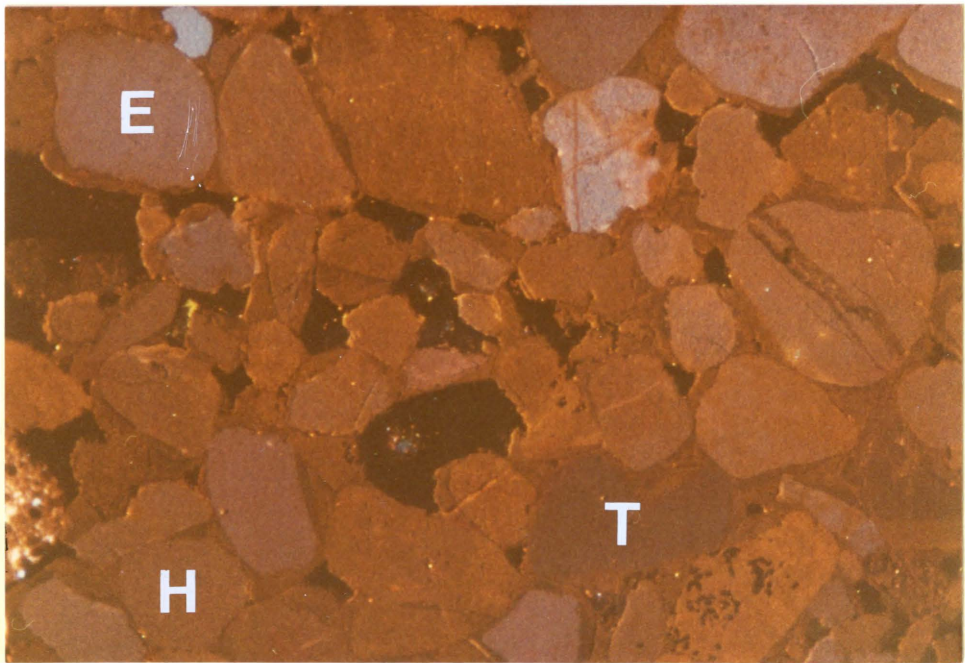
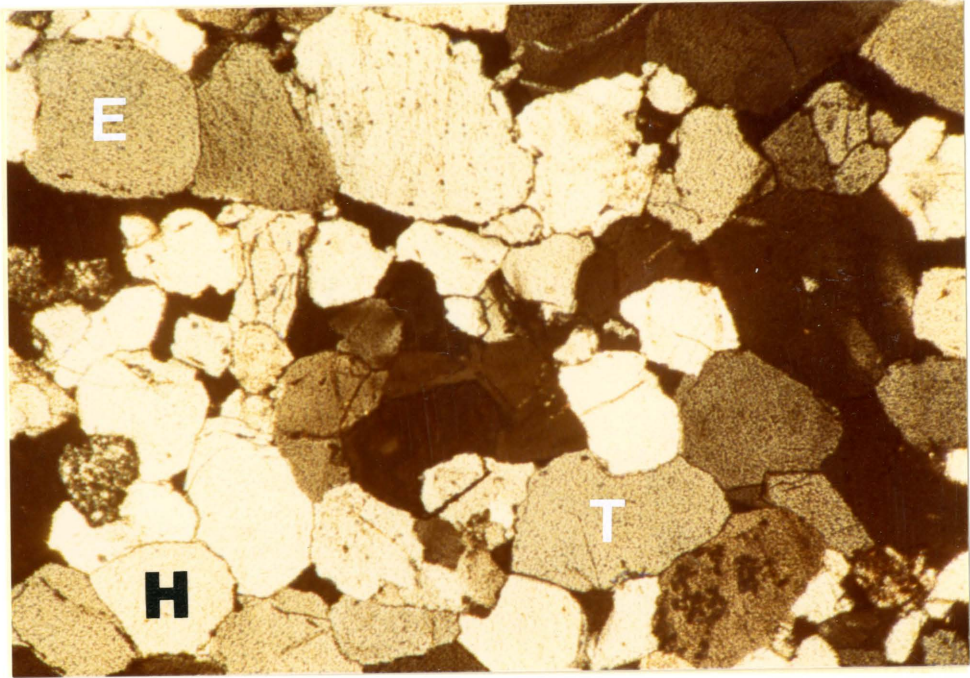
n= 100 counts per grain

contact strengths and average grain contacts calculated from the CL study are on average 35% and 23% lower than those calculated from the transmitted light study, respectively.

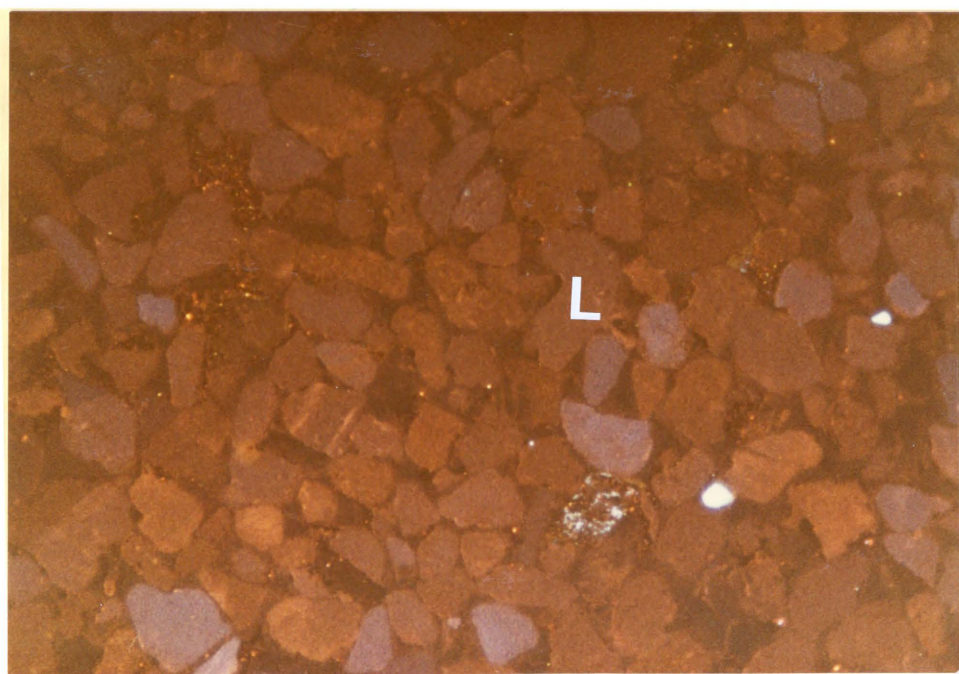
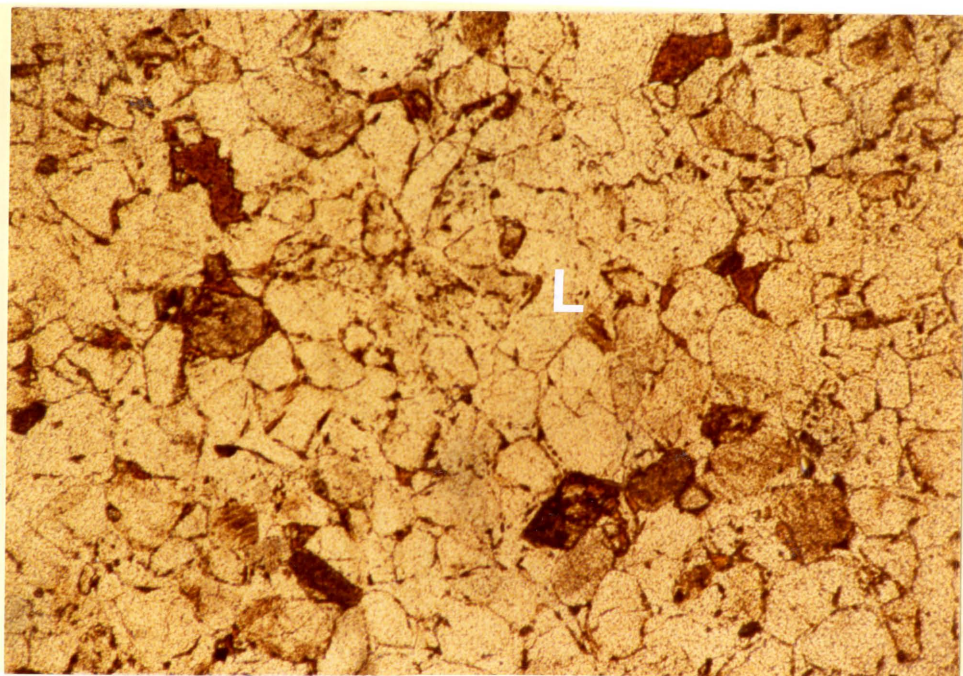
In the transmitted light study, approximately 55% of all the contacts were concavo-convex and sutured. Under transmitted light these contacts give every appearance of interpenetration and pressure solution. The CL study shows however, that roughly 25% of these contacts are nothing more than authigenic overgrowths that have grown together in concavo-convex and sutured patterns [see plates 3-24a,b, 3-25a,b, 5-1a and 3-2b]. Thus, the CL grain contact study represents the true measure of pressure solution within the Whirlpool Sandstone.

The contact strengths obtained for the Whirlpool Sandstone at the Haul Road and Jolley Cut outcrops are 1.6 and 1.2 respectively. The average number of contacts per grain in these locations is 4.0 and 3.5. These last figures are larger than what would be expected from normal grain packing alone [Gaither, 1953], and thus are an indication of pressure solution. However, roughly 85% of all the contacts are tangential in nature, suggesting that pressure solution has been minimal. This high number of tangential contacts may also reflect the early formation of quartz and calcite cements which would impede

Plates 3-24a,b: CL photograph showing the differences  
in contact description between  
transmitted light and CL. Sample  
VIS 1, 63X magnification, top XN,  
bottom CL.



Plates 3-25a,b: CL photograph showing the differences in contact description between transmitted light and CL. Sample VIS 6, 63X magnification, top PPL, bottom CL.



mechanical compaction [Gardiner, 1982]. Evidence of this would be the presence of the primary quartz cement discussed earlier and the fact that calcite cement is observed to be surrounded by later generations of silica cement [see chapter 5, plates 3-7a,b and 5-1a].

As demonstrated above, pressure solution was not a major factor in the diagenesis of the Whirlpool Sandstone, yet, quartz cement comprises roughly 20% of the samples studied. It is possible that the primary quartz cement observed has its origin from local silica, due to pressure solution, but there must have been an external source or sources of free silica in order to precipitate the massive, later generation, quartz cement.

Fuchtbauer [1978] suggests two other possible sources for free silica: i] diffusion of silica from surrounding shales and ii] to a lesser degree from dissolution of quartz stylolites within sandstones. Diagenetic conversion of smectite or interlayered smectite-illite to pure illite can also be a major source of silica [Towe, 1962]. This is not applicable to the Whirlpool Sandstone due to the low diagenetic temperatures and shallow depth of burial that the Whirlpool has experienced [see chapter 5].

The most likely source of the silica is the diffusion of silica from surrounding shales. The Whirlpool rests between 300 m of red shale below, the Queenston Formation

and many m of shale on the top, the Cabot Head Formation. It is very likely that enough silica could be derived from these shales to more than account for the silica cementation observed.

The average number of contacts per grain and the contact strength appear to decrease towards the northwest. This trend could be reflecting the lower burial depths of the Whirlpool Sand in the Hamilton area and is thus a function of lateral movement away from the centre of the depositional basin.

Classification, Provenance and Maturity:

Classification:

It has been demonstrated above that the CL technique gives a more accurate measure of the amount of quartz and quartz cement. It has also been shown that the identification of feldspars is routine with CL, but is difficult to impossible with transmitted light. Due to the above points, CL point count results for quartz and feldspar have been used to classify the Whirlpool Sandstone. It was unfortunate that the Luminoscope<sub>TM</sub> used did not have higher objectives available for it made the study of rock fragments impossible. Instead, the rock fragment population was determined using transmitted light and then combined with the CL data.

Tables 3-13 and 3-14 represent compilations of



TABLE 3-13

POINT COUNT RESULTS: QUARTZ, FELDSPAR AND ROCK FRAGMENTS

LOCATION	SAMPLE NUMBER	QUARTZ Q	FELDSPAR F	ROCK FRAGMENTS RF
HAUL ROAD CUT	VIS 1	100.0	t	t
	VIS 7	95.8	3.8	0.4
	VIS 6	94.2	3.0	2.7
	VIS 4	98.3	0.7	t
	VIS 2	98.5	1.5	t
	VIS 3	95.6	3.0	1.5
ART PARK	ART BASE	97.2	0.4	2.4
	ART 2	95.7	0.4	3.9
	ART 5	94.5	0.9	4.5
	ART 7	98.7	t	1.3
	ART 8	99.6	t	0.4
	ART 12	89.7	3.7	6.6
WHIRLPOOL	WHIRL 1	94.4	2.8	2.8
JOLLEY CUT	JOLL 6	91.3	3.0	5.7
	JOLL 5	96.2	0.4	1.9
	JOLL 4	93.8	4.8	1.4
	JOLL 3	95.3	1.0	3.7
	JOLL 1	92.1	4.4	3.5
SYDENHAM ROAD CUT	SYD 1	93.0	6.6	0.5
	SYD 2	93.9	6.1	t

Q and F values from Cathodoluminescent Microscopy, Point Count Results

RF values from Transmitted Light Microscopy, Point count Results

t= mineral not counted, but present in slide

**TABLE 3-14** POINT COUNT RESULTS: ROCK FRAGMENTS AND SRF COMPONENTS, TRANSMITTED LIGHT MICROSCOPY

LOCATION	SAMPLE NUMBER	ROCK FRAGMENT TYPES			COMPONENTS OF SRF		
		SRF	MRF	VRF	CHERT	PHOSPHATE	SANDSTONE SHALE
HAUL ROAD CUT	VIS 1	49.0	51.0	-	63.3	18.4	20.4
	VIS 7	38.0	62.0	-	60.5	23.7	15.8
	VIS 6	47.0	53.0	-	41.7	20.8	35.4
	VIS 4	35.0	65.0	-	45.7	40.0	14.3
	VIS 2	41.0	59.0	-	34.1	61.0	4.9
	VIS 3	45.0	55.0	-	44.4	53.3	6.1
ART PARK	ART BASE	30.0	70.0	-	37.1	11.4	51.4
	ART 2	45.0	55.0	-	62.2	20.0	17.8
	ART 5	42.0	58.0	-	40.5	2.4	57.1
	ART 7	26.0	74.0	-	69.2	15.4	15.4
	ART 8	29.0	71.0	-	75.9	10.3	13.7
	ART 12	30.0	70.0	-	26.7	13.3	60.0
WHIRLPOOL	WHIRL 1	44.0	56.0	-	52.4	7.1	40.3
JOLLEY CUT	JOLL 6	42.0	58.0	-	47.6	16.7	35.7
	JOLL 5	37.0	63.0	-	37.8	13.5	48.6
	JOLL 4	43.0	57.0	-	25.6	11.6	62.8
	JOLL 3	52.0	48.0	-	59.6	7.7	32.7
	JOLL 1	35.0	65.0	-	40.0	22.8	37.1
SYDENHAM ROAD CUT	SYD 1	43.0	57.0	-	37.2	34.9	27.9
	SYD 4	39.0	61.0	-	46.2	23.1	30.8

n= 100 point counts per slide

--= mineral not present in slide

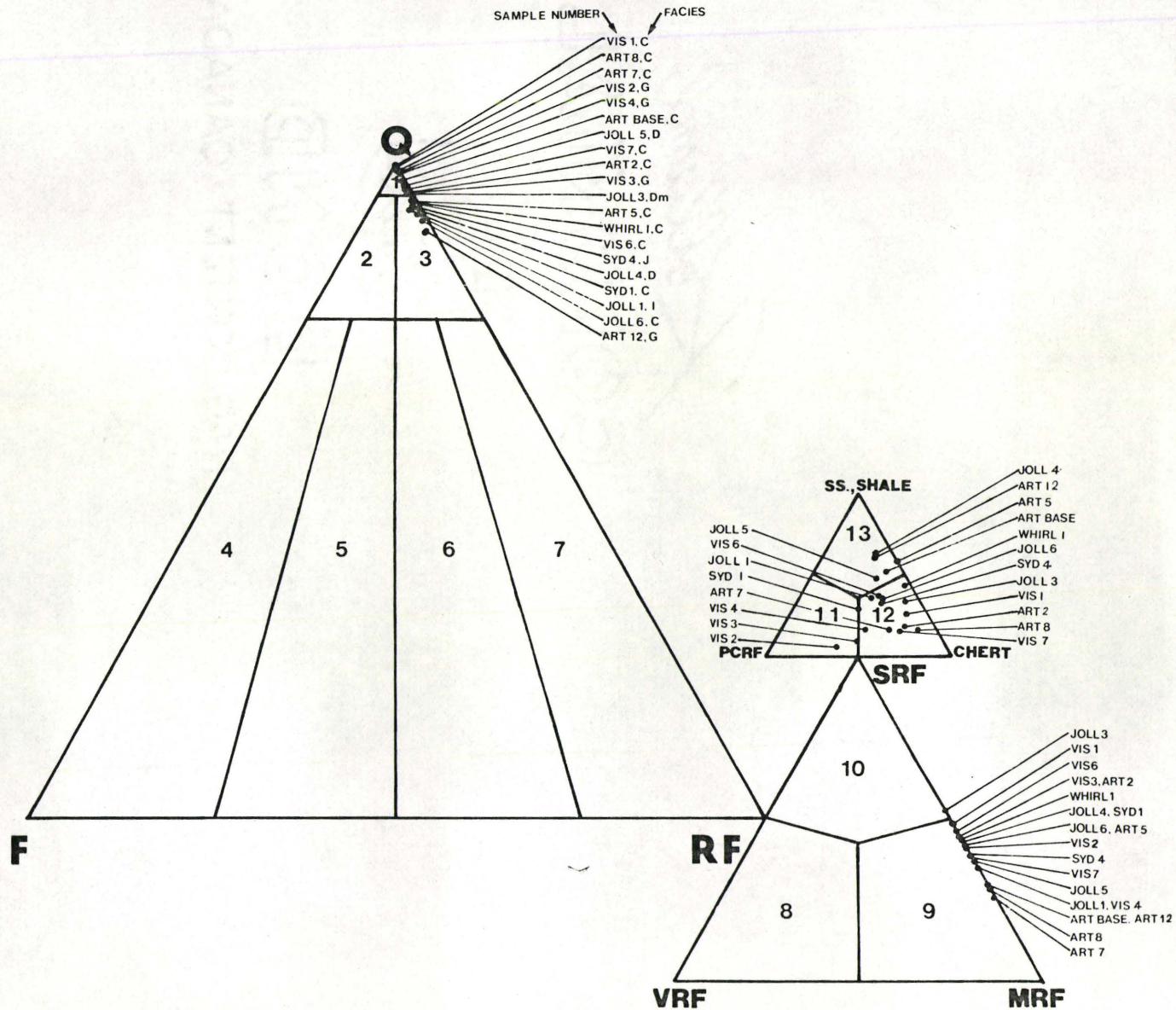
quartz, feldspar and rock fragment data and figure 3-1 displays the Folk [1978] classification diagram with results from the twenty thin sections studied plotted. All samples are classified as Quartzarenites or Sublitharenites.

Provenance:

It has been well documented in the literature that the source beds of the Whirlpool Sandstone are pre-existing sediments lying to the southeast [see chapter 1]. Alling [1936] believed that most of the quartz was derived from a pre-existing sandstone and Holstein [1936] thought that the restricted variety of heavy minerals present suggested a pre-existing sediment source.

It has long been accepted that sedimentary rocks comprising only quartz and the most stable heavy minerals, such as zircon and tourmaline, are products of recycled sediments [Blatt et al, 1980, page 286]. The Whirlpool Sandstone would seem to fit in this category, as it is composed of, on average, 70% quartz and only zircon and tourmaline are abundant as detrital heavy minerals. The presence of low grade metamorphic rock fragments and quartz grains containing large inclusions of vermicular chlorite suggest that the Whirlpool had a bimodal source, for these grains could not be expected to survive recycling. Thus, the source of the Whirlpool Sandstone appears to be primarily pre-existing sediments with minor input from low grade

Figure 3-1: Classification of the Whirlpool Sandstone  
after Folk, 1978.



metamorphic and hydrothermal veined terrain.

Two methods were used in order to determine the provenance of the sedimentary source beds.

Quartz varieties were plotted on a diagram proposed by Basu et al [1975]. They demonstrated that a double ternary plot of monocrystalline and polycrystalline quartz grains revealed the provenance of medium sand size quartz grains.

Basu et al. feel that this method should not be applied to mature sediments, i.e. Quartzarenites, for recycling will progressively move the quartz population towards the left corner of the diagram. Strictly speaking this method should not be applied to the Whirlpool Sandstone, but it has been used to give a rough idea of the original provenance.

Table 3-15 displays the results of the quartz classification and figure 3-2 is the plot after Basu et al, [1975]. The original provenance of the Whirlpool is shown to be in middle to high grade metamorphic terrain. When we consider that there has been at least one episode of recycling, the actual source could have had more low grade metamorphic character.

Triangular diagrams showing framework populations of quartz, feldspar, polycrystalline quartzose lithic fragments and unstable lithic fragments have been shown by

TABLE 3-15

MONOCRYSTALLINE, POLYCRYSTALLINE QUARTZ:  
TRANSMITTED LIGHT MICROSCOPY

LOCATION	SAMPLE NUMBER	MONOCRYSTALLINE		POLYCRYSTALLINE	
		<5° UNDUL.	>5° UNDUL.	>3 crystals per grain	2-3 crystals per grain
HAUL ROAD CUT	VIS 1	67.0	20.0	11.0	2.0
	VIS 7	73.0	22.0	4.0	1.0
	VIS 6	79.0	17.0	4.0	t
	VIS 4	67.0	22.0	9.0	2.0
	VIS 2	72.0	22.0	4.0	2.0
	VIS 3	74.0	19.0	6.0	1.0
ART PARK	ART BASE	77.0	13.0	9.0	1.0
	ART 2	74.0	19.0	5.0	2.0
	ART 5	70.0	15.0	14.0	1.0
	ART 7	70.0	18.0	12.0	t
	ART 8	70.0	17.0	10.0	3.0
	ART 12	77.0	16.0	6.0	1.0
WHIRLPOOL	WHIRL 1	73.0	13.0	12.0	1.0
JOLLEY CUT	JOLL 6	70.0	21.0	9.0	t
	JOLL 5	72.0	20.0	8.0	t
	JOLL 4	72.0	18.0	9.0	1.0
	JOLL 3	69.0	16.0	14.0	1.0
	JOLL 1	75.0	14.0	9.0	2.0
SYDENHAM ROAD CUT	SYD 1	75.0	20.0	4.0	1.0
	SYD 4	71.0	20.0	8.0	1.0

n= 100 point counts per slide

t= mineral not counted, but present in slide

Dickinson and Suczek [1979] to distinguish the key provenance types. Two diagrams were prepared: 1] a plot: i] of stable quartzose grains, Q, including both monocrystalline quartz grains and polycrystalline quartzose lithic fragments [chiefly chert grains]; ii] monocrystalline feldspar grains, F; iii] unstable polycrystalline lithic fragments, L, of two kinds, volcanic, metavolcanic and sedimentary, metasedimentary rock fragments. 2] a plot of: i] monocrystalline quartz grains, Qm; ii] monocrystalline feldspar grains, F; iii] total lithic fragments, L<sub>t</sub>, composed of unstable lithic fragments and stable quartzose lithic fragments.

Tables 3-16 and 3-17 represent the results of the framework classification and figure 3-3 displays the results on the triangular plots described above. The provenance of the Whirlpool Sandstone is shown to lie in Recycled Orogenic terrain with a shift into the Continental Block field brought about by the maturity of the Whirlpool Sandstone's framework.

Dickinson and Suczek [ibid.] describe Recycled Orogenic terrain as consisting of folded and faulted strata, from which recycled detritus of sedimentary and metasedimentary origin is prominent. Since, the metamorphic grade in these orogenic rocks ranges from low to high grade, it would appear as if the framework plots after Dickinson and



TABLE 3-16

STABLE MONOCRYSTALLINE QUARTZOSE GRAINS, PLUS STABLE QUARTZOSE LITHIC FRAGMENTS/MONOCRYSTALLINE FELDSPAR GRAINS/UNSTABLE POLYCRYSTALLINE LITHIC FRAGMENTS

LOCATION	SAMPLE NUMBER	Q	F	L
HAUL ROAD CUT	VIS 1	99.1	0.9	t
	VIS 7	95.6	3.2	1.2
	VIS 6	94.4	2.7	2.9
	VIS 4	98.2	1.4	0.4
	VIS 2	97.2	1.4	1.4
	VIS 3	97.1	2.5	0.4
ART PARK	ART BASE	97.2	0.4	2.4
	ART 2	96.4	0.4	3.2
	ART 5	94.0	0.8	5.2
	ART 7	98.8	t	1.2
	ART 8	100.0	t	t
	ART 12	91.8	3.7	4.5
WHIRLPOOL	WHIRL 1	94.2	2.7	3.1
JOLLEY CUT	JOLL 6	94.6	2.9	2.5
	JOLL 5	99.2	0.4	0.4
	JOLL 4	94.3	4.5	1.2
	JOLL 3	98.0	1.0	1.0
	JOLL 1	94.2	4.4	1.4
SYDENHAM ROAD CUT	SYD 1	92.7	5.6	1.7
	SYD 4	92.0	5.2	2.8

Q and L values from Transmitted Light Microscopy, Point Count Results

F values from Cathodoluminescent Microscopy, Point Count Results

t= mineral not counted, but present in slide

TABLE 3-17

STABLE MONOCRYSTALLINE QUARTZOSE GRAINS/MONOCRYSTALLINE  
FELDSPAR GRAINS/UNSTABLE POLYCRYSTALLINE LITHIC FRAGMENTS,  
PLUS STABLE QUARTZOSE LITHIC FRAGMENTS

---

LOCATION	SAMPLE NUMBER	Qm	F	L <sub>t</sub>
HAUL ROAD CUT	VIS 1	86.2	0.9	12.9
	VIS 7	91.1	3.2	5.7
	VIS 6	90.3	2.7	7.0
	VIS 4	88.0	1.4	10.9
	VIS 2	91.7	1.4	6.9
	VIS 3	89.0	2.8	8.2
ART PARK	ART BASE	86.7	0.4	12.9
	ART 2	88.6	0.4	11.0
	ART 5	79.9	0.8	19.3
	ART 7	86.8	t	13.2
	ART 8	87.8	t	12.2
	ART 12	83.9	3.7	12.4
WHIRLPOOL	WHIRL 1	82.7	2.7	14.6
JOLLEY CUT	JOLL 6	83.8	2.9	13.3
	JOLL 5	90.2	0.4	9.4
	JOLL 4	84.6	4.5	10.9
	JOLL 3	82.2	1.0	16.8
	JOLL 1	84.4	4.4	11.2
SYDENHAM ROAD CUT	SYD 1	88.4	5.6	6.0
	SYD 4	84.1	5.2	10.7

---

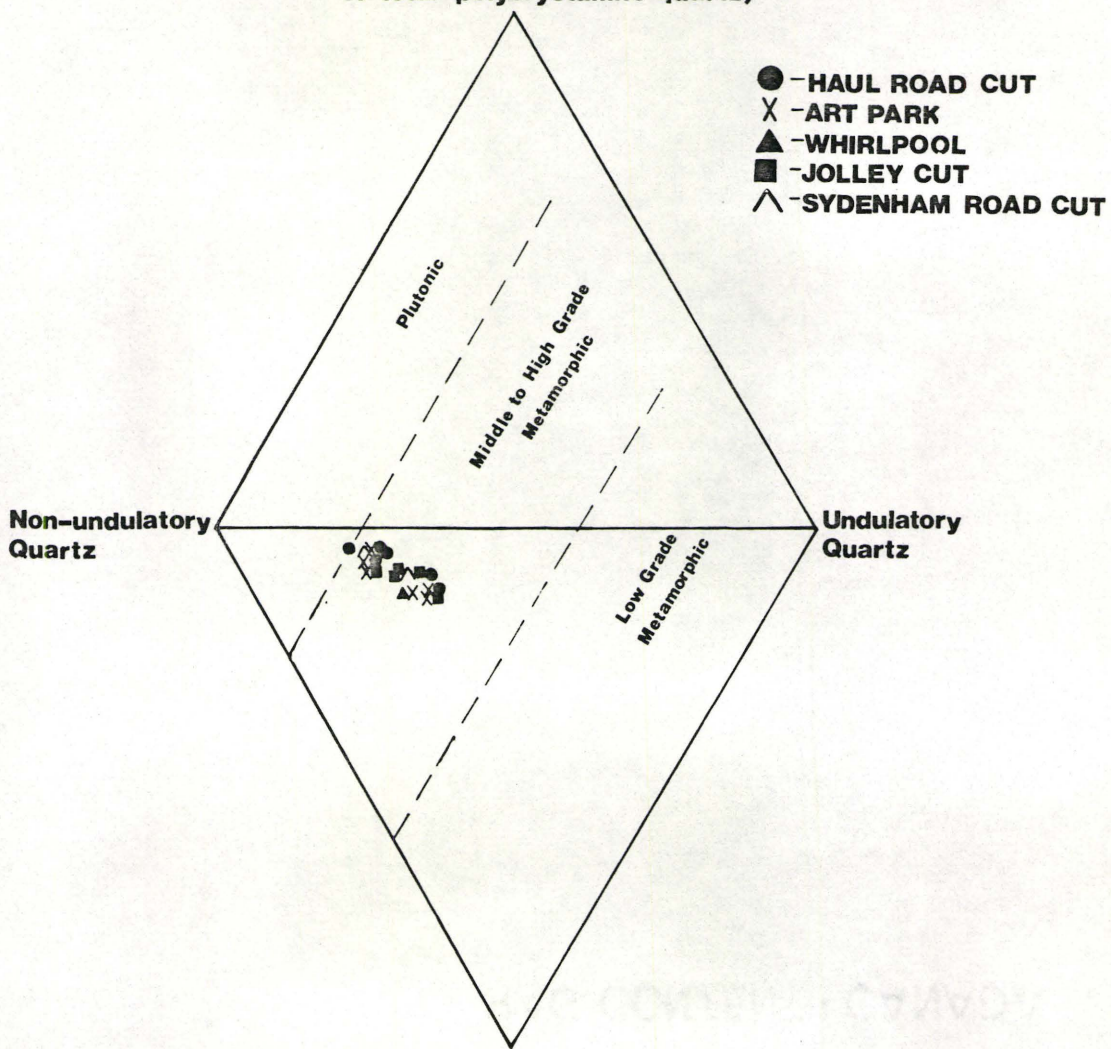
Qm and L<sub>t</sub> values from Transmitted Light Microscopy,  
Point Count Results

F values from Cathodoluminescent Microscopy, Point  
Count Results

t= mineral not counted, but present in slide

Figure 3-2: Quartz varieties of the Whirlpool Sandstone plotted on diagram proposed by Basu et al (1975) suggests a provenance of middle to high grade metamorphic with some plutonic character.

**Polycrystalline Quartz**  
(2-3 crystals per grain;  $\geq 75\%$   
of total polycrystalline quartz)



**Polycrystalline Quartz**  
( $>3$  crystals per grain;  $>25\%$   
of total polycrystalline quartz)

Figure 3-3: Constituent varieties of the Whirlpool Sandstone plotted on diagrams proposed by Dickenson and Suczek, (1979) suggests recycled orogenic provenance with a shift towards continental block provenance brought about by the maturity of the Whirlpool Sandstone's framework.

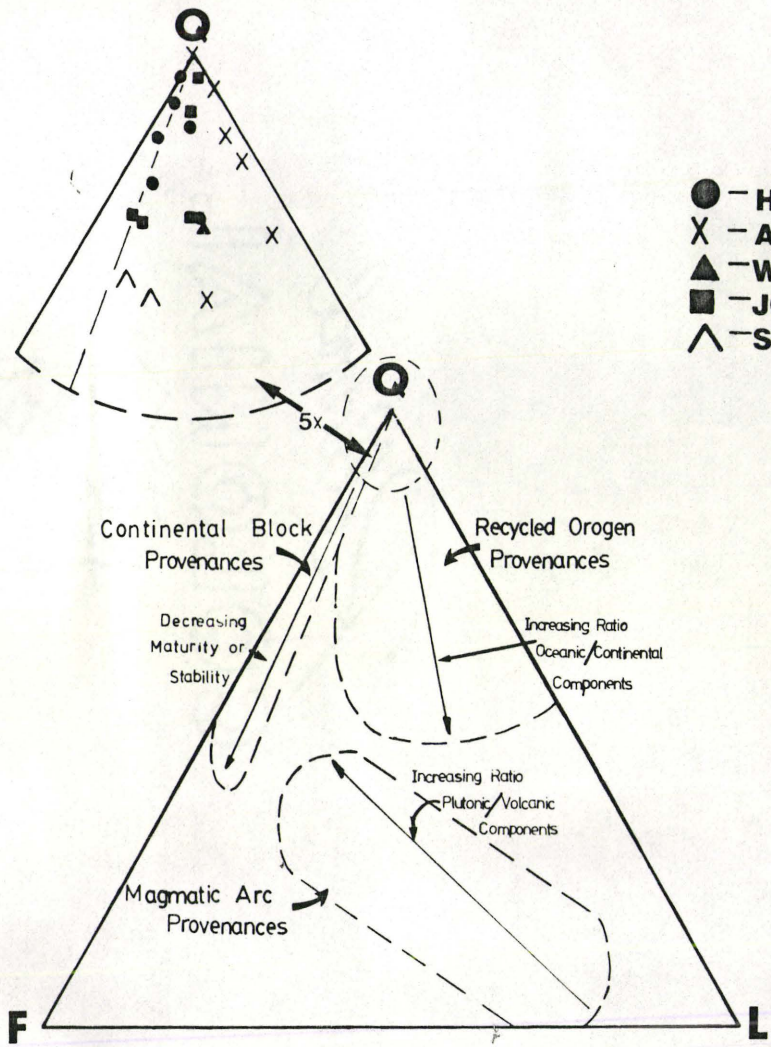
Q<sub>m</sub>= monocrystalline quartz grains

Q= monocrystalline quartz grains plus stable polycrystalline quartzose lithic fragments

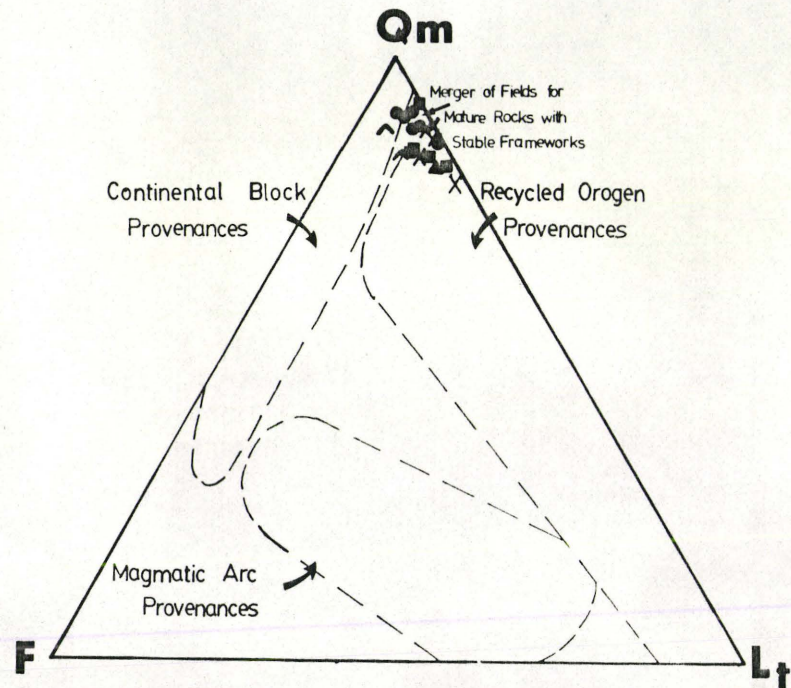
F= monocrystalline feldspar

L= unstable polycrystalline lithic fragments of two types, volcanic, metavolcanic and sedimentary, metasedimentary rock fragments

L<sub>t</sub>= total unstable lithic fragments



- - HAUL ROAD CUT
- X - ART PARK
- ▲ - WHIRLPOOL
- - JOLLEY CUT
- ∧ - SYDENHAM ROAD CUT



Suczek [ibid.] are in agreement with the quartz variety plots after Basu, et al [1975].

Both of the methods used point to a source region comprised of pre-existing sediment, derived from the Appalachians. This conclusion is consistent with the literature [see chapter 1].

#### Maturity:

The Whirlpool Sandstone can be considered to be mineralogically mature, due to its monocrystalline quartz rich nature, relative lack of unstable lithic fragments and the presence of only the most stable detrital heavy minerals, zircon and tourmaline [Blatt et al, 1980].

Following the textural maturity of Folk [1974] detrital clays account for much less than 5% of the total mineral abundance, quartz grains are subangular to well rounded and are in general well sorted. Therefore, the Whirlpool Sandstone is texturally mature.

#### Porosity

Ten thin sections were impregnated with blue epoxy in order to determine the porosity of the Whirlpool Sandstone.

An average porosity of 5.7% was obtained [see Tables 3-2a,b to 3-5a,b] agreeing roughly with the value obtained by Seyler [1981]. Porosity ranged from a maximum of 9.3%, in the ART sample, to a minimum of trace, in the JOLL 3 sample.

Virtually all the porosity is secondary in nature. It was formed by the dissolution of feldspar [see plates 3-26a,b and 3-27a,b] calcite cement [see plates 3-28a,b and 3-32b] and sedimentary rock fragments [see plate 3-29b].

Almost all of the primary intergranular porosity has been occluded by second generation massive quartz cement [see plates 3-30a and 5-1a]. In many of the samples calcite cement has occluded any remaining primary porosity [see plate 3-30b].

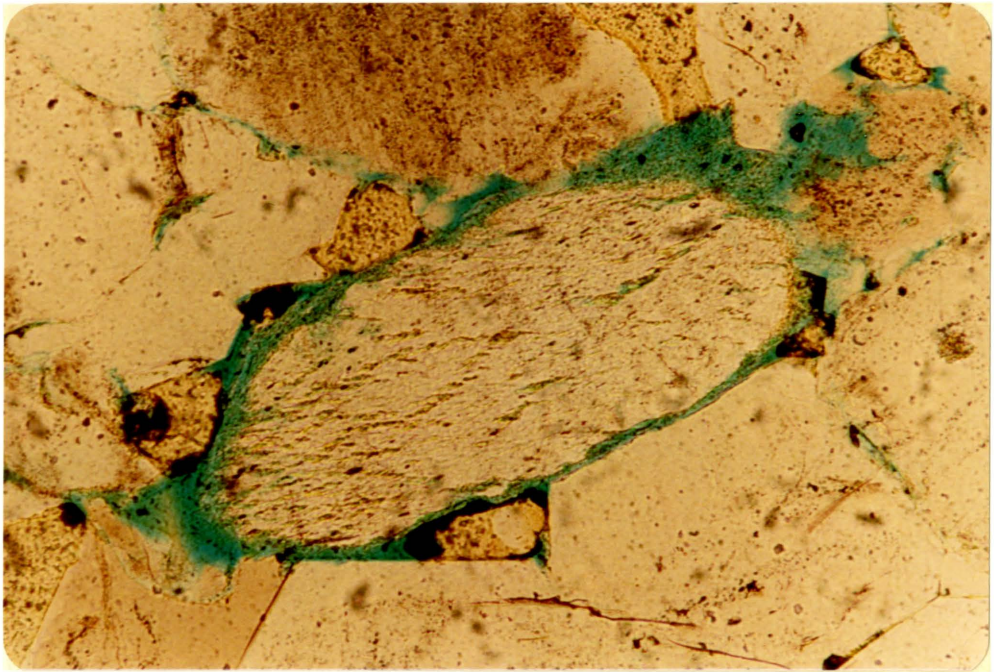
#### Weathering Cavities:

Near the base of Facies C, at the Niagara Gorge outcrops, there exists, in a narrow band roughly 30 cm wide, an accumulation of round, superficial, weathering cavities. These cavities exist on the vertical and horizontal faces of the outcrops and range in diameter from 1.0 to 0.5 cm. Plate 2-4a, displays these cavities in outcrop and plates 3-31a,b and 3-32a,b, display the cavities in thin section.

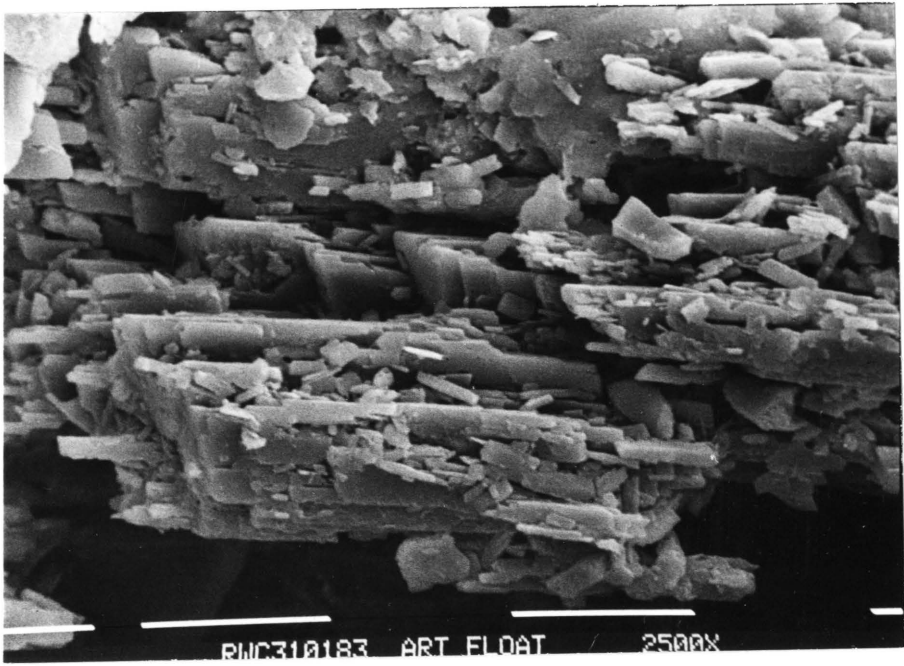
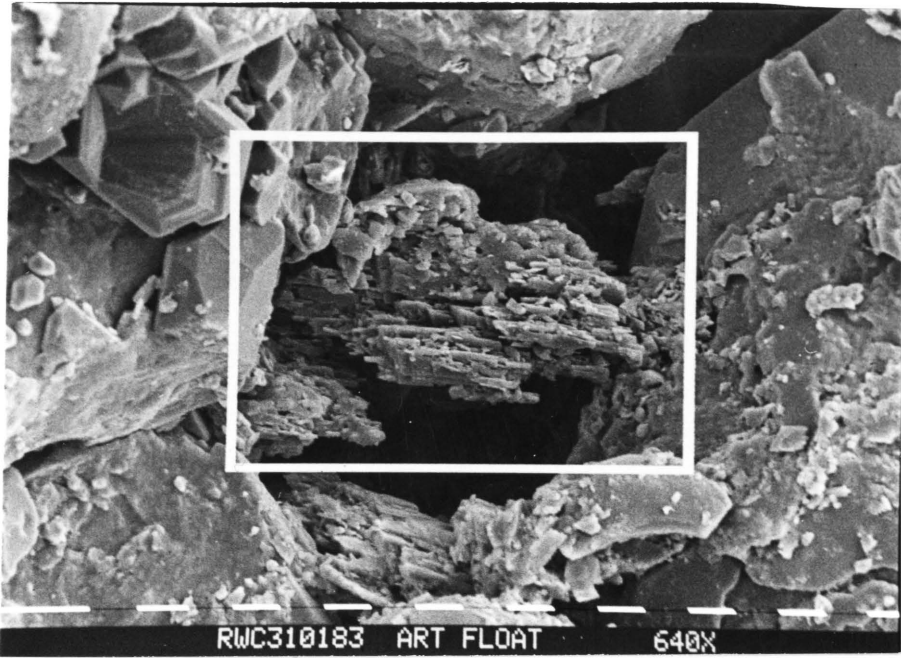
Seyler [1981] interpreted these structures to be worm burrows. If they were worm burrows, then one would expect to see a well defined muddy matrix that the worms were digesting [M.J. Risk, personal communication]. The Whirlpool Sandstone however, is essentially mud free. Also, one would expect to see grain rotation along the edges of the burrows [M.J. Risk, pers. com.]. No such grain rotation is



Plate 3-26: Dissolution of microcline leading to  
the formation of secondary porosity.  
Sample ART BASE, 160X magnification, PPL.



Plates 3-27a,b: Dissolution of feldspar leading  
to the formation on secondary  
porosity. Sample ART BASE, scale  
bar divisions equal 10 microns.



Plates 3-28a,b: Dissolution of calcite leading to the formation of secondary porosity. Sample VIS 1, top, scale bar divisions equal 100 microns, bottom, scale bar divisions equal 10 microns.

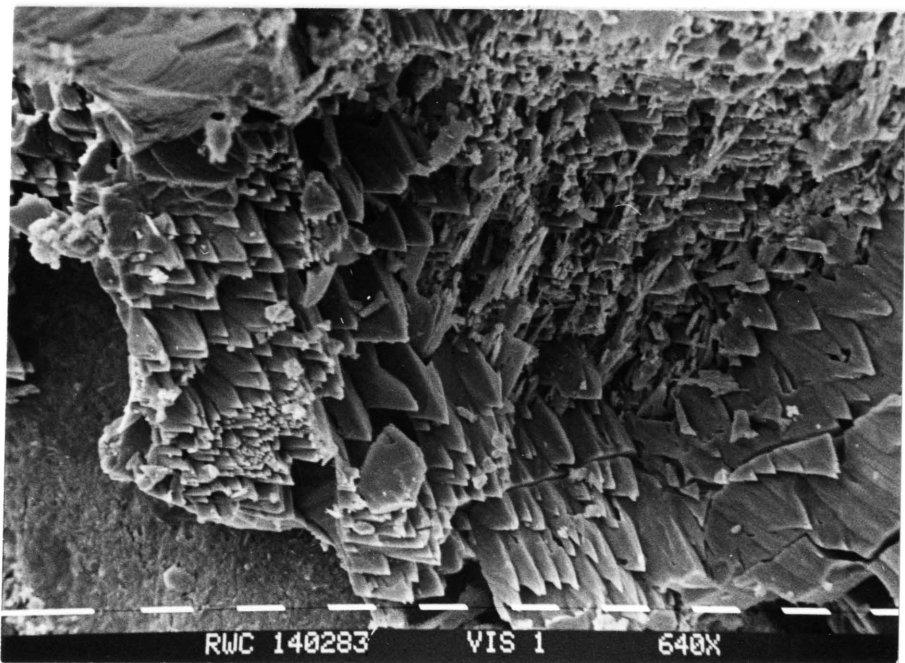
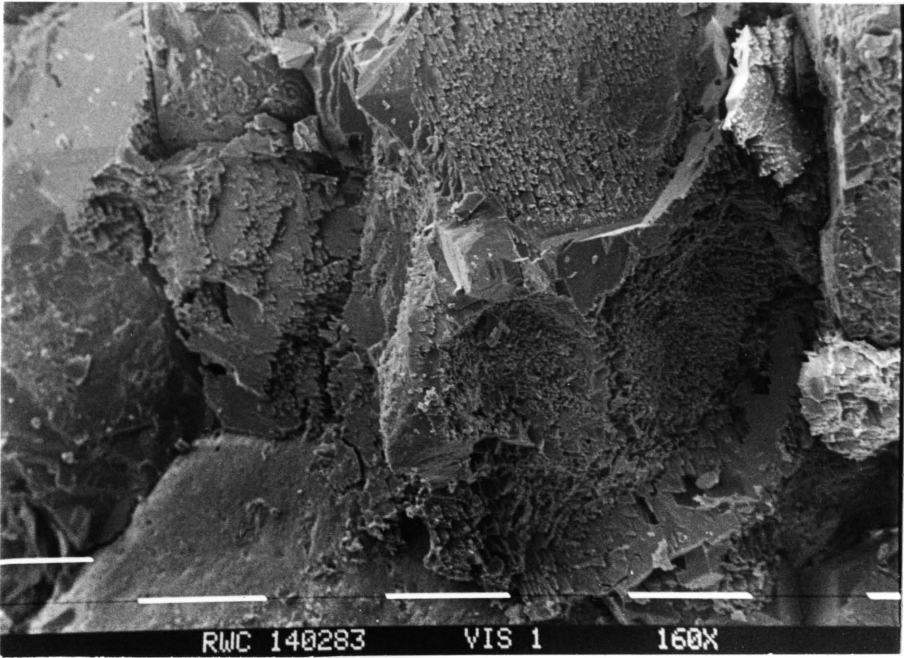


Plate 3-29a: Dissolution of an SRF leading to the formation of secondary porosity. Sample ART 2, 160X magnification, PPL. Note the small amount of primary interparticle porosity [arrow].

Plate 3-29b: Secondary porosity formed due to the dissolution of a grain, see oblong shaped pore. Sample ART BASE, 160X magnification, PPL. Note the small amount of interparticle porosity.

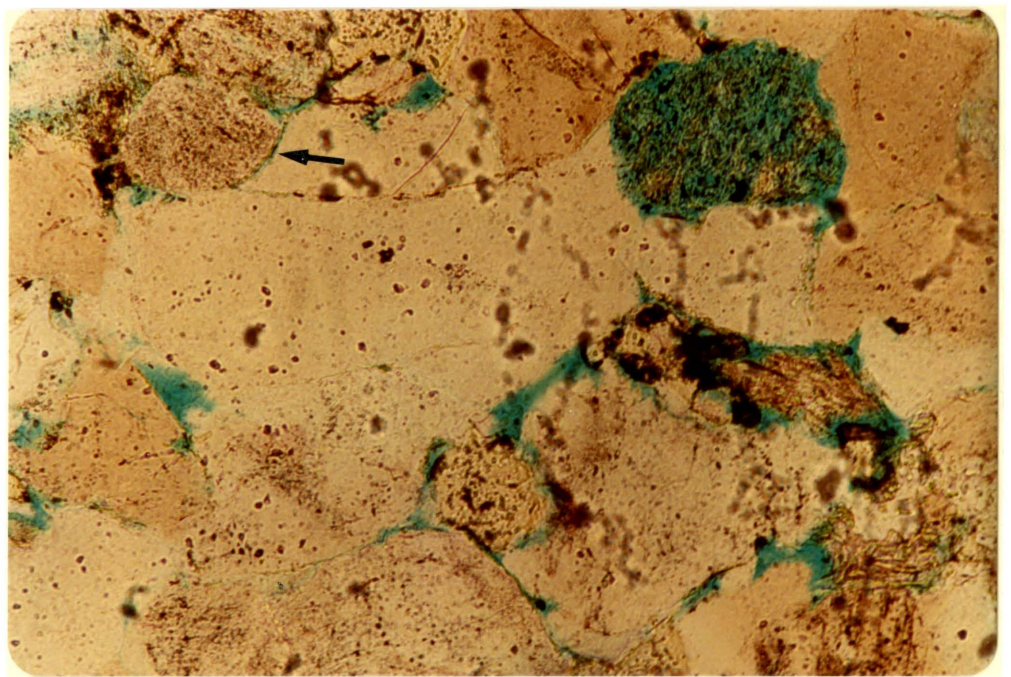
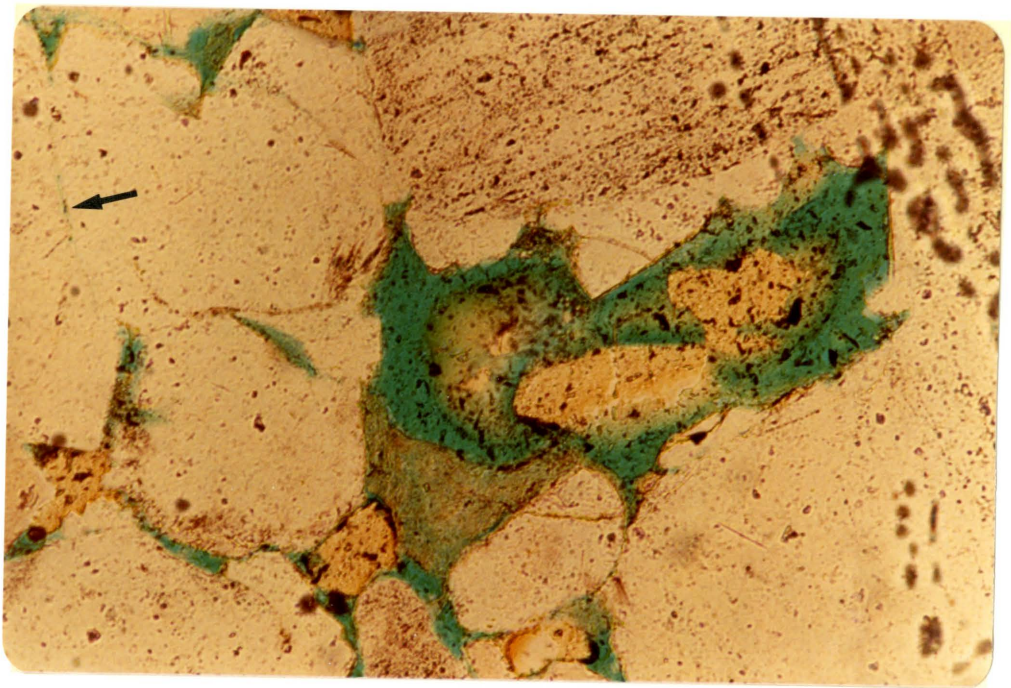
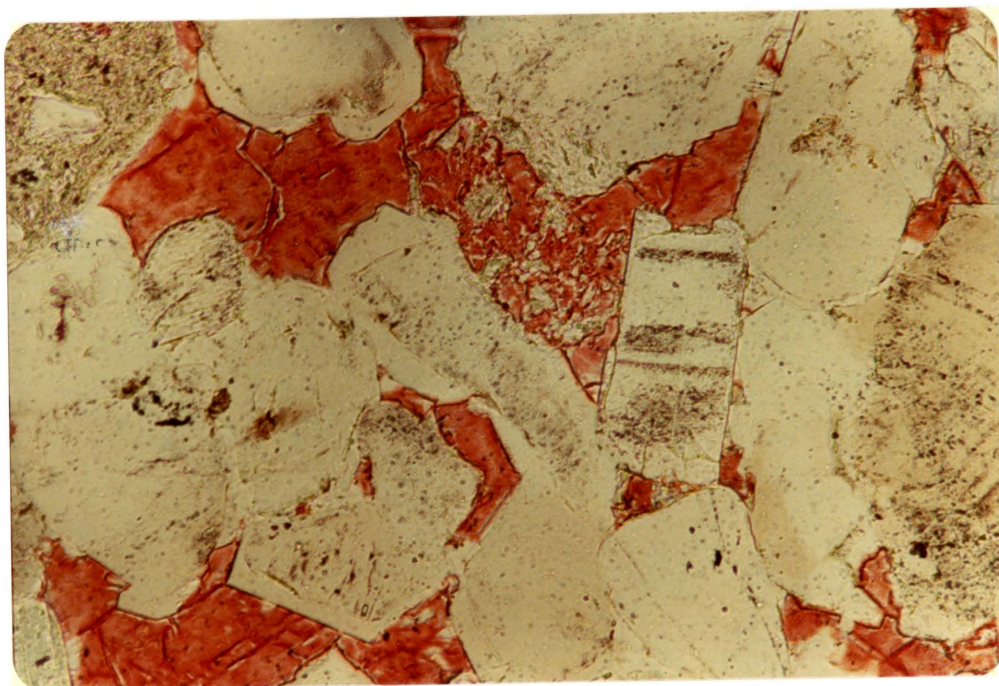
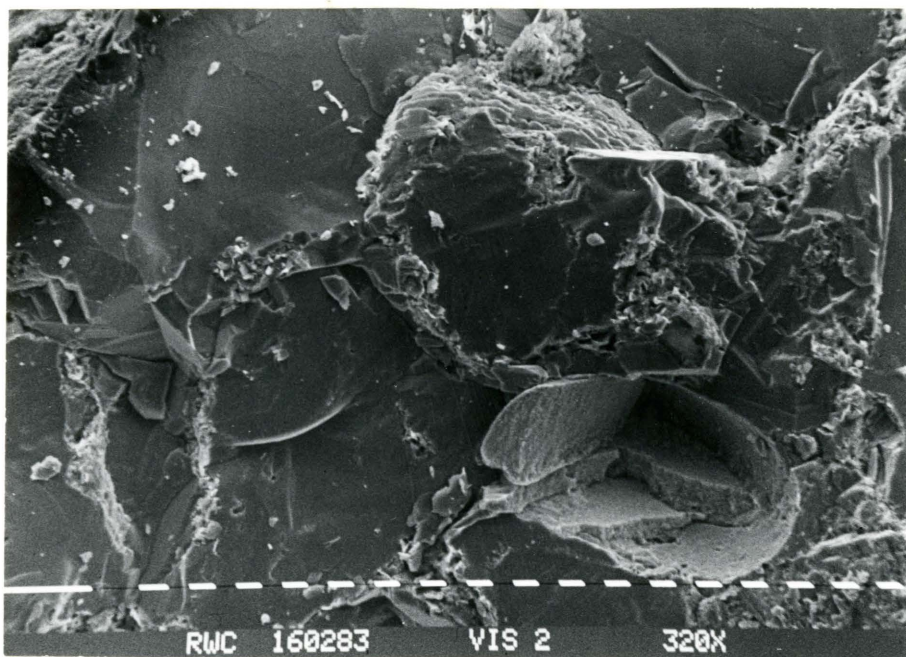




Plate 3-30a: Secondary, massive quartz cement, occluding all porosity. Sample VIS 2, scale bar divisions equal 10 microns.

Plate 3-30b: Occlusion of all remaining porosity by nonferroan calcite cement. Sample JOLL 3, 63X magnification, PPL.



Plates 3-31a,b: CL photograph showing weathering cavity. Note, lack of grain rotation, the "fallen away" character of the grains and the dissolution features of the patchy calcite. Sample ART BASE, 63X magnification, top PPL, bottom CL.

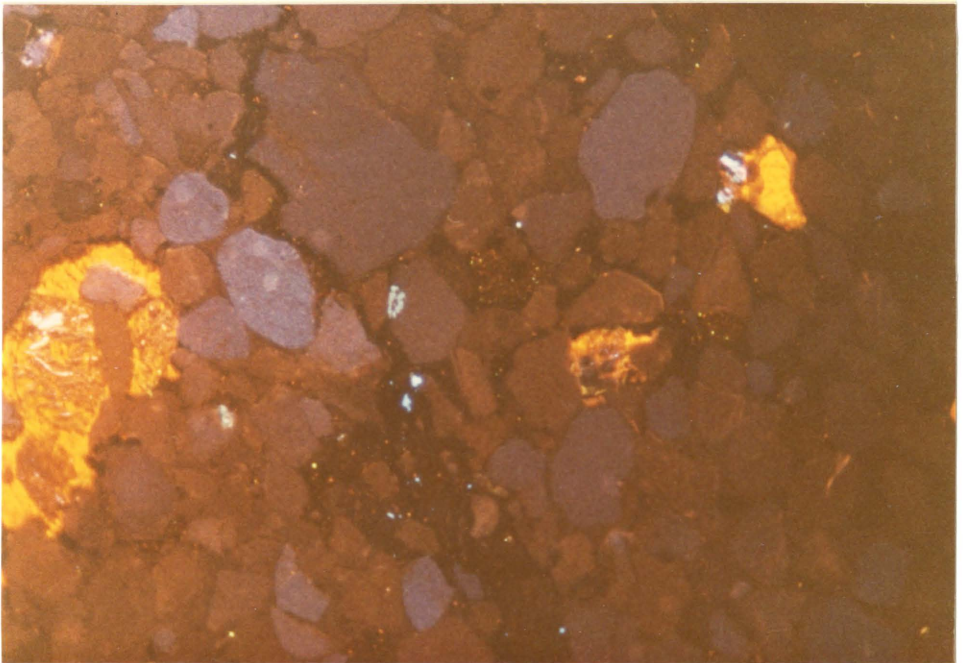
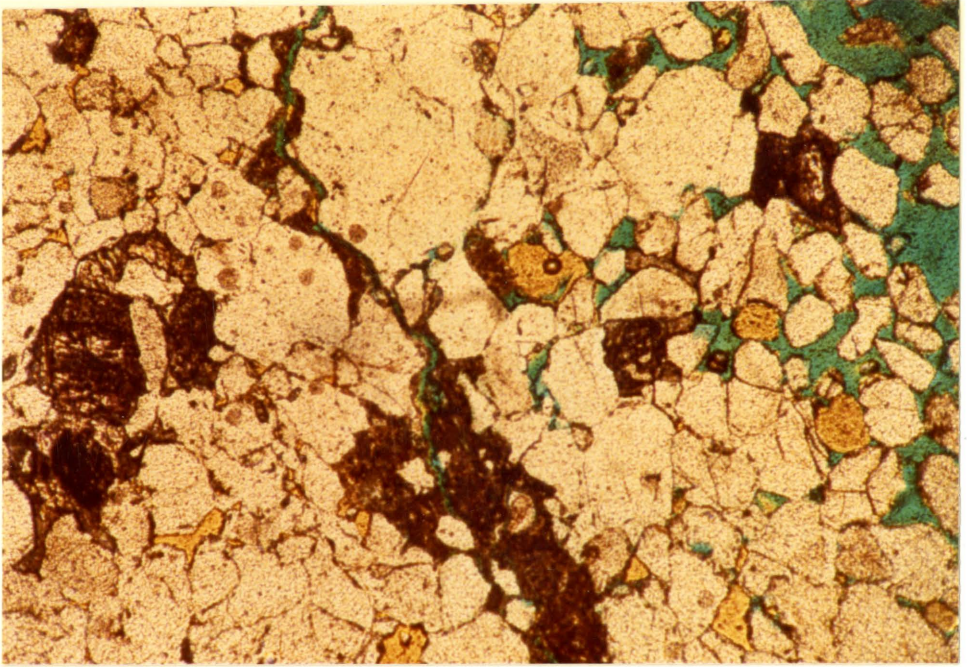
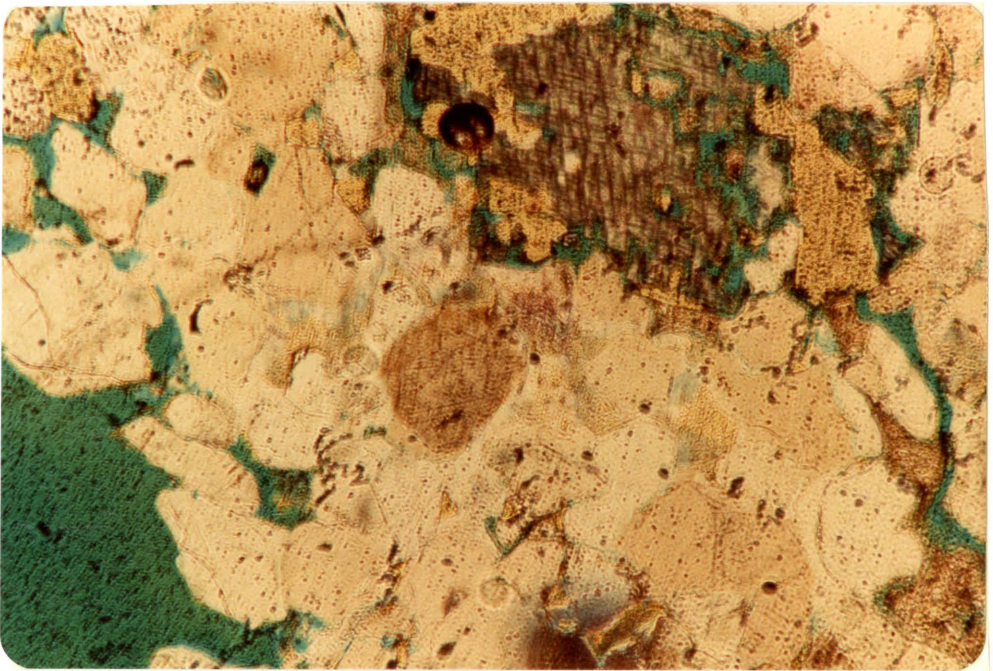
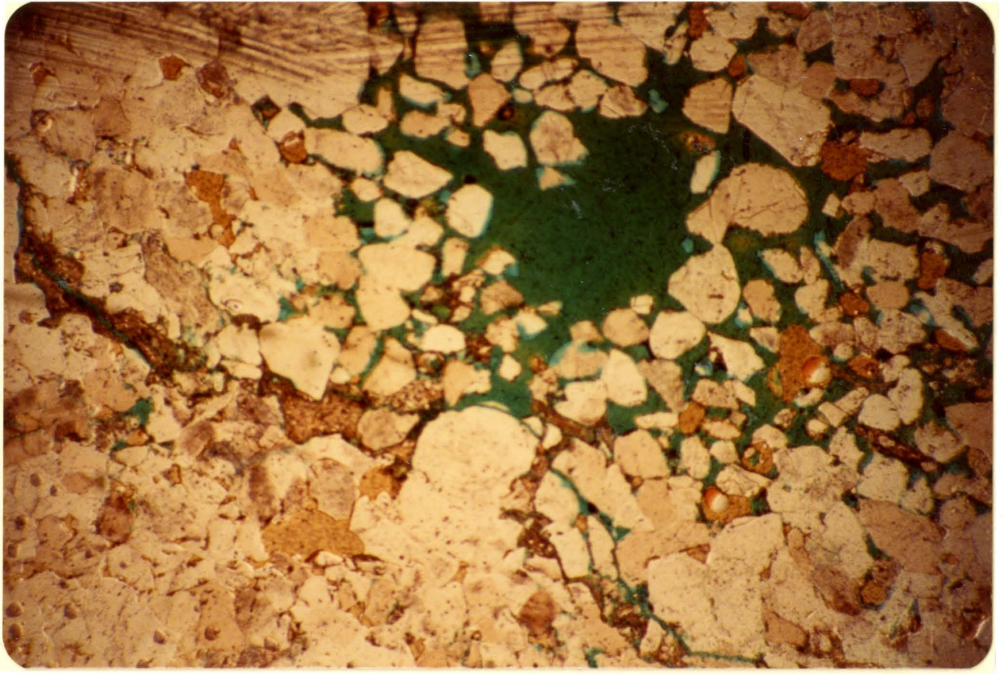


Plate 3-32a: Weathering cavity showing no grain rotation. Note, the gradual increase in dissolution porosity towards the cavity. Sample ART BASE, 25X magnification, PPL.

Plate 3-32b: Dissolution of patchy calcite leading to the formation of weathering cavity. Sample ART BASE, 63X magnification, PPL.



observed. Instead, the grains appear to have simply fallen away, into the cavities [see plates 3-31a and 3-32a].

The Whirlpool is coarsest at the very base and coarsens to the southeast [Geitz, 1952]. Thus, the structures are confined to the coarsest grain size observed in the Whirlpool. It appears as though the formation of the cavities is a function of grain size, i.e. the coarser the grain size, the smaller the surface area of the grains that is cemented. If patchy calcite cement were to weather away [see plate 3-32b] a small cavity would be formed. The larger, less cemented grains would gradually be weathered out and fall into the cavity, exposing fresh grains to the weathering solutions. The process will continue, with a snowball type effect, until a large cavity is formed.

In the areas having finer grain sizes, the grains will be held more strongly by cement and the weathering process will be retarded. Another control on the formation of the cavities could be proximity to the water laden Queenston Shale.

#### Minus Cement Porosity:

Rosenfeld [in Fuchtbauer, 1974] defined minus cement porosity as the porosity that would occur if all cement was dissolved away, thus indicating the porosity of the sand prior to cementation.

Table 3-18 displays the minus cement porosity calculated

TABLE 3-18

MINUS CEMENT POROSITY: CATHODOLUMINESCENT MICROSCOPY

LOCATION	SAMPLE NUMBER	GRAINS	CEMENT	POROSITY	MATRIX	MINUS CEMENT POROSITY
ART PARK	ART BASE	71.0	23.3	5.7	t	29.0
	ART 2	68.2	25.3	6.5	t	31.8
WHIRLPOOL	WHIRL 1	70.7	23.0	6.3	t	29.3
JOLLEY CUT	JOLL 6	73.3	16.7	10.0	t	26.7
	JOLL 5	67.3	18.3	14.0	t	32.2
	JOLL 4	75.4	13.3	11.3	t	24.6
	JOLL 3	69.7	30.6	t	t	30.6
	JOLL 1	65.7	33.0	1.3	t	34.3
SYDENHAM ROAD CUT	SYD 1	67.0	21.0	12.0	t	33.0
	SYD 4	71.0	17.0	12.0	t	29.0

n= 300 point counts per slide



for the ten thin sections that were impregnated with blue epoxy. An average of 30.0% minus cement porosity was obtained, with values ranging from a maximum of 34.3% in the JOLL 1 sample, to 24.6% in the JOLL 4 sample.

Evaluation of Cathodoluminescent Microscopy as Applied to Sedimentological Research:

Cathodoluminescent Microscopy offers a great deal of new information for sedimentological research.

This study has demonstrated the advantage of CL when dealing with sandstones that have extensive quartz cement, but this technique can also be applied to routine mineral analysis.

The identification of detrital feldspar is routine using CL and in fact once a colour/mineral pair has been established, colour can be used as the sole criterion for identification with only random checks to ensure consistency. Dolomitization of carbonates is easily detected as well as zonation in both minerals. This can yield valuable information concerning the diagenesis of the sediment.

CL is relatively inexpensive, safe and easy to use and requires the same sample preparation as transmitted light microscopy.

Its only drawback is the gradual destruction of the thin sections by the high energy electron beam. Thin sections will become "baked" after long exposure to the beam, causing

the grains to fracture as the mounting medium contracts.

CL offers a new approach to petrographic studies that will become routine in the future and better understood as more research is carried out [see Appendix 1 for description of CL technique, i.e., thin section preparation, general use, photography, etc.].

## CHAPTER 4

### C L A Y M I N E R A L O G Y

#### Introduction:

In order to determine a diagenetic history for the Whirlpool Sandstone a study of the clay mineralogy was attempted.

Clay mineral identification was carried out using X-ray Diffraction and Scanning Electron Microscopy. X-ray diffraction alone cannot be used to distinguish effectively between allogenic and authigenic clays. Rather, direct observation of clay morphologies and textural relationships via the SEM is used.

#### X-ray Diffraction:

X-ray identification of clay minerals involves matching the recorded X-ray powder patterns of standard clays, i.e. peak positions [or d-spacings] peak profiles and peak intensities, against unknown X-ray powder patterns.

Peak position, expressed as an angle  $2\theta$ , is dependant on the wavelength of the radiation used, usually  $\text{CuK}\alpha$ , and can be converted to d-spacings via the Bragg equation:

$$n\lambda = 2d\sin\theta$$

Most crystalline substances give integral orders of Bragg reflections from equally spaced lattice planes. Thus, they are easily identified by comparative analysis, as they always have the same form. Clays however, can contain layers of unequal spacings, due either to unequal expansion or contraction of layers resulting from varying cationic substitutions, or from mixed layering of two or more different structural types, i.e. dioctahedral or trioctahedral layers. Thus, comparative analysis of clays can sometimes give erroneous results.

It is for the above reason that XRD analyses should be made in conjunction with SEM analyses.

In order to minimize the inherent differences between standards and unknowns a series of standard clays, Illite No. 35, Kaolinite No. 4 and Ripidolite Chlorite No. CCa-1, and four unknowns, ART BASE, SYD 4, JOLL 1 and WHIRL 1, were processed under identical conditions. The standards and unknowns were then analyzed on a Phillips X-ray Diffractometer.

In order to achieve maximum peak intensity it is imperative that basally oriented clay mounts be used. Orientation of the clay particles in a basal manner enhances the  $00\ell$  intensities and retards the  $hk\ell$  intensities. This is due to the fact that the X-rays normally used in XRD analysis are readily absorbed by clay materials. Thus, a

very thin surface layer, where orientation is most likely to occur, will contribute most to the peak intensities. Since, the definition of a recognizable peak is two times the base line noise, the higher the intensities of the clay peaks the more chance there is of identification.

#### Analysis:

Samples were prepared and analyzed using a procedure modified from Gardiner [1982] [see Appendix 3 for a complete description of XRD technique]. Figures 4-1 to 4-3 are XRD traces of the standard clays analyzed and figures 4-4 and 4-5 are XRD traces of the ART BASE and SYD 4 samples.

#### Results:

##### Standard Clays

The most intense peaks on the standard clay XRD traces, figures 4-1 to 4-3, represent basal reflections, i.e. 001, 002, etc. All other, less intense, peaks are low order reflections, i.e.  $hk\ell$ . The sharp and well developed profiles of all the peaks are an indication of the highly crystalline nature of the standard clays.

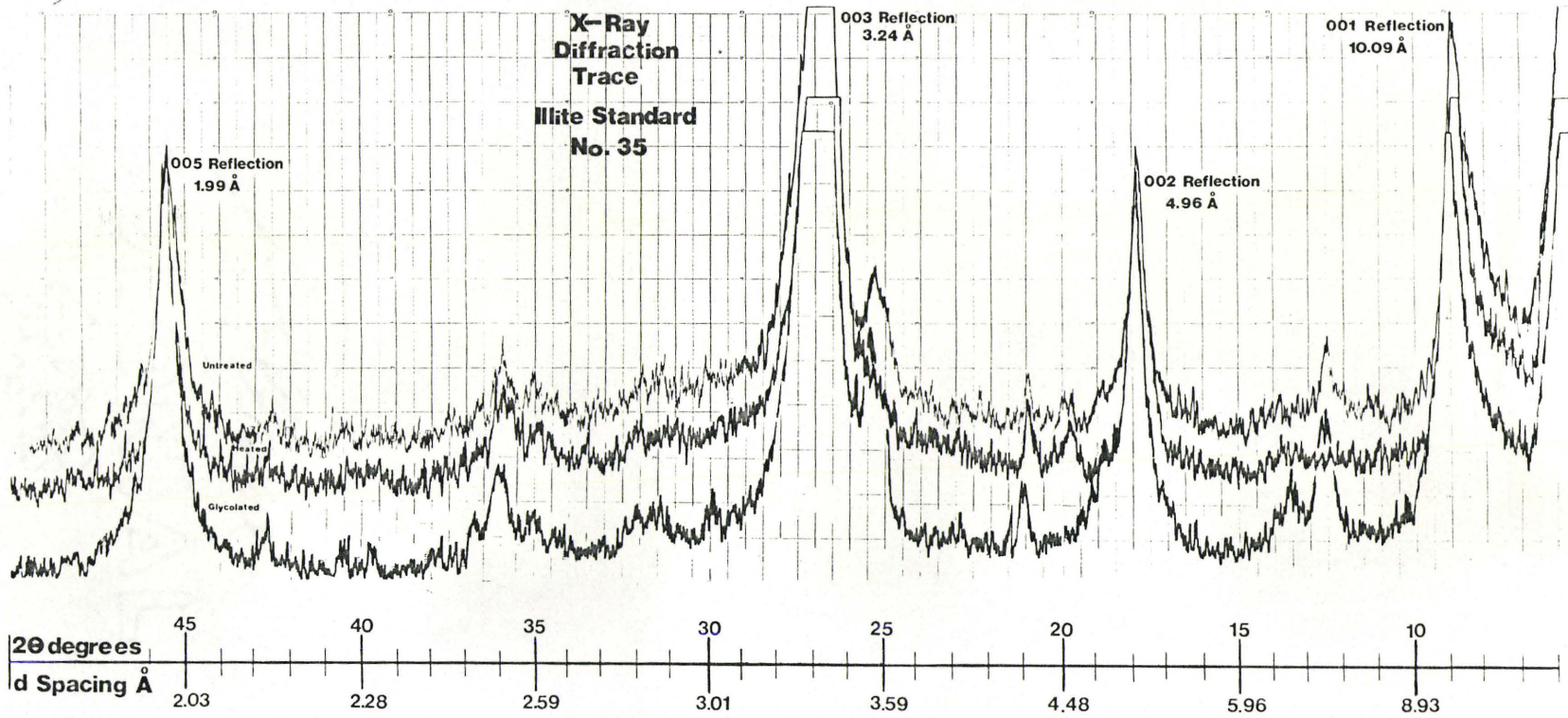
##### Illite

The Illite standard used was the Fithian Illinois, Illite Standard No. 35, verified at Columbia University by R.J. Holmes.

The sharp and intense peaks at 10.09 Å, 4.96 Å,

**FIGURE 4-1**

134



3.24 Å and 1.99 Å represent the 001, 002, 003, and 005 basal reflections of Illite [Thorez, 1975] [refer to figure 4-1].

As expected, these basal reflections were not affected by glycolation or heating. The lower order peaks at  $12.5^\circ$  and  $25.5^\circ$   $2\theta$  have been destroyed by heating. This can be explained by the presence of mixed layer character in the standard.

#### Kaolinite

The Kaolinite standard used was the Macon, Georgia, Kaolinite No 4, verified by R.J. Holmes at Columbia University.

The sharp and intense peaks at 7.12 Å, 3.56 Å and 2.40 Å, represent the 001, 002, and 003, basal reflections of Kaolinite [DR. H.D. Grundy, personal communication] [refer to figure 4-2]. As expected, these peaks were destroyed by heating, due to the formation of an amorphous meta-Kaolin structure [Carroll, 1970]. Glycolation, as expected, did not affect these peaks.

#### Chlorite

The Chlorite standard used was the Flagstaff Hill, El Dorado County, California, Ripidolite [chlorite] CCa-1, supplied by the Clay Mineral Society, from the Clay Mineral Repository.

The sharp and intense peaks at 7.00 Å and 4.70 Å,

FIGURE 4-2

136

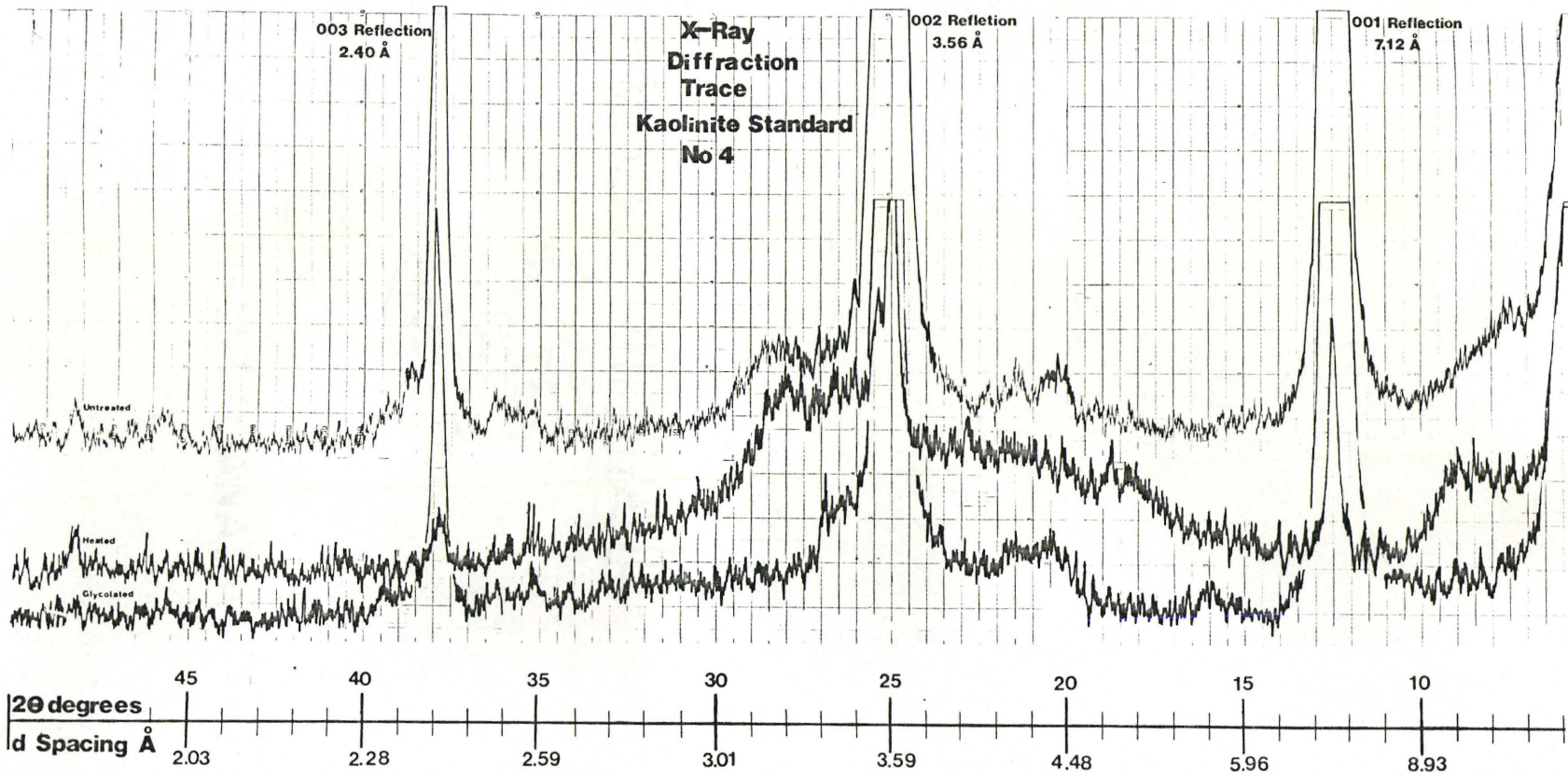
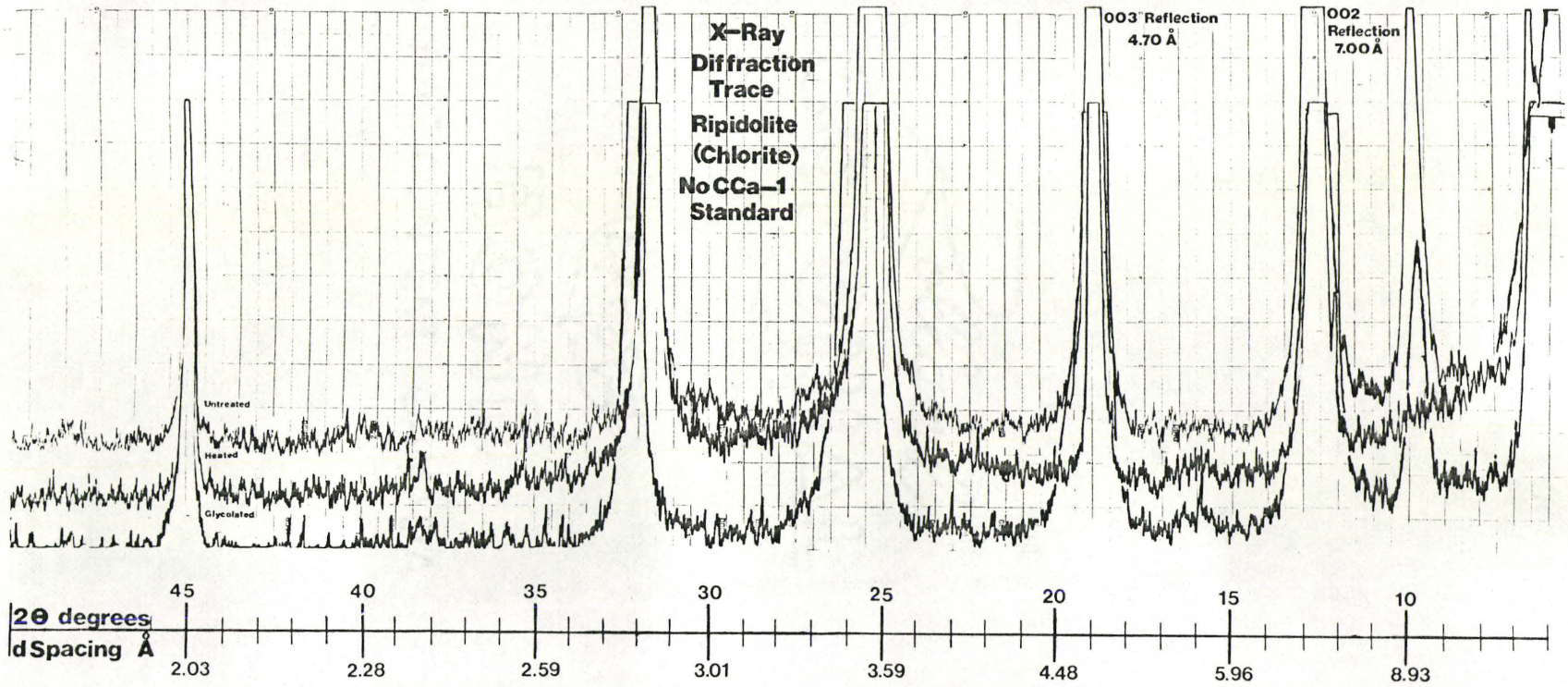




FIGURE 4-3

137



represent the 002 and 003, basal reflections of chlorite [Dr. H.D. Grundy, personal communication][refer to figure 4-3]. It should be noted that the 001 basal reflection,  $14.0 \text{ \AA}$ , occurs at around  $4^\circ 2 \theta$ . The equipment used could not resolve peaks lower than  $7^\circ 2 \theta$ .

As expected the basal reflection peaks were not affected by heating or glycolation. However, a lower order reflection peak at  $9.9^\circ 2 \theta$  was destroyed by heating, while two other peaks at  $25^\circ$  and  $31.5^\circ 2 \theta$ , were shifted down field by glycolation. These observations can be explained by the presence of mixed layer character in the standard.

#### Unknown Samples

Out of the four samples analyzed, only two, ART BASE and SYD 4, gave good results [refer to figures 4-4 and 4-5].

Comparative analysis was applied, using the standard traces prepared. The only clay present in the Whirlpool Sandstone in the study area appears to be authigenic illite.

Identification was based on the presence of the 001, 002, 003 and 005 basal reflections of illite and their behaviour when heated and glycolated. The identification was confirmed by studying the character of the lower order reflections at  $13^\circ$ ,  $25^\circ$  and  $42.5^\circ 2 \theta$ .

FIGURE 4-4

139

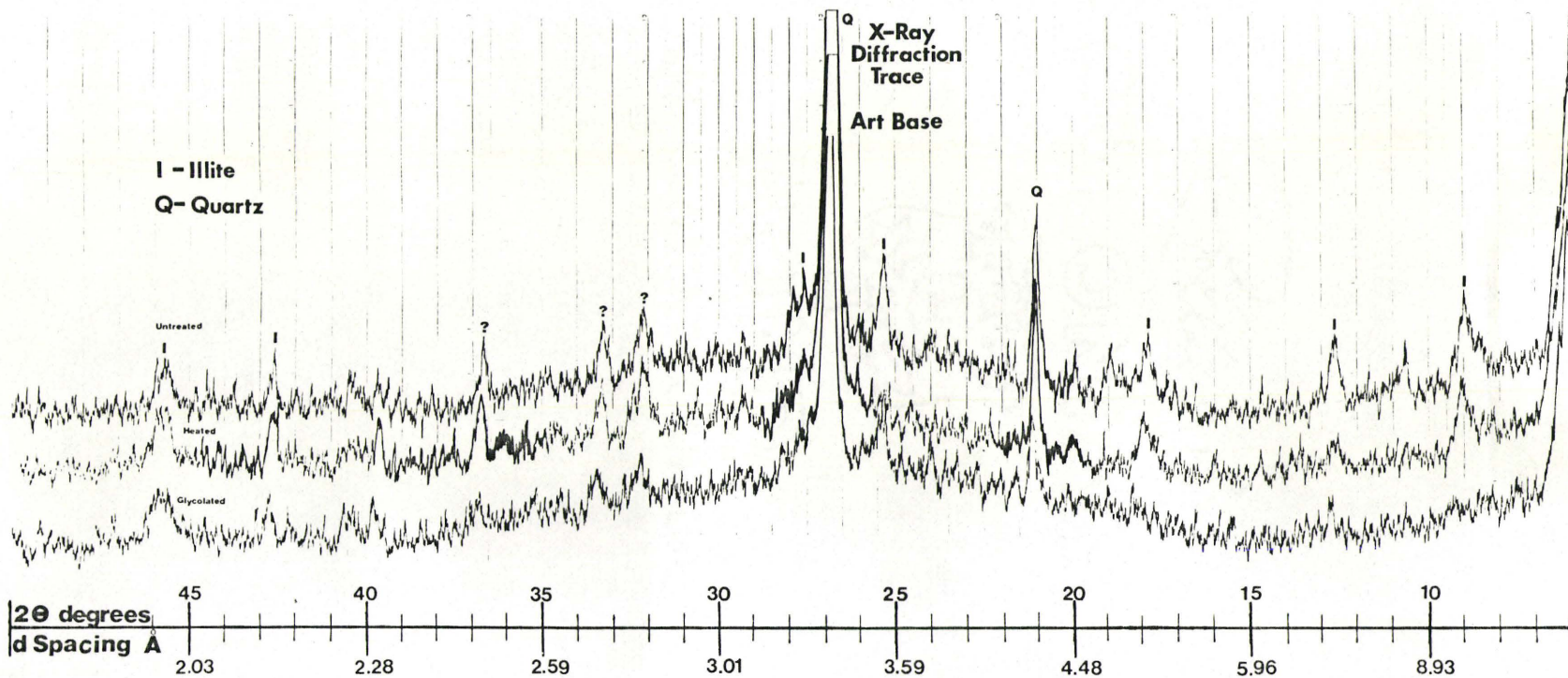
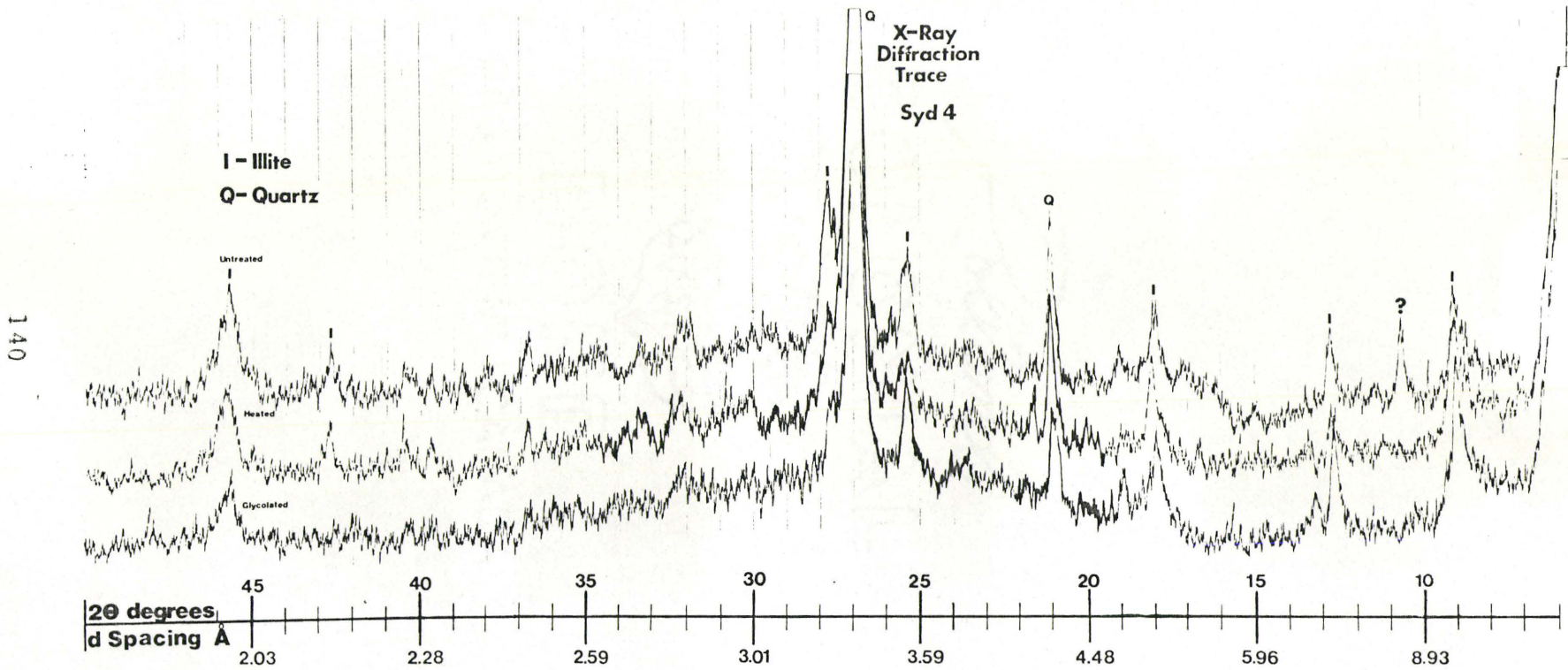


FIGURE 4-5



The lower order peak at  $25^{\circ} 2 \theta$ , was initially identified as the 002 Kaolinite peak. However, after studying the illite standard it was noted that the  $25^{\circ} 2 \theta$  standard peak has a similar profile and behaviour when heated. Also, Dr. Grundy has pointed out that the  $25^{\circ} 2 \theta$  peak of the samples was not broad enough to be a Kaolinite peak, and no other Kaolinite peaks exist in the trace. This conclusion is verified by the SEM study, no Kaolinite was found. Thus, the  $25^{\circ} 2 \theta$  peak is a lower order reflection of an illite clay showing some mixed layer character.

All of the illite peaks are sharp and well defined. This reflects the highly crystalline nature of the illite and suggests that all of the illite is authigenic in origin.

The sharp and intense peaks at  $21^{\circ}$  and  $26.75^{\circ} 2 \theta$ , represent the 100 and 011 reflections of quartz [Borg and Smith, 1969]. These peaks are the result of the crushing of quartz grains below 2 microns in size during sample preparation.

There also exist several less intense peaks that cannot be identified. These peaks are marked with a question mark, see figures 4-4 and 4-5, and are not characteristic of any common clay minerals.

#### Scanning Electron Microscopy:

##### Method

Rock chips, roughly 0.5 to 1.0 cm<sup>3</sup> in size were mounted on aluminum stubs with silver conductive paint. A gold coating, 360 Å thick, was applied to the chips using a Polaron E 5100 sputter coater. The rock chips were then examined with a Phillips 501B SEM. Unfortunately, the SEM used does not have energy dispersive analysis capability, EDAX, and thus all identification was done via comparison with published photographs, i.e. AAPG Memoir #28.

Six samples were examined, ART BASE, WHIRL 1, VIS 1, VIS 2, JOLL 1 and SYD 4. The ART BASE, WHIRL 1, SYD 4 and JOLL 1 samples were prepared from rock chips taken from the same area that had been sampled for XRD analysis.

In order to facilitate using the lower magnifications and thus obtaining maximum resolution, samples were in general taken from the coarser facies of the Whirlpool.

#### Results:

Authigenic illite was the only clay mineral identified. It was present in four morphologies.

The most common morphology observed consisted of pore lining, wispy, laths growing from the surface of quartz overgrowths [see plates 4-1a,b and 4-2a]. The next common morphology consisted of pore lining, short digitate flakes, with wispy, lath like, projections on

Plate 4-1a: Most common illite morphology, pore lining laths. Sample WHIRL 1, scale bar divisions equal 10 microns.

Plate 4-1b: Same area as above but magnified. Scale bar divisions equal 10 microns.

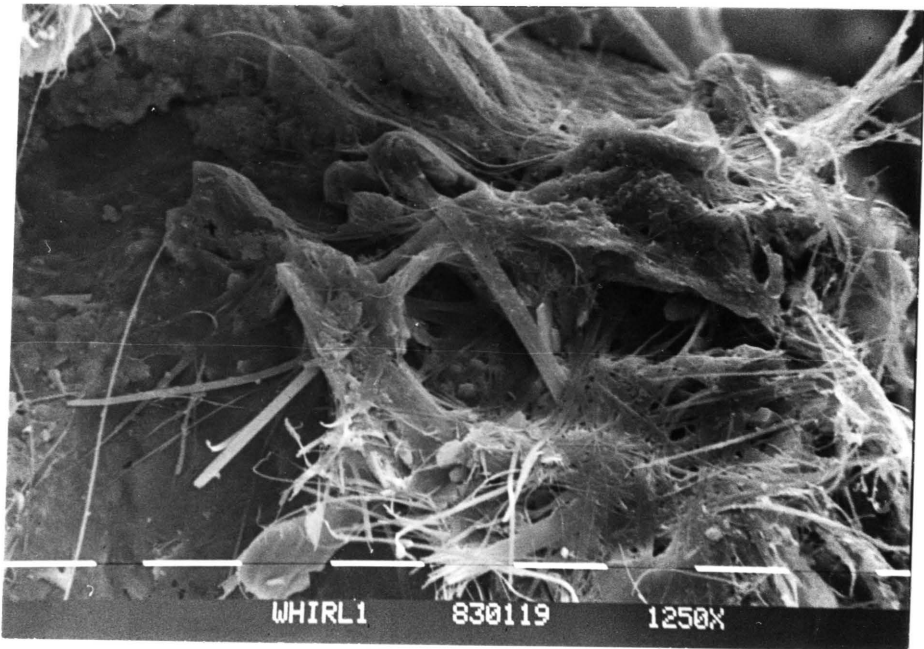
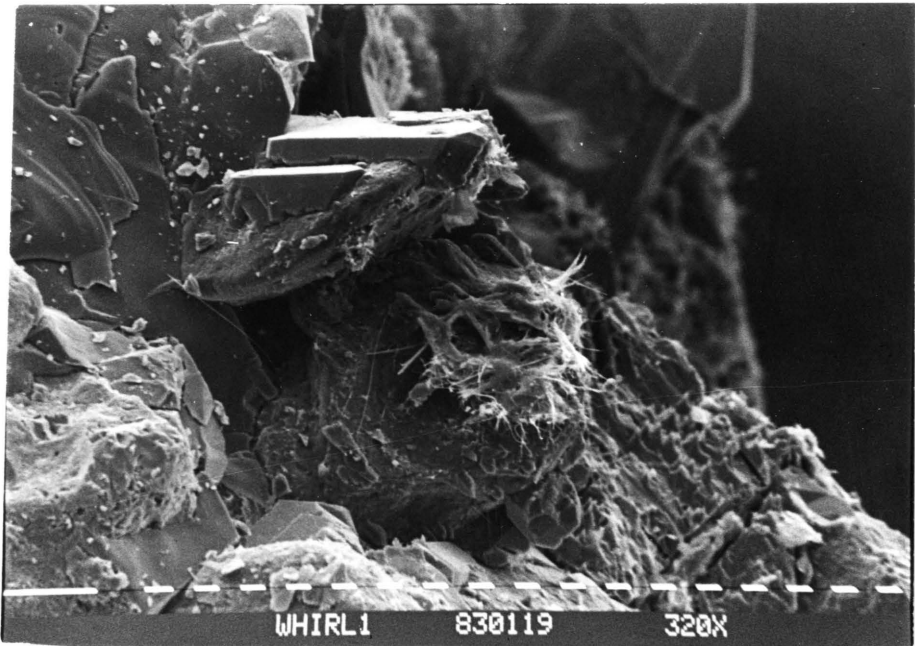
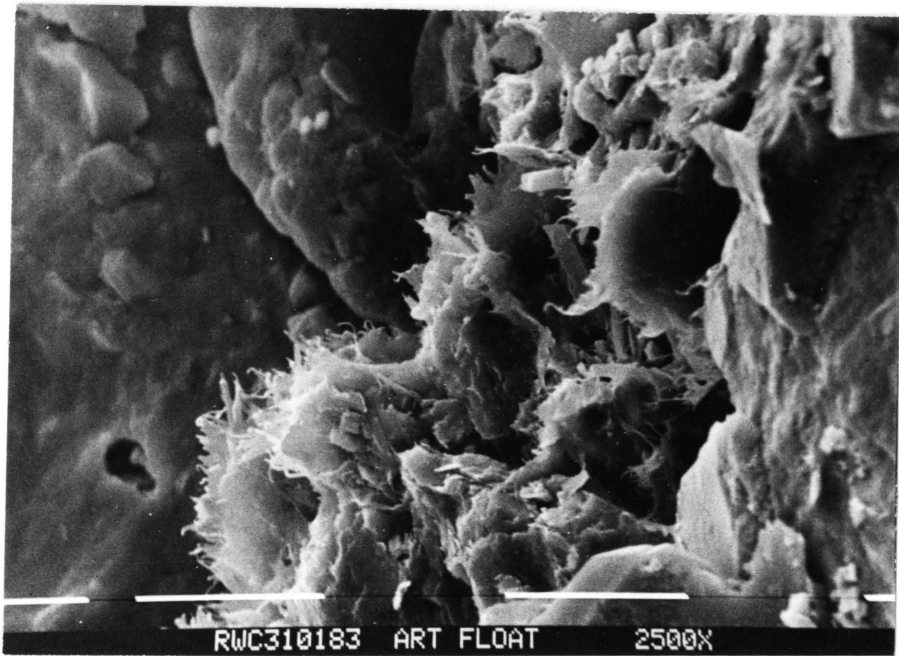
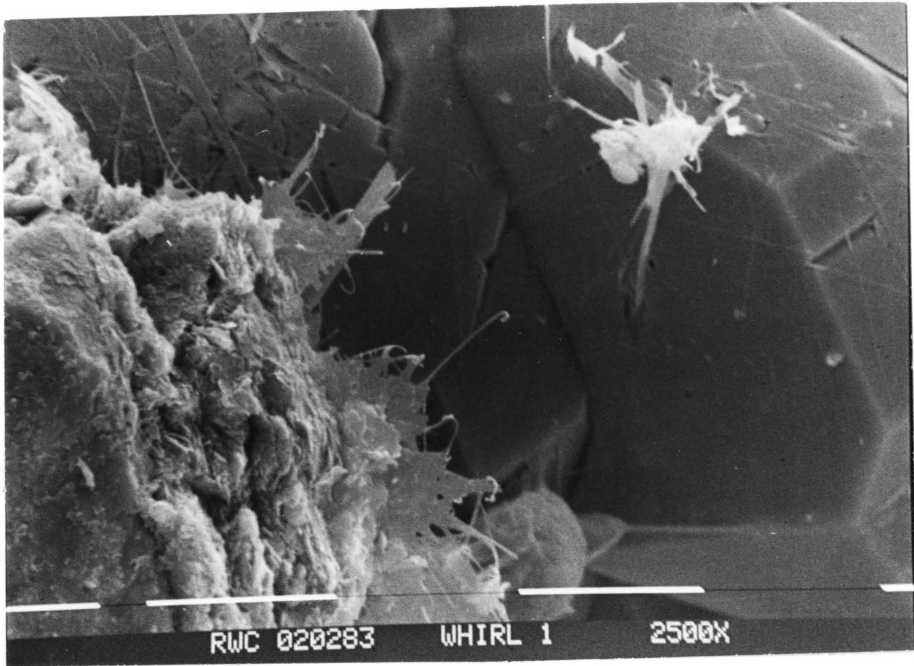




Plate 4-2a: Pore lining, wispy laths of illite.  
Sample WHIRL 1, scale bar divisions equal  
10 microns.

Plate 4-2b: Second most common illite morphology, pore  
lining, short digitate flakes, with wispy,  
lath like projections on their edges.  
Sample ART BASE, scale bar divisions equal  
10 microns.



their edges [see plate 4-2b]. The third most common morphology consisted of "spaghetti" like laths bridging pore space [see plate 4-3a]. The least common morphology observed was a "mudcrack" illite found on detrital quartz grain surfaces only [Gardiner, 1982] [see plate 4-3b].

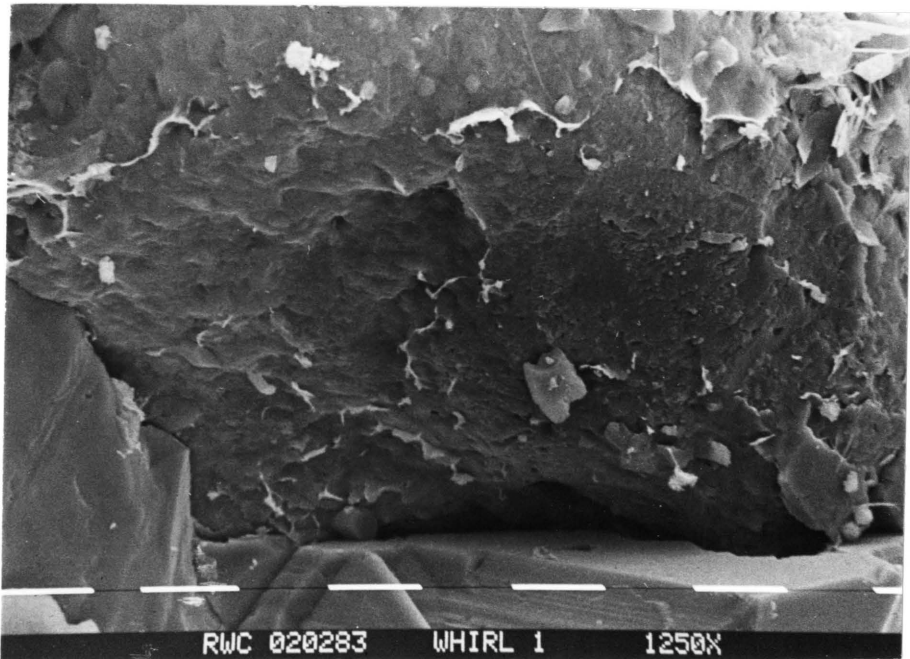
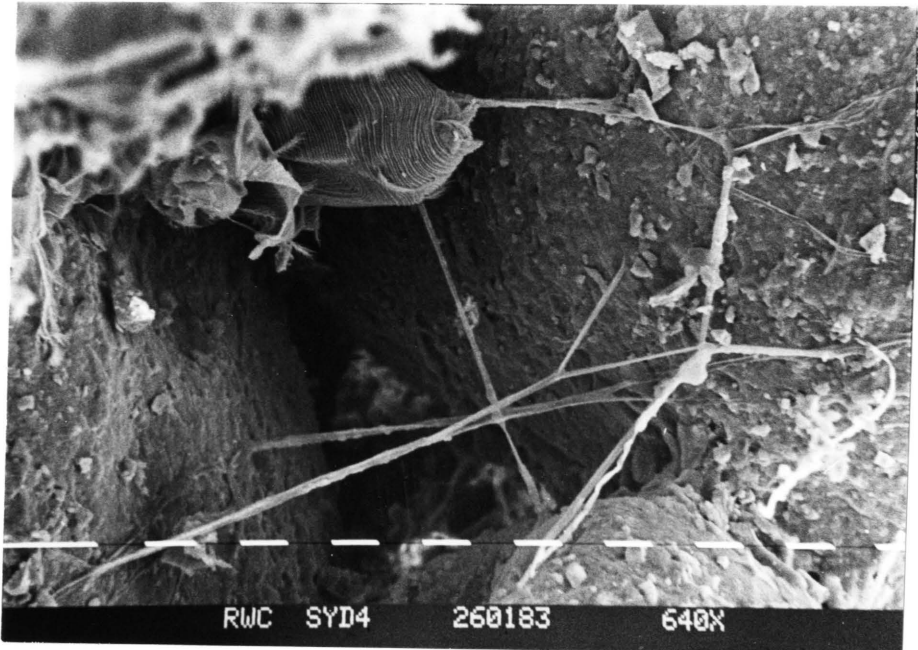
It is difficult to tell if the different morphologies represent varying times of formation. One exception might be the "mudcrack" illite. The "mudcrack" illite is found only on the surfaces of detrital quartz grains [see plate 4-3b], thus it seems reasonable to suggest that it is this illite morphology that is seen rimming quartz grains under transmitted light [see plate 3-15]. This illite is always surrounded by quartz cement and thus would be younger than the quartz cement. In areas where the illite rim was well developed, the quartz overgrowths would not be able to nucleate [Scholle, 1979] and thus, would remain in the free pore space. This exposed illite might represent the "mudcrack" illite observed under the SEM.

Dr. G.V. Middleton [personal communication] has suggested that this illite could either be detrital in origin, or have been mechanically infiltrated into the lower, coarser, units by influent surface waters, shortly after deposition by a process described by Walker [1976].

The digitate illite might represent a mixed layer

Plate 4-3a: Third most common illite morphology, pore bridging, spaghetti like laths. Sample SYD 4, scale bar divisions equal 10 microns.

Plate 4-3b: Least common illite morphology, "mudcrack" type illite on surface of detrital quartz grain. Sample WHIRL 1, scale bar divisions equal 10 microns.

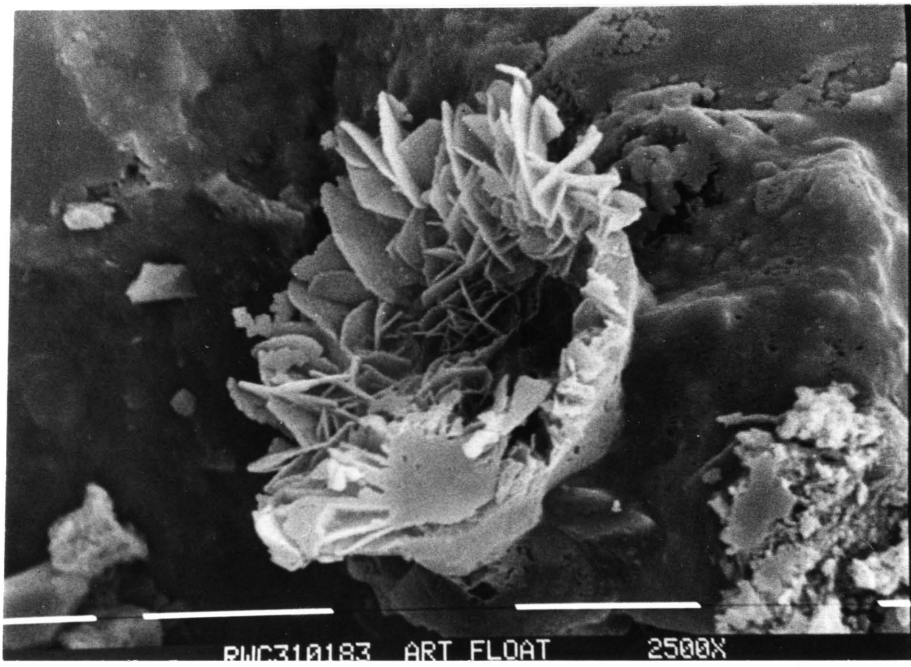
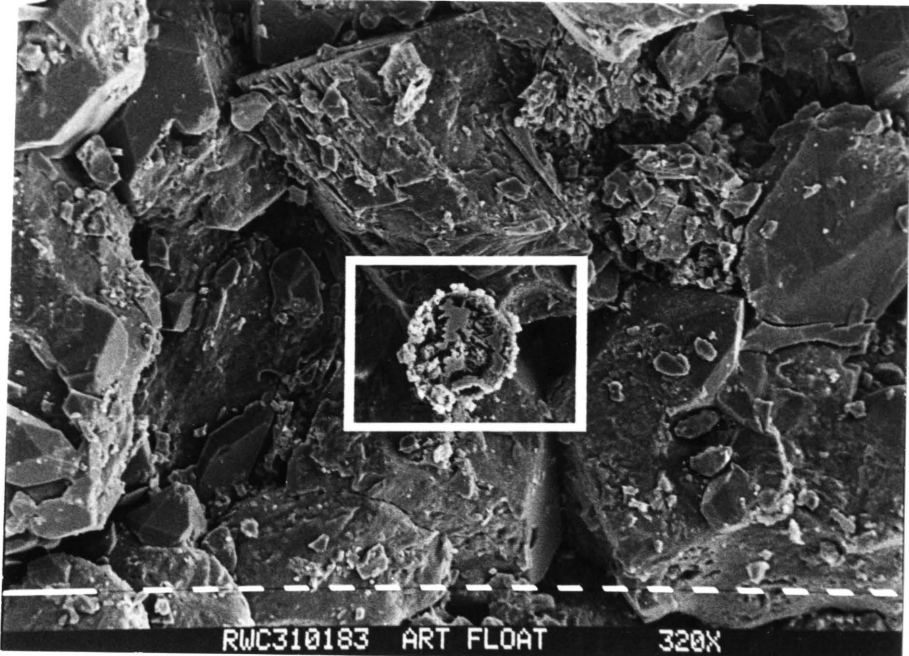


assemblage, with the pristine illite structure comprising the greater fraction [Potocki, 1981]. This mixed layer assemblage may be reflected in the XRD analysis. It is possible that the lower order peak at  $25^{\circ}$ , in the SYD 4 and ART BASE samples is from this mixed layer morphology.

In addition to the authigenic illite, an unidentified clay mineral, thought to be chlorite, was observed. The mineral has grown from the surface of quartz overgrowths in a shape very similar to a flower [see plates 4-4a,b].

Plate 4-4a: Unidentified clay mineral displaying flower like morphology, possibly chlorite. Sample ART BASE, scale bar divisions equal 10 microns.

Plate 4-4b: Unidentified clay mineral displaying flower like morphology, possibly chlorite. Sample ART BASE, scale bar divisions equal 10 microns.





## CHAPTER 5

### D I A G E N E S I S

#### Introduction:

Any diagenetic history of the Whirlpool Sandstone must explain: 1] the large amount [20%] of authigenic quartz cement that must have had an external source.

2] the occurrence of small amounts of patchy pyrite cement.

3] the formation of authigenic illite clay and the lack of any other authigenic or detrital clays.

4] the presence of ferroan and nonferroan calcite and zoned dolomite cements.

5] the fact that the processes that formed these minerals occurred at very low diagenetic temperatures.

#### Diagenetic Theory and Definitions:

Sand, originally in a non-equilibrium assemblage, seeks to equilibrate with changing physical and chemical conditions as soon as it is buried. The process of equilibration is known as diagenesis.

Hurst and Irwin [1981] have recognized seven factors that affect sandstone diagenesis:

- i] temperature

- ii] pressure
- iii] detrital mineralogy
- iv] porewater composition
- v] sedimentary facies
- vi] tectonics
- vii] time

The most important factor affecting sandstone diagenesis is porewater composition. This is due to the relatively high permeability of sandstone, which can allow the periodic flushing and replacement of porewaters of different composition. If the time between flushings is long, then the sandstone mineralogy will re-equilibrate, i.e. all unstable minerals will be replaced. If however, this time is short, then it is possible to get only partial replacement, i.e. illite coatings on authigenic kaolinite [Hurst and Irwin, 1981].

The porewater composition history of a sandstone can only be inferred. Clues can be found in the authigenic mineralogy, the tectonic history of the area, and the depositional environment of the sandstone.

Choquette and Pray [1970] have formulated a system of diagenetic regimes to be used when describing the diagenetic history of a rock. Eodiagenesis is defined as the regime at or near the surface of sedimentation where the chemistry of the interstitial fluids is mostly controlled by the surface environment. Mesodiagenesis is the subsurface

burial regime where strata have sealed the interstitial fluids of the sandstone from the effects of chemical agents at the surface. Telodiagenesis represents the unsealing of the sandstone due to uplift and erosion.

Maximum Diagenetic Temperature:

The maximum diagenetic temperature experienced by a sandstone can be calculated if the maximum depth of burial and the geothermal gradient for the area are known.

The Silurian rocks in the study area, i.e. the Whirlpool Sandstone to the Lockport Formation, are roughly 100 m in thickness, with a substantial thickening trend to the south east. Elsewhere in Southern Ontario, the Lockport Formation, the top of the Silurian in the study area, is overlain by roughly 800 m of Upper Silurian, Devonian and Mississippian sediments [Middleton, 1982].

Thus, the Whirlpool Sandstone has experienced a depth of burial of at least 900 m. Hewitt [1982] demonstrated, from a study of increased shale compaction, using interval transit times from sonic logs [after Magara, 1975, p. 20] in northern Lake Erie, that there has been roughly 530 m of erosion among the units from the Silurian to the Mississippian. If we assume that all of the erosion has occurred in the Mississippian sediments, then the Whirlpool Sandstone would have experienced a maximum depth of burial of roughly 1400 m. This last assumption is not totally correct for periods of

intense erosion are recognized in the Silurian and Devonian sediments [Sandford, 1969]. The above figure however, still provides a rough maximum to work with.

Judge and Beck [1973] calculated a geothermal gradient of  $2.58 \text{ }^{\circ}\text{C}/100 \text{ m} \pm 0.01$ , for the southern Ontario area, from a bore hole in Elgin County. Thus, if we assume that this geothermal gradient has remained fairly constant in the geologic past, the maximum diagenetic temperature experienced by the Whirlpool Sandstone could range from a minimum of  $23^{\circ} \text{ C}$ , to a maximum of  $36^{\circ} \text{ C}$ . This low diagenetic temperature is substantiated by studies of conodont and acritarch colouration carried out by Legall [1980] which indicate a maximum sub-surface temperature in the Silurian not greater than  $60^{\circ} \text{ C}$ . Also, gas wells in Lake Erie have revealed temperatures in the Silurian of roughly  $20^{\circ} \text{ C}$  at depths of 700 m [Judge and Beck, 1973].

Since all the units thicken substantially to the southeast, it is reasonable to assume that this reflects movement into the centre of the depositional basin. Thus, the depth of burial of the Whirlpool Sandstone in the Niagara Gorge would be greater than in the Hamilton area [roughly 100-200 m] and thus, a slightly higher maximum diagenetic temperature could be expected [ $3$  to  $5^{\circ} \text{ C}$ ] for the sediment at the Niagara Gorge.

Eodiagenesis:

### Mechanical Porosity Reduction

The main process operating during eodiagenesis is the mechanical reduction of porosity, [Schmidt and McDonald, 1979]. In the Whirlpool Sandstone mechanical compaction has reduced initial porosity by 10%, if one assumes an initial sediment porosity of 40% [Blatt et al., 1980, p. 417] and a calculated minus cement porosity of 30% [Chapter 3].

Mechanical compaction occurs by grain slippage, rotation and ductile grain deformation. Evidence for grain slippage and rotation is not observed, but these processes are associated with pressure solution. There does exist evidence to suggest that minor amounts of pressure solution have occurred, i.e. concavo-convex and sutured grain contacts [see plates 3-24a,b and 3-25a,b].

### Early Pore Fluid Composition

The initial pore fluids of the Lower Whirlpool Sandstone beds would have been fresh in nature. But, with the marine transgression, the fresh water would have been flushed and replaced with seawater. Thus, we are dealing with the early diagenesis of a sand with marine porewater, i.e. it is unlikely that the fresh water was present long enough to have any pronounced, or observable effects on the sediment.

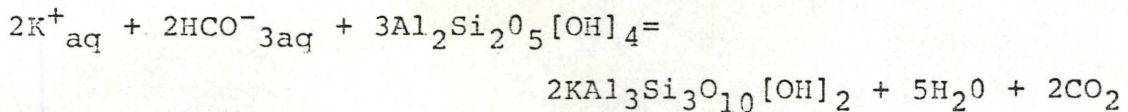
Aerobic bacteria present near the sediment-water interface utilize free oxygen and release CO<sub>2</sub>, when consuming

organic constituents in the sediment. This effectively lowers the pH of the porewater from 8.0 to approximately 6.5, depending on the amount of detrital carbonate present [Collins, 1975]. If a large amount of detrital carbonate is present, it will buffer the pH, maintaining it at higher levels. In the case of the lower Whirlpool sand, carbonate probably was not present. At depths greater than 0.5 m below the sediment-water interface free oxygen is no longer available. Anaerobic bacterial activity serves to elevate the pH to roughly 9.0 [ibid.]. If any detrital carbonate remains below this depth, it will be protected from further dissolution until later on in the mesodiagenetic regime. Also, any organic material that has survived to these levels will go on to form hydrocarbons at greater depth [ibid.].

#### Early Clay Diagenesis

Any detrital clays deposited along with the lower fluvial sands of the Whirlpool would have been transported from the source area, without alteration [Rhoten and Smeck, 1981]. Alteration will take place during halmyrolysis and early diagenesis. Halmyrolitic alteration occurs when detrital clays from fresh water environments mix with seawater. In the Whirlpool, this would occur, after deposition, during the marine transgression. It is difficult to fix the types of detrital clays that could be expected, due to the fact that the source beds were largely pre-existing sediment. If we

consider that early clay diagenesis takes place in the top few meters of sediment [ibid.] and that in this period any excess bicarbonate not reacting to form bicarbonate could react with detrital kaolinite to form illite by a reverse weathering reaction:



[Berner, 1971, p. 181], then it would be possible to form illite early in the diagenetic history. Since illite would not be expected to be stable in a fluvial system, the "mudcrack" illite described in Chapter 4 might have been formed by the above process. It is impossible to ascertain if the "mudcrack" illite was formed by conversion of kaolinite in situ, or by the infiltration of already transformed kaolinite, down into the lower units of the Whirlpool, in a manner described by Walker [1976]. It should be noted that the formation of carbonate is highly favoured; thus, not much excess bicarbonate would exist and little illite could be formed in the above manner. The "mudcrack" illite is still consistent with this hypothesis for it exists in small amounts only. The large scale formation of authigenic illite occurs later on in the mesodiagenetic regime.

#### Formation of Pyrite

The principal factors that limit the amount of pyrite, or any sulphide, which can form in a sediment, are the availability

of reduced sulphur and the concentration and reactivity of iron compounds [ibid., p. 203]. Figure 5-1 displays the pyrite stability field, on an Eh vs.  $pS^2$  diagram [after Berner, 1971, p. 196].

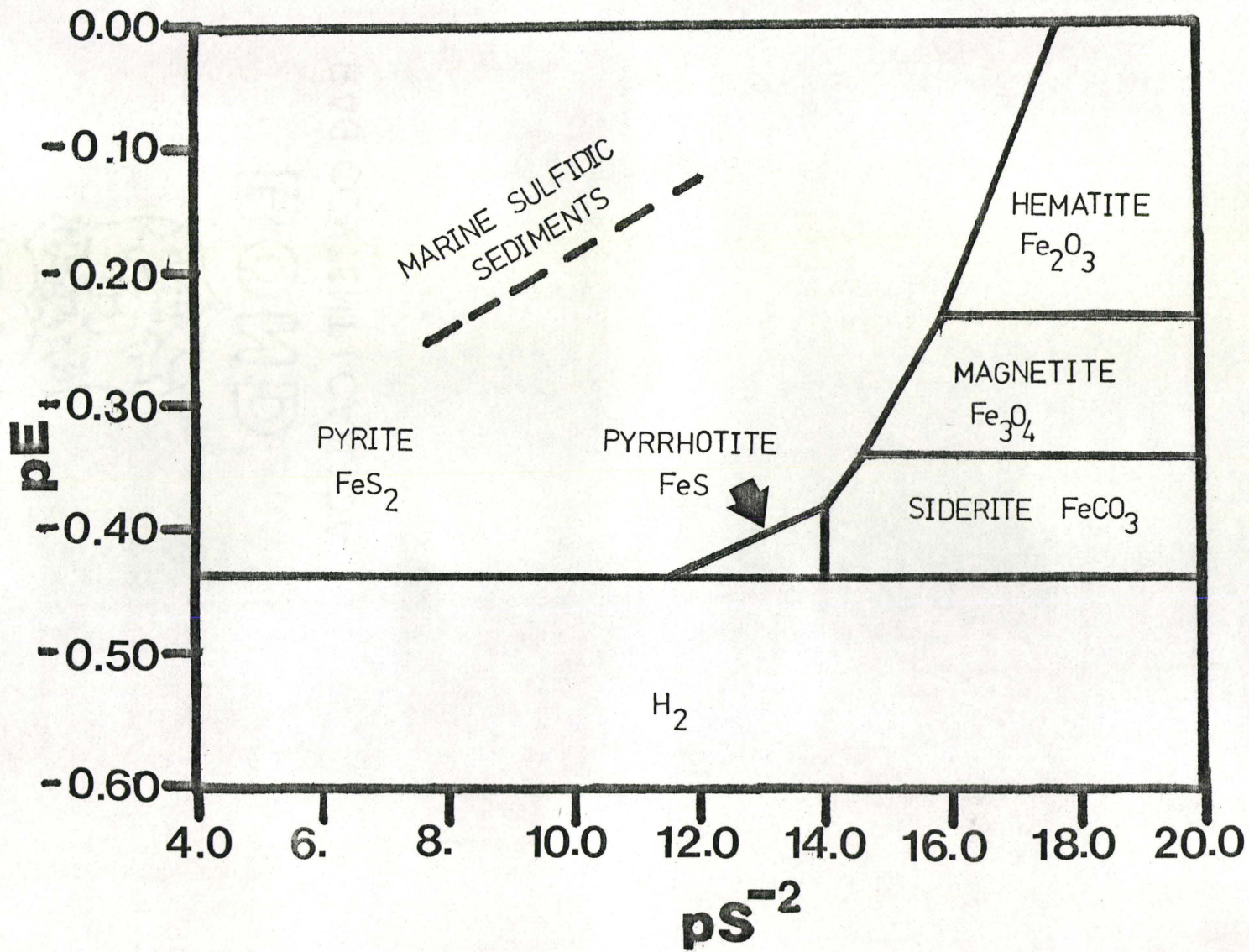
There are two possible sources of reduced sulphur. Sulphur reducing bacteria can produce  $H_2S$  if there are available concentrations of dissolved sulfate and metabolizable organic matter [ibid, p. 200-207]. Middleton [personal communication] has suggested a second source, the up-dip migration of  $H_2S$  bearing fluids from areas deep within depositional basins where the maturation of hydrocarbons is occurring.

Since the lower units of the Whirlpool Sandstone are fluvial in origin, large amounts of organic matter would not be expected. Thus, the relatively early migration of  $H_2S$  bearing fluids, up-dip from the southeast, seems to be the only logical source of reduced sulphur. Middleton has also suggested that these reducing fluids could account for the reduced zone at the top of the Queenston Formation described in Chapter 2.

One might expect the pyrite cement to be more extensive in the study area if the above hypothesis is considered, due to the release of large amounts of reduced iron from the Queenston Formation. However, Candy [1963] has shown that little iron has moved from this reduced zone,



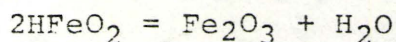
Figure 5-1: Eh vs.  $pS^{-2}$  diagram for pyrite, pyrrhotite, hematite, magnetite and siderite.  
pH = 7.37,  $\log P_{CO_2} = -2.40$ ,  $T = 25^\circ C$ ,  
 $P_{total} = 1 \text{ atm}$ . The field marked  $H_2$  corresponds to the area where water is unstable relative to  $H_2$  gas. Measurements of modern marine sulphidic sediments fall closely along the dashed line [after Berner, 1971, p. 196].



rather it has simply been reincorporated into ferrous iron minerals, e.g., Fe-chlorite. Even without reduced iron from the Queenston, the concentration of iron in the pore fluids should have still been substantial. Thus, there must have been some other, unidentified control on the formation of pyrite.

### Hematite Formation

Hematite is formed primarily from the alteration of ferromagnesian minerals [Walker, 1974]. However, it is possible to form hematite from goethite:



[Berner, 1971, p. 197]. Hematite is stable only at high Eh and  $pS^{-2}$  values and is unstable in the pyrite field [see figure 5-1]. Thus, the hematite present in the Whirlpool Sandstone must have formed before the pyrite cement and later been reduced, leaving only minor amounts as rims around detrital quartz grains.

### Eodiagenetic Cements

Porosity filling cements are almost exclusively formed in the mesodiagenetic regime, but there is good evidence that suggests that there has been early cementation in the Whirlpool.

The fact that mechanical compaction has only reduced initial porosity by 10% on average suggests that there has been early cementation that has partially lithified the

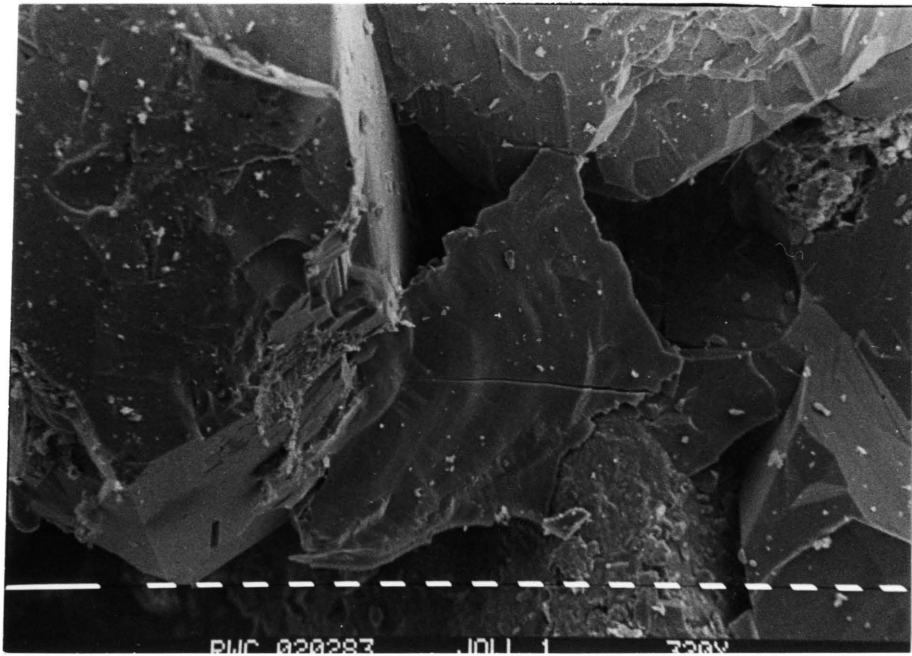
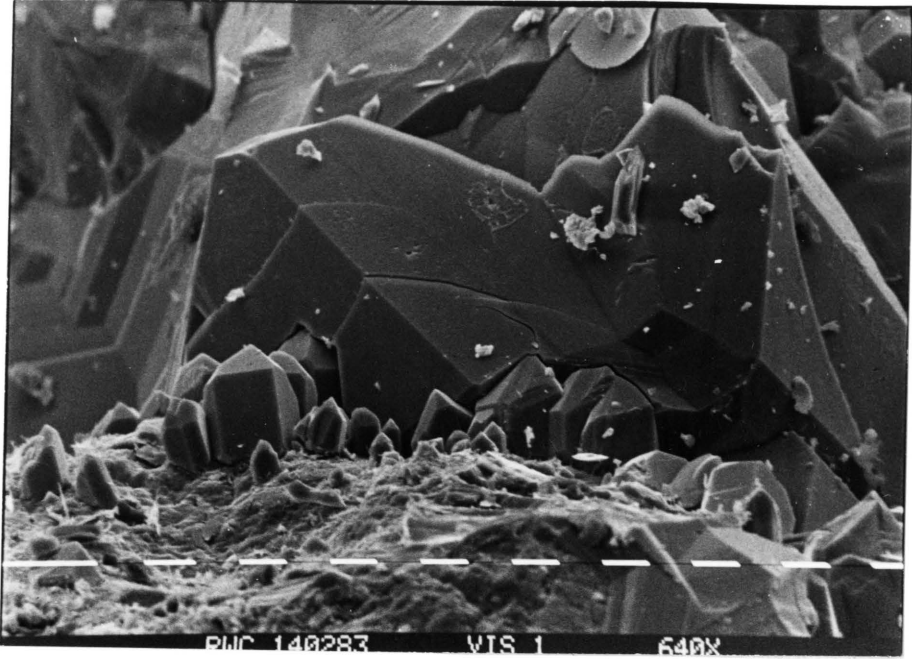
sediment, thereby inhibiting mechanical compaction.

The first cement to have formed appears to be quartz [see plate 3-1a and 5-1a] possibly in response to pressure solution, brought about by mechanical compaction [Robin, 1978]. This cement is observed to be present as isolated, euhedral, single crystals of quartz on the surface of detrital quartz grains. Minor ferroan calcite cement is seen to be replacing detrital quartz grains and is surrounded by the second generation massive quartz cement [see plate 3-7a]. Galloway [1974] recognized the presence of early stage pore filling calcite cement and attributed it to a near "sedimentation surface" process. Boles and Frank [1979] suggest that the source of calcite cements may be from the conversion of smectite to illite. This process will release  $\text{Ca}^{+2}$  which will lead to the formation of calcite cement, until sufficient iron and magnesium are released to stabilize other minerals.

Elevated levels of  $\text{Ca}^{+2}$  could be introduced into the Whirlpool Sandstone early in its diagenetic history by the early migration of pore fluids up-dip from deep within the depositional basin. It has already been demonstrated that migratory fluids containing  $\text{H}_2\text{S}$  were responsible for the eodiagenetic precipitation of pyrite. Thus it seems reasonable to suggest that these same fluids were rich in  $\text{Ca}^{+2}$  due to the conversion of smectite to illite in the shale units deep

Plate 5-1a: Photograph showing primary and secondary massive quartz cements. Sample VIS 1, scale bar divisions equal 10 microns.

Plate 5-1b: Photograph showing third generation, pore bridging quartz cement. Sample WHIRL 1, scale bar divisions equal 10 microns.



within the depositional basin to the southeast, where the diagenetic temperatures were higher [Boles and Franks suggest temperatures greater than 60° C].

The volume of these early cements is insignificant compared to mesodiagenetic quartz and calcite cements.

#### Mesodiagenesis:

It is during the mesodiagenetic regime that the bulk of primary interparticle porosity is reduced by the formation of authigenic cements. It is also during this regime that the major proportion of secondary porosity developed.

Four textural stages in mesodiagenesis have been recognized by Schmidt and McDonald [1979]. Figure 5-2 displays these stages and their effects on porosity. Figure 5-3 schematically demonstrates the major processes that have affected porosity during mesodiagenesis in the Whirlpool Sandstone [after Schmidt and McDonald, 1979].

#### Quartz Cement:

Quartz cementation occurs at, or near, the maximum depth of burial [Dr. G.V. Middleton, personal communication]. During this period, pore fluids are oversaturated with respect to silica and precipitation occurs, via nucleation on detrital quartz grains [see figure 5-4].

The secondary, massive quartz cement identified in the Whirlpool was formed at this time [see plate 5-1a].

Figure 5-2: Textural changes of porosity during mesodiagenesis indicating progressive burial (after Schmidt and McDonald, 1979).



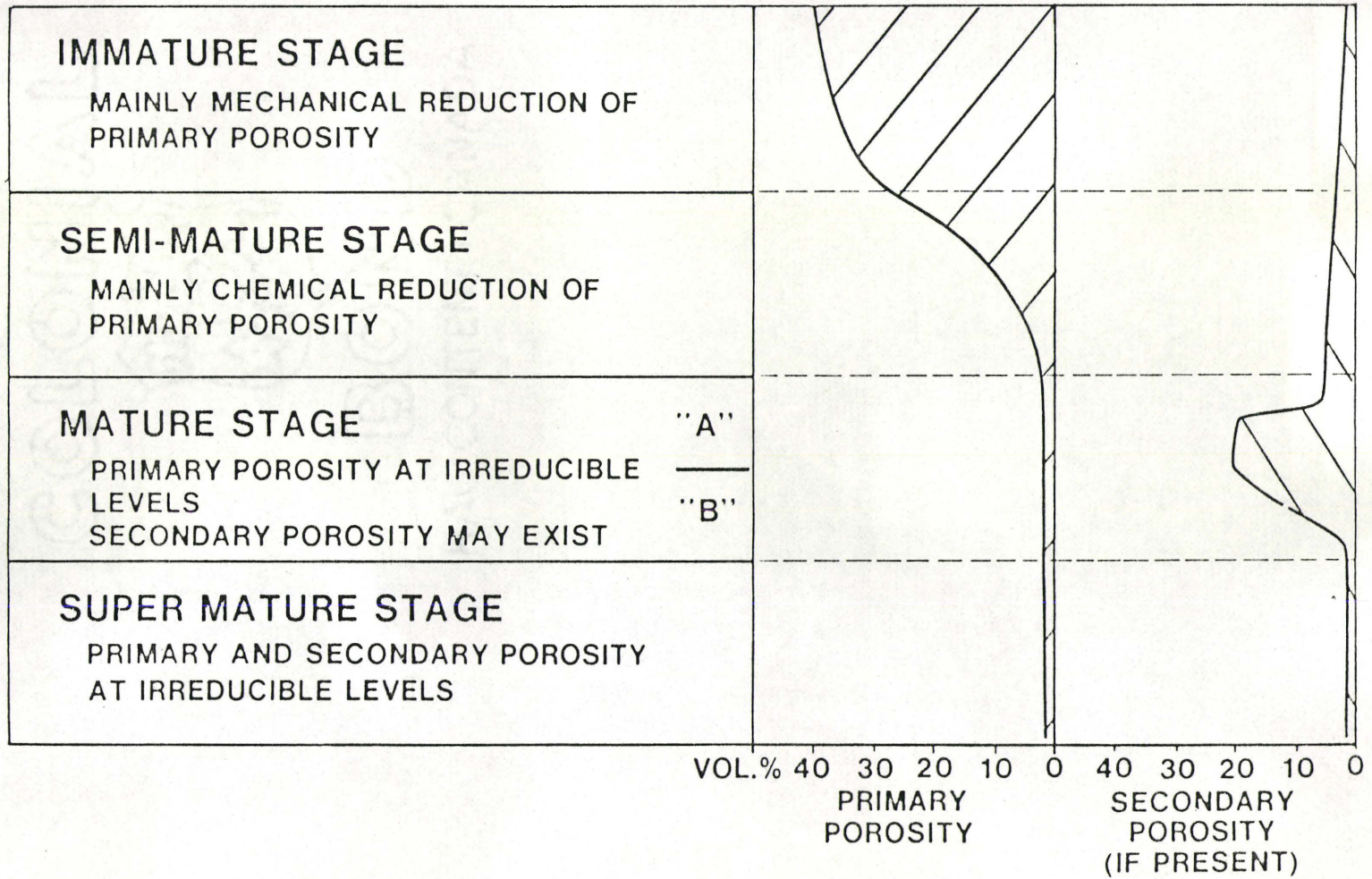


Figure 5-3: Schematic representation of the major processes affecting porosity during mesodiagenesis in the Whirlpool Sandstone. (after Schmidt and McDonald, 1979)

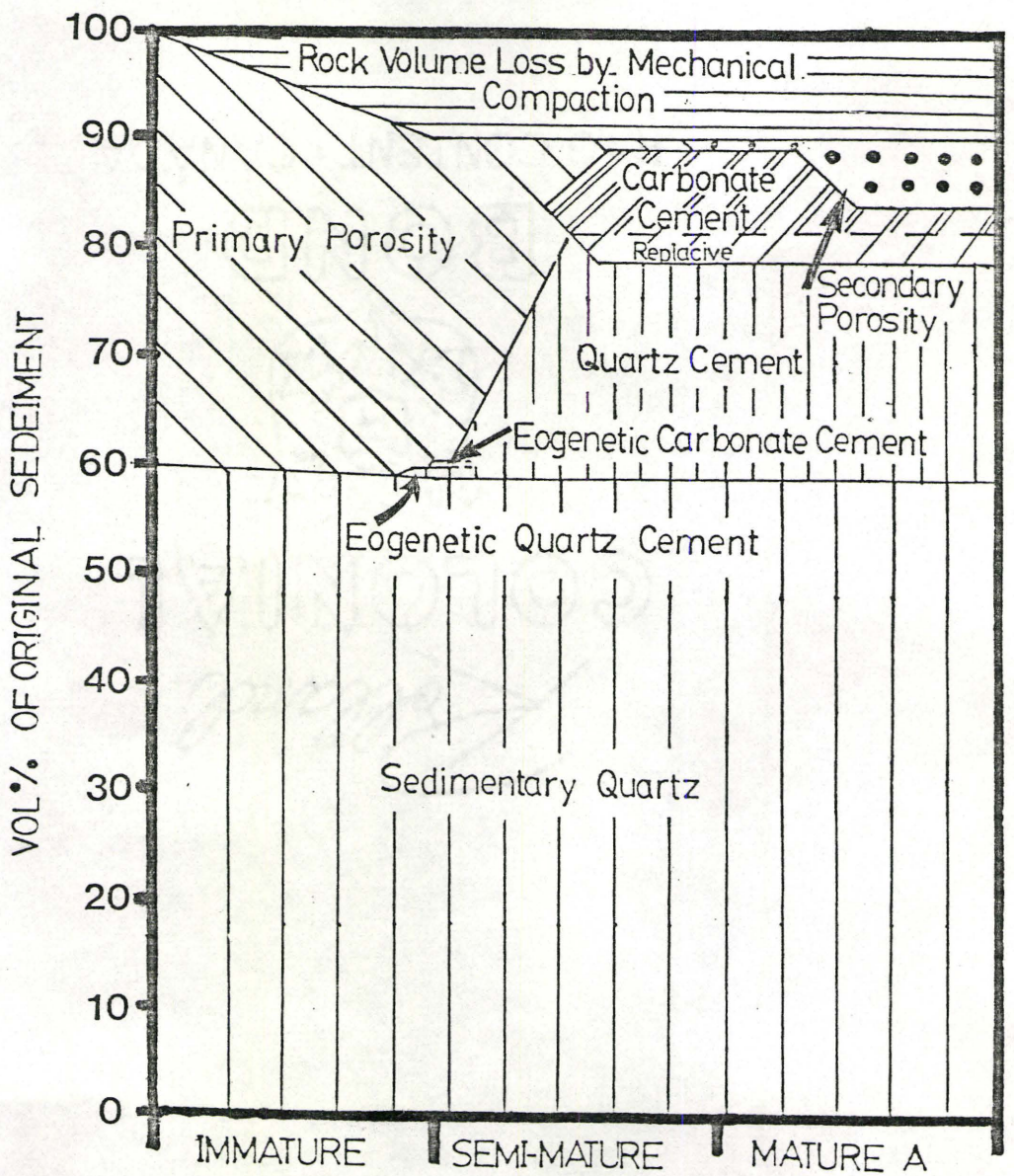
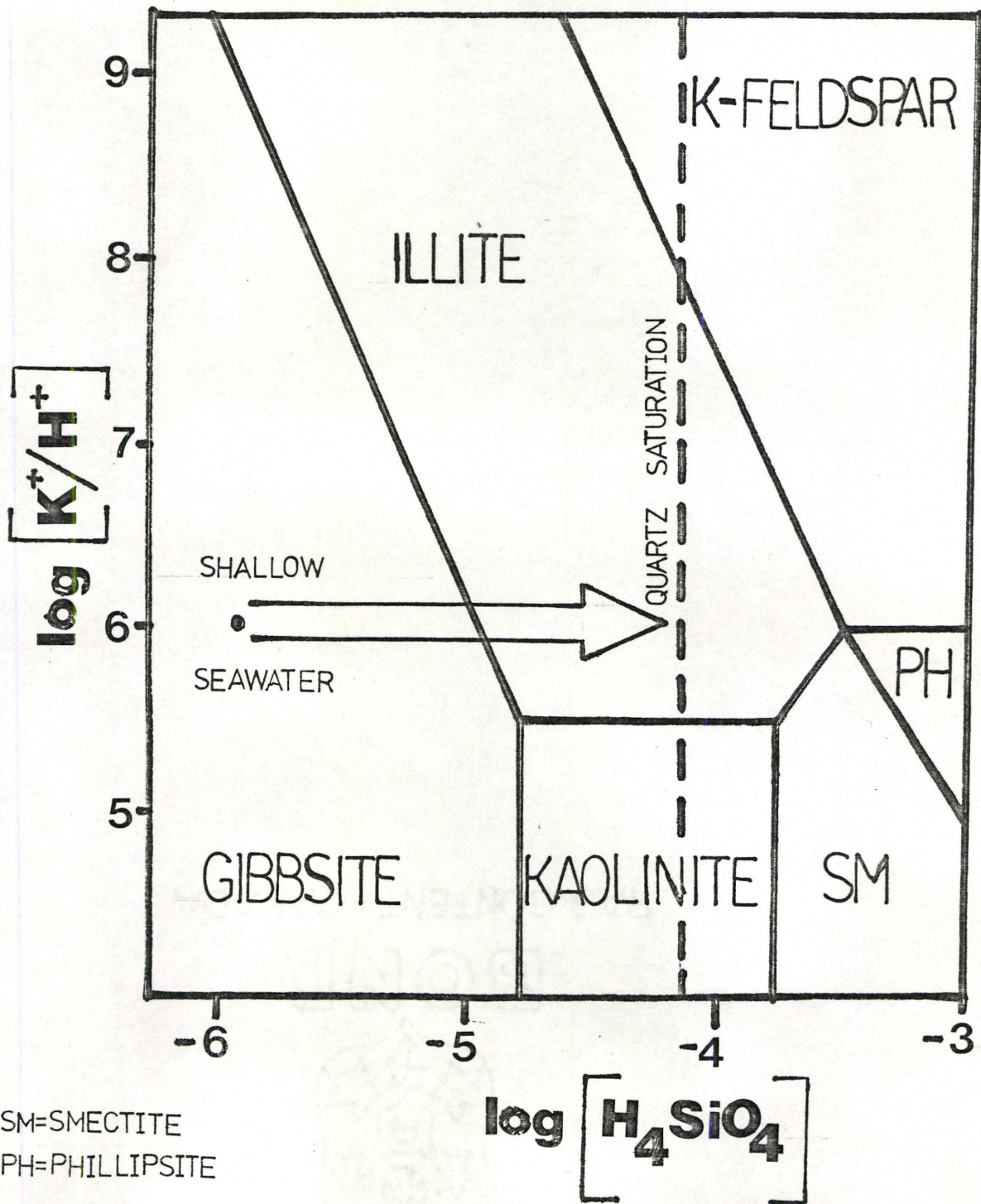


Figure 5-4:  $\text{Log}(K^+/H^+)$  vs.  $\text{log}(H_4\text{SiO}_4)$  diagram showing the changing chemical composition of the porewaters in the Whirlpool Sandstone. Fluids first reached quartz saturation causing precipitation of quartz overgrowths. Soon after the direct precipitation of illite occurred. (after Drever p. 102)



SM=SMECTITE  
 PH=PHILLIPSITE

As described in Chapter 3, there are several possible origins for this cement. The most logical source appears to be diffusion of free silica from the surrounding shales. There exists a problem with this hypothesis due to the fact that the units within the study area never experienced the high diagenetic temperatures necessary to promote this reaction. Boles and Franks [1979] have demonstrated that the illitization of smectite occurs at temperatures in the 60 to 175°C range. Legall [1980] has demonstrated that the maximum diagenetic temperature experienced by the Whirlpool Sandstone was less than 60°C, thus, the conversion of smectite to illite could not have occurred locally. It is possible; however, that this process did generate the free silica found as authigenic quartz cement in the study area, only it occurred deep within the depositional basin to the southeast. Thus, the authigenic quartz cement would have precipitated in response to migrating pore fluids saturated in silica [Middleton, personal communication].

Land and Dutton [1978] suggested a similar source for the quartz cement in the Strawn Series of Pennsylvanian Sandstones in Texas. They calculated that  $10^5$  volumes of a 10 ppm silica pore fluid would be needed to produce 10% quartz cement in each  $\text{cm}^3$  of rock. They also suggested that this water might have been derived from the dewatering of compacting shales at a late stage of burial. Bjorlykke [1979]

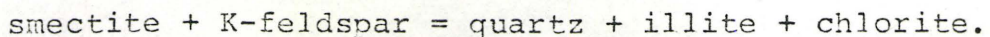
suggests that even allowing for channelized flow of water from large volumes of basinal shales moving up-dip through sandstones it would be impossible to produce the great volume of water needed to precipitate large amounts of silica cement. Blatt [1979] concluded that silica released from mudrocks is insufficient to cement sandstones. Bjorlykke [1979] also suggests that it might be possible to cement small thicknesses of sandstone if higher fluxes of water can be moved through the sandstone, e.g., groundwater circulation.

The Whirlpool Sandstone is surrounded by large thicknesses of relatively impermeable shales [800 m of Queenstone shale alone] and the thicknesses of these shales increase rapidly to the southeast. The Whirlpool Sandstone would present a highly porous medium for movement of water out of the basin. Thus, it is possible that great volumes of water could have been channelled out of the basin through the Whirlpool [Middleton, personal communication]. Since the volume of shale is so large, a great deal of diagenetically derived water could have been produced and travelled out through the Whirlpool. Also, it is possible that an aquifer system was present on the west side of the Appalachians, similar to the system that is present today on the east side of the Rockies.

Thus, it is possible that there existed large amounts

of silica saturated waters deep within the depositional basin to the southeast of the study area, but the ability of large volumes of this water to travel such long distances [on the order of 1000 km] through increasingly cement filled pore spaces in the Whirlpool, is not known. A great deal more work needs to be done on the Whirlpool Sandstone in the northwest and the southeast in order to determine the existence of trends in the quartz cementation.

A third generation of quartz cement present only in very minor amounts has also been identified [see plate 5-1b]. It consists of pore bridging quartz cement that has grown on the massive quartz overgrowths. The source of this cement probably lies in the formation of secondary porosity due to the dissolution of feldspars. Thus, it seems reasonable to suggest that it also post-dates the calcite cement, since the calcite cement is observed to conform to the original outline of now badly weathered feldspars. The feldspars could have been dissolved by water containing large amounts of CO<sub>2</sub>, producing free silica and kaolinite, [see equation above], or by the following reaction developed by Hoffman and Hower [1979]:



This last mode of formation would seem more reasonable as no authigenic kaolinite is observed and the bulk of the feldspar in the Whirlpool is badly weathered microcline.



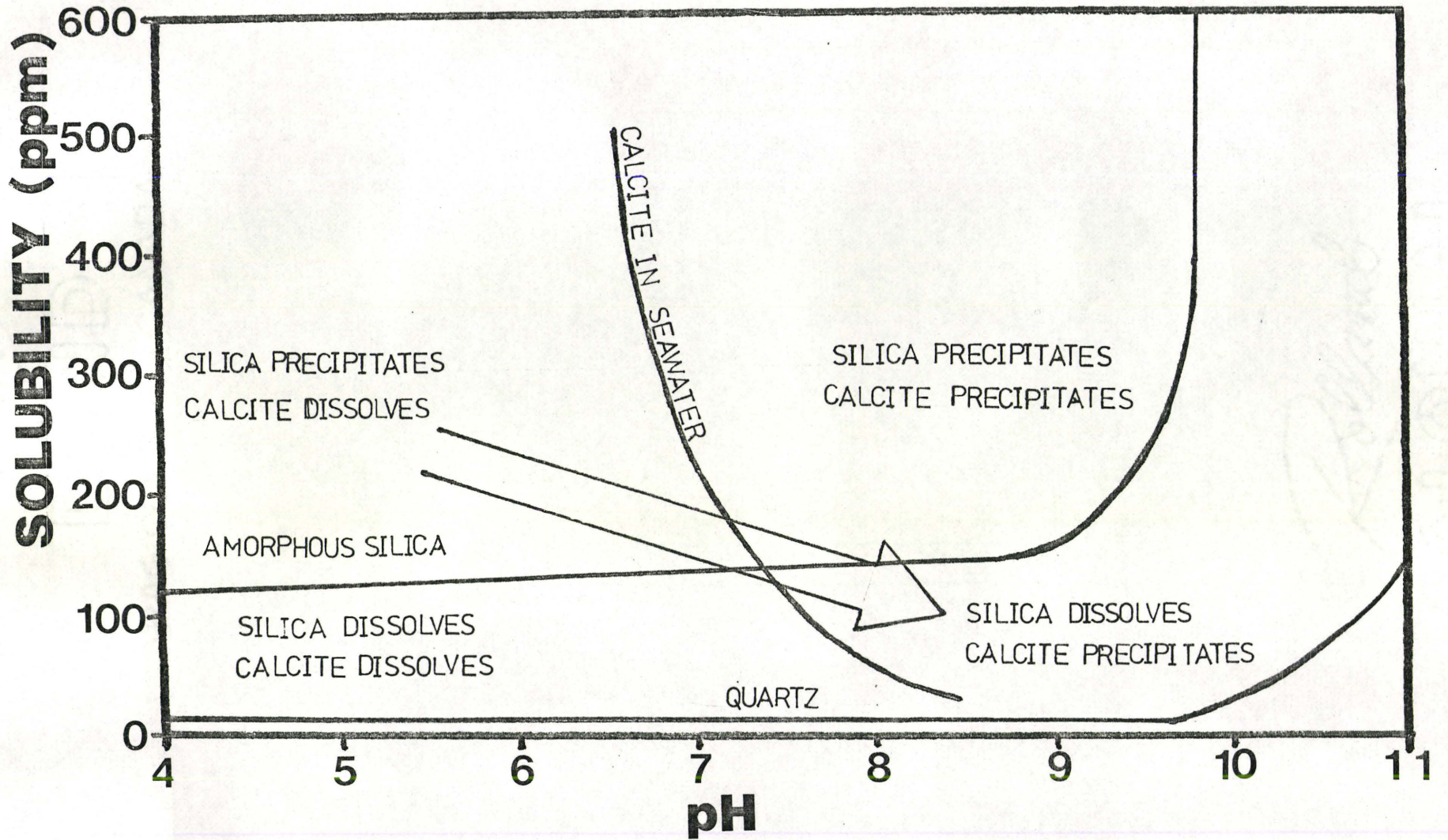
### Carbonatization:

The bulk of the carbonate cement has formed after the mesodiagenetic quartz cementation. There is also evidence that suggests that calcite cement has replaced quartz overgrowths and detrital grains to a minor extent [see plate 3-7b]. It has also been demonstrated that there is more calcite cement in the upper marine units of the Whirlpool than in the lower fluvial units. Since the amount of calcite cement is not constant throughout the Whirlpool, it is unlikely that the source of the cement was the up-dip migrating pore fluids. Rather, it seems more reasonable to suggest that the calcite was derived from local detrital carbonate deposited in the upper marine beds. Schmidt and McDonald [1979] also suggest that the source of calcite cement is local detrital shell material.

If we assume that the detrital carbonate is the source of the calcite cement, then the chemical environment in the sandstone must have been such that the carbonate was dissolved without substantial mixing of the  $\text{Ca}^{+2}$  rich fluids with the bulk porewaters. The environment must have then changed drastically in order to precipitate the calcite cement.

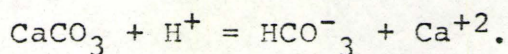
The migrating pore fluids that carried in the free silica that formed the quartz cement would have been acidic in nature [see figure 5-5]. Thus, it is possible that these fluids caused the dissolution of the detrital carbonate. The

Figure 5-5: Solubility vs. pH diagram showing the changing nature of the porewater in the Whirlpool Sandstone during diagenesis [after Blatt et al, 1980, p. 348].



only way in which the  $\text{Ca}^{+2}$  rich fluids could be kept from mixing with the bulk pore fluids would be due to the fact that the porosity of the Whirlpool had been progressively occluded by the quartz cement and thus, the movement of the  $\text{Ca}^{+2}$  fluids down into the fluvial beds would have been inhibited. Quartz cementation probably ceased when the porosity of the Whirlpool had been lowered to the extent that fluid migration was inhibited. Thus, the calcite cement probably precipitated from static pore fluids.

The dissolution of carbonate is controlled by the reaction:



If we assume that the pH of the pore fluids was such that  $\text{HCO}_3^-$  was the dominant species [pH=6.3 to 9.3] and that after the pore water became static the pH was controlled by mineral reactions with an aqueous phase; then the addition of  $\text{CO}_2$  would have increased the amount of  $\text{HCO}_3^-$  via the dissociation of  $\text{H}_2\text{CO}_3$ . This would lead to an increase in the solubility product for the above reaction and calcite would have been precipitated [Hutcheon, 1982]. The source of the  $\text{CO}_2$  might have been the decay of organic detritus in the upper marine beds. The type of mineral reactions needed to control the pH might have been the alteration of feldspars, or perhaps the alteration of detrital and early authigenic clays to illite [see formation of illite, chapter 5].

There is evidence that suggests that calcite has played a part in the alteration of microcline [see plates 3-6a,b].

Both ferroan and nonferroan calcite cement have been observed [see chapter 3]. Ferroan calcite is calcite that contains small amounts of FeO. The ferroan cement appears to be more abundant, in general, than the nonferroan and it also post-dates it [see plate 3-5b]. The nonferroan calcite is most abundant in the upper marine beds of the Whirlpool [see Tables 3-2a,b to 3-5a,b], which suggests that the nonferroan calcite has reprecipitated close to where it was dissolved, i.e., there has been little mixing with the bulk pore fluids.

#### Decarbonatization

The major proportion of secondary porosity has probably been formed due to the dissolution of calcite cement during decarbonatization. The dissolution of calcite can result either from decrease in pH, or by the mixing of two chemically dissimilar waters i.e., fresh and saline, resulting in a mixture undersaturated with respect to calcite [Stanton, 1977].

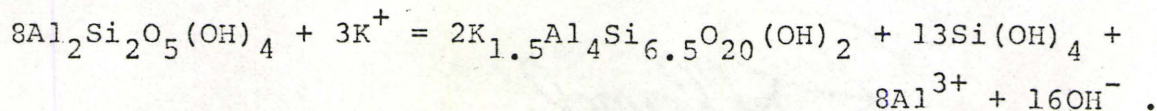
The pH can be lowered due to shale diagenesis in overpressurized zones, or by the maturation of organic hydrocarbons [ibid.]. It is hard to envisage these processes occurring locally in the study area due to the low diagenetic temperatures. Also, since the porosity of the Whirlpool at this

time would have been reduced to very low levels [less than 5%] due to quartz and calcite cementation there would have been no up-dip migration of pore fluids. Thus, the dilution effect from the release of local intershale water during diagenesis is favoured, i.e., there probably was enough porosity left to allow the movement of local shale water up into the Whirlpool.

### Illite Formation

The only clay mineral identified in the Whirlpool Sandstone is authigenic illite. The illite has two possible sources. All of the illite is highly crystalline in nature, suggesting direct precipitation from alkaline, cation rich, pore fluids, resulting in the growth of wispy laths from illitic cores on quartz overgrowths [Güven et al., 1980] [see plates 4-1a,b to 4-3a]. The second origin could lie in the recrystallization of previously existing detrital and/or earlier authigenic clays to illite.

Hurst and Irwin [1981] believe that the most important factor controlling the conversion of kaolinite to illite is an influx of  $K^+$ :



They feel that temperature may not play as important a part in this process as first determined by Hancock and Taylor [1978]. Thus, it is possible that even with the low

diagenetic temperatures experienced by the Whirlpool, that all of the pre-existing clays were totally recrystallized to illite. This conclusion is perhaps substantiated by the findings of Weaver [1960] who noted the dominance of illite with age, suggesting some type of transformation process that converts most clays to illite with time.

#### Dolomitization

Minor amounts of dolomite cement are observed in the Whirlpool Sandstone [see plates 3-5a,b and 3-8]. It is present as isolated rhombs, or replacing ferroan calcite cement. The CL study has revealed that the dolomite is zoned [see plates 3-21a,b to 3-23a,b].

Stanton [1977] described the formation of dolomite as occurring due to a decrease in the amount of available iron relative to magnesium. Thus, the formation of dolomite in the Whirlpool could be in response to the removal of FeO from the pore fluids by the formation of ferroan calcite.

Amieux [1982] feels that the zonation in dolomites is due to rapidly changing pore fluid composition. Since the dolomite in the Whirlpool is late stage, it is possible that the control on the zonation was related to the restricted amount of porosity present after authigenic cementation, i.e. since the movement of the pore fluid was inhibited, dolomite would initially precipitate relatively rich in iron, then before remixing could occur an iron poor generation of

dolomite would precipitate. The pore fluid would have then had time to remix and the cycle would be repeated. The texture that this process would produce is displayed in plate 3-23a,b.

#### Changes in Pore Fluid Composition

In order to infer the porewater compositional history of a sandstone, one needs three critical facts, the initial and final porewater compositions and the porewater composition needed to precipitate out the various authigenic minerals observed.

The initial porewater in the Whirlpool Sandstone was a seawater origin. The composition of seawater today is known and it is assumed that it has not changed substantially over geologic time.

The present day porewater composition of the Whirlpool Sandstone in the northeastern Lake Erie area has been determined from wells drilled by Consumer's Gas. In this area the Whirlpool is found at the 300 m level and water has been collected via bottom hole drill stem testing. Unfortunately, analyses for  $K^+$  were not performed. Table 5-1 displays the major ion analysis for the Leep Frog Wildcat Well. The reliability of this data is hard to ascertain, due to the fact that drill stem testing will give water samples that are contaminated with drilling mud. Even with drilling mud contamination, it is difficult to



TABLE 5-1

Formation Water Analysis of the Leep Frog Wildcat Well

Dissolved Solids	mg/L	Other Properties	
<b>Cations</b>		Ph	6.6
Na <sup>+</sup>	4,400	Specific Gravity	
Ca <sup>2+</sup>	2,000	60/60 F	1.009
Mg <sup>2+</sup>	486		
Ba <sup>2+</sup>	-		
<b>Anions</b>			
Cl <sup>-</sup>	11,500		
SO <sub>4</sub> <sup>-2</sup>	283		
CO <sub>3</sub> <sup>-2</sup>	-		
HCC <sub>3</sub> <sup>-</sup>	78		
Total Dissolved			
Solids	18,747		

Data courtesy of Consumers' Gas

account for such high salinity unless we assume that the porewater was saline before drilling. Thus, oil and gas and saline porewaters exist in a sandstone that has experienced very low diagenetic temperatures [approximately 30° C]. It is impossible to form gas and oil at these temperatures and it is difficult to envisage the occurrence of low temperature diagenetic reactions that would lead to the creation of saline porewaters. Two possible solutions to these problems exist. It might be argued that the present day geothermal gradient calculated by Judge and Beck has not been constant in the past, i.e., it was much higher. This seems unreasonable due to the fact that the basement rocks in the area are Precambrian in age and are very stable now and have been stable for a very long period of time. The second solution entails the migration of oil and gas and saline pore fluids, up-dip, from areas deep within the depositional basin to the southeast. Thus, the oil and gas could have formed in areas having diagenetic temperatures within the oil and gas "windows" and then migrated up-dip into the present day hydrocarbon reservoirs found in the Whirlpool Sandstone [Middleton, personal communication]. The migration of hydrocarbons and porewaters seems to agree with the mineralogy observed and it definitely solves the problems associated with the low diagenetic temperatures.

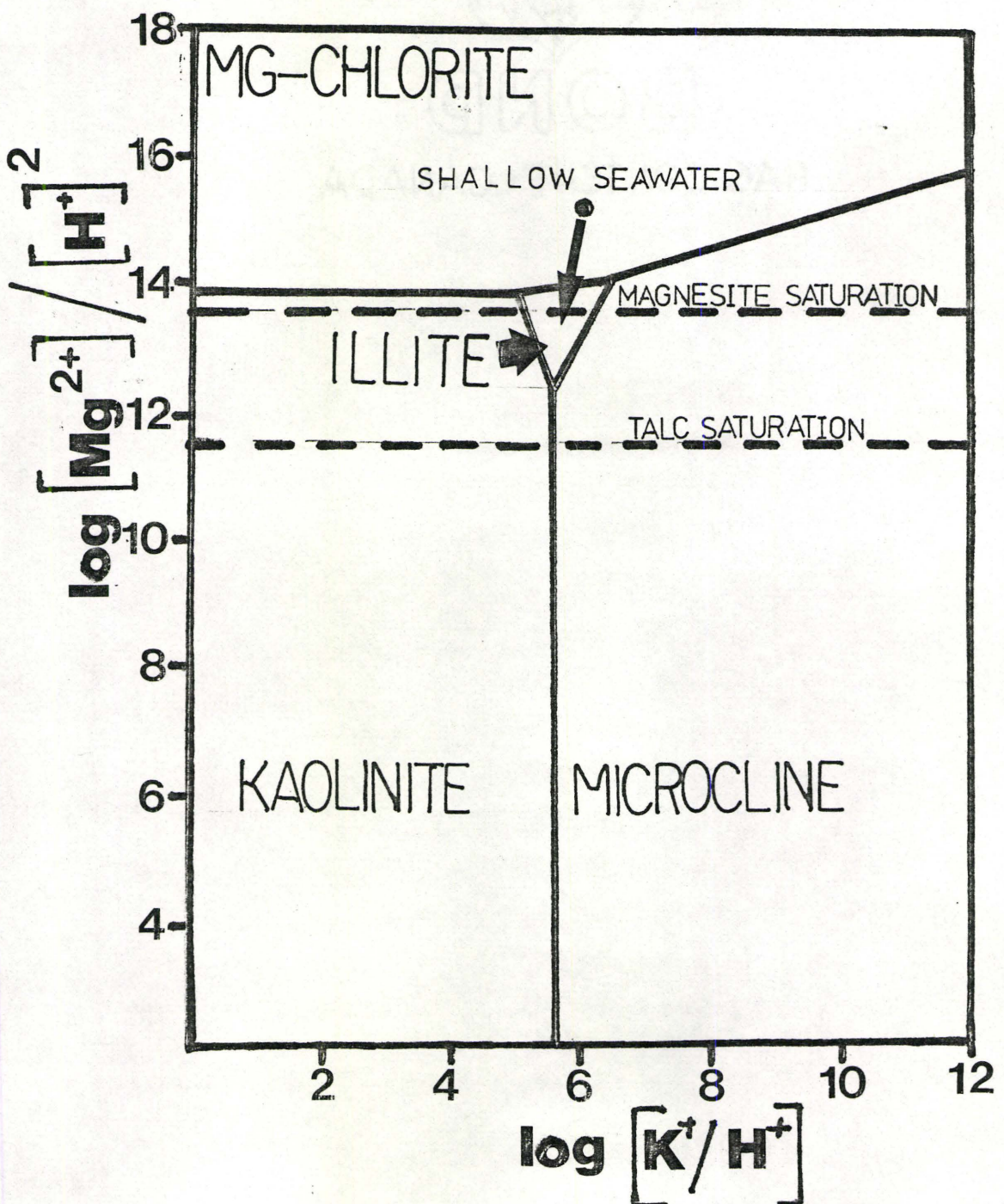
The Medina Group experienced a period of emergence

shortly after the deposition of the Neagha Shale. Thus, porewaters would have been flushed by fresh water. It is unlikely however, that the Whirlpool Sandstone ever came into contact with this fresh water, due to its depth of burial. Also, there is no mineralogic evidence that suggests the presence of fresh water, i.e., authigenic kaolinite.

Figures 5-4 and 5-6 trace the compositional changes of the pore fluids during diagenesis. Figure 5-4 is a plot of  $\log[K^+/H^+]$  vs.  $\log[H_4SiO_4]$ , while figure 5-6 is a plots of  $\log[mg^{+2}]/[H^+]^2$  vs.  $\log[K^+/H^+]$ . The following pore fluid history is inferred:

- 1] Deep in the depositional basin to the southeast of the study area, the maturation of hydrocarbons led to the formation of  $H_2S$  which was dissolved in pore waters that eventually migrated up-dip in the Whirlpool Sandstone into the study area. These reducing fluids produced a reduced zone at the top of the Queenston Formation and caused the precipitation of pyrite.
- 2] Free silica was released to the pore water deep within the depositional basin due to the conversion of smectite to illite in the surrounding shales, when a diagenetic temperature of 60 to 175°C had been reached. Large volumes of water were generated at this time due to the dewatering of

Figure 5-6:  $\log [\text{Mg}^{2+}] / [\text{H}^+]^2$  vs.  $\log [\text{K}^+/\text{H}^+]$  diagram showing the changing chemical composition of the porewaters of the Whirlpool Sandstone. Chlorite is initially stable in seawater. The porewaters gradually move into the illite field after the formation of quartz overgrowths [after Helgeson, p. 41, 1969].



shales and/or the circulation of groundwater. This water then migrated up-dip in the Whirlpool Sandstone into the study area, where it became saturated with respect to silica, causing quartz overgrowth precipitation. The pore fluid never fell far below the quartz saturation concentration of  $10^{-4}$  mg/L due to the fact that the overgrowths have remained in equilibrium with the pore fluids.

- 3] The fluid that carried in the free silica for the quartz cementation was acidic in nature. It caused the dissolution of local detrital carbonate in the upper marine beds of the Whirlpool. The  $\text{Ca}^{+2}$  rich fluids were prevented from circulating into the bulk pore fluids due to the fact that the quartz cementation had occluded most of the porosity. After the pore fluids became static, i.e., all fluid migration had stopped, the pH of the porewater became dependant on mineral reactions like the alteration of feldspar and/or the alteration of detrital and early authigenic clays to illite. The pH of the porewater was such that  $\text{HCO}_3^-$  was the dominant carbonate species [pH= 6.3 to 9.3]. Then, the addition of  $\text{CO}_2$  from the decay of

organic material in the upper marine beds increased the amount of  $\text{HCO}_3^-$  via the dissociation of  $\text{H}_2\text{CO}_3$  and calcite was precipitated.

- 4] After calcite cementation had been completed, the release of local, intershale water due to diagenesis led to a porewater composition that was undersaturated with respect to calcite.
- 5] Minor amounts of dolomite cement were formed in response to a decrease in the amount of available iron relative to magnesium due to the removal of FeO from the porewater by the formation of ferroan calcite. This dolomite shows zonation that reflects rapid changes in porewater composition, i.e., the concentration of iron relative to manganese. It is possible that this zonation is a function of the lack of available pore space in the Whirlpool at this time.
- 6] During the formation of calcite and dolomite cements, the pore fluids became increasingly alkaline and rich in  $\text{K}^+$ , leading to the direct precipitation of illite and the total recrystallization of all pre-existing clays. The pore fluid must have retained this composition

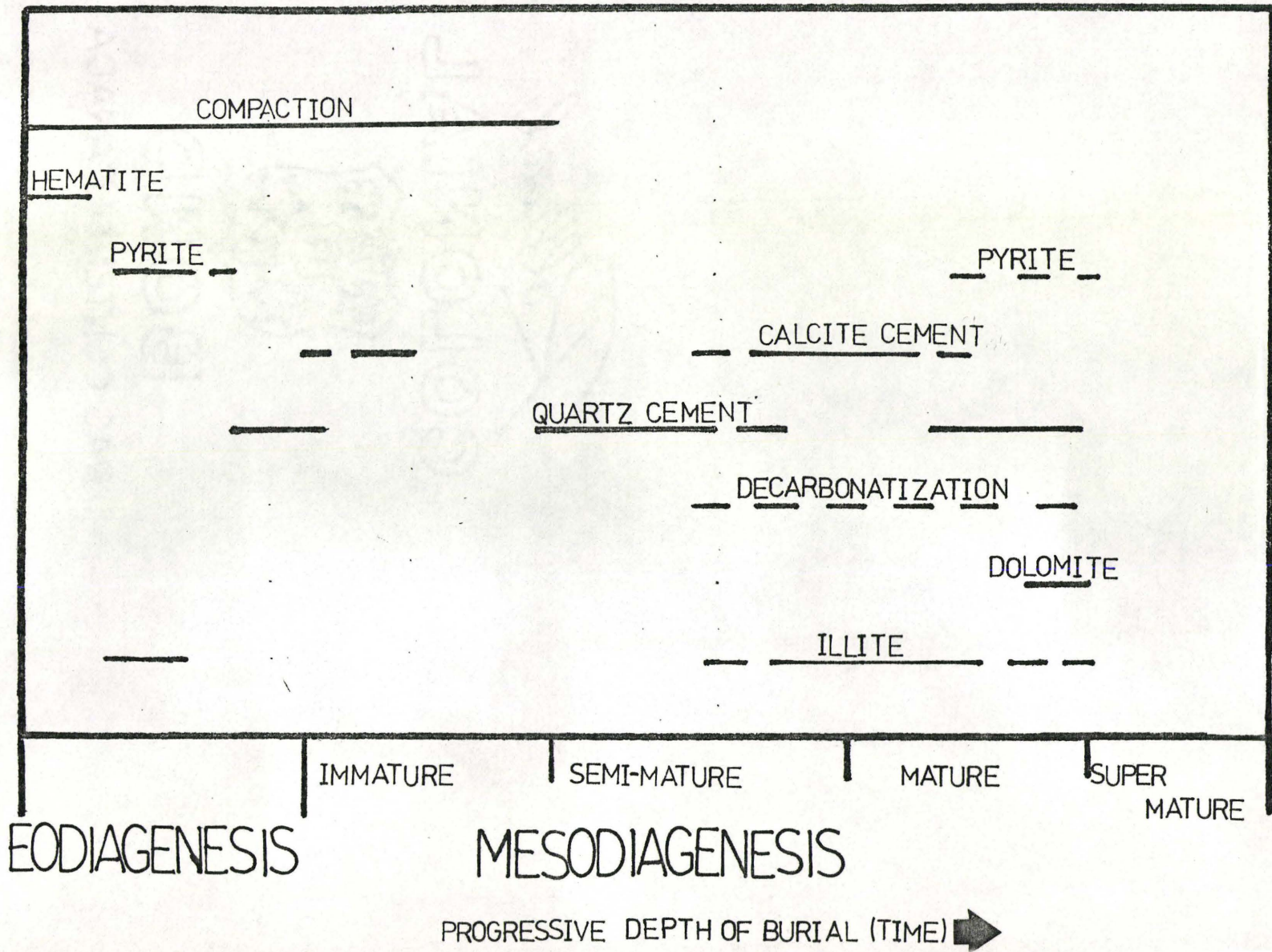
for a long period of time due to the fact that illite recrystallization is complete and no other clay minerals are observed.

### Mineral Paragenesis

Figure 5-7 is a schematic representation of the paragenetic sequence of authigenic mineral formation in the Whirlpool Sandstone during diagenesis. This sequence has been prepared from the observation of authigenic mineralogy and the known tectonic history of the area. The individual timing of mineral formation with respect to the diagenetic stages can only be inferred, but the overall sequence of minerals relative to one another is known from textural evidence.



Figure 5-7: Schematic representation of the paragenetic sequence of mineral formation during the diagenesis of the Whirlpool Sandstone (after Gardiner, 1982).



## CHAPTER 6

### C O N C L U S I O N S

- 1] The sedimentary structures and constituents observed to be present in the lower two-thirds of the Whirlpool Sandstone in the study area appear to be consistent with the sandy braided fluvial depositional model that has been proposed by C.J. Salas [1983] from work done on the Whirlpool in the Georgetown area.
- 2] The upper one-third of the Whirlpool Sandstone has been deposited in a near shore, shallow marine environment.
- 3] The vertical and Northwest fining trends present in the Whirlpool Sandstone as described by Geitz [1952] appear to be well developed within the study area.
- 4] The minerals and constituents found in the Whirlpool Sandstone in the study area are: quartz, present as detrital grains and authigenic overgrowths; feldspar, dominantly microcline; opaque and heavy minerals, opaques present as authigenic and secondary precipitates; chert, phosphatized fossil fragments and rock fragments; ferroan and nonferroan calcite and dolomite cements; authigenic illite clay and detrital muscovite.
- 5] All samples are classified as Quartzarenites or

Sublitharenites after Folk [1974]. The source of the Whirlpool Sandstone appears to lie to the southeast in Recycled Orogenic terrain with the bulk of the sediment derived from pre-existing sediments, and with minor input from low grade metamorphic and hydrothermally veined terrain.

- 6] Under transmitted light, approximately 55% of all grain contacts appeared to be concavo-convex or sutured in nature. Under CL, these contacts give every appearance of interpenetration and pressure solution; however, the Cathodoluminescent study showed that roughly 25% of these contacts are nothing more than authigenic quartz overgrowths that have grown together in concavo-convex and sutured patterns. Thus, the CL represents the accurate measure of the extent of pressure solution that has occurred in the Whirlpool Sandstone.
- 7] Using CL, it has been determined that roughly 85% of all grain contacts are tangential in nature, thus, pressure solution has been minimal. The high number of tangential contacts may be reflecting the early cementation of the Whirlpool Sandstone by quartz and calcite which impeded mechanical compaction.
- 8] The increase of calcite cement and the decrease in the average number of grain contacts and contact strength to the northwest may reflect lower burial depths

and thus, they are functions of lateral movement away from the centre of the depositional basin.

- 9] An average porosity of 5.7% was obtained for the Whirlpool Sandstone with values ranging from a minimum of trace to a maximum of 9.3%. Virtually all of the porosity is secondary in nature and was formed during mesodiagenesis by the dissolution of calcite cement, feldspar and sedimentary rock fragments.
- 10] The round, superficial cavities, near the base of the Whirlpool Sandstone, described as worm burrows by Seyler [1981] have been re-interpreted as simple weathering cavities that initially formed due to the dissolution of patchy calcite cement and then grew as a function of grain size.
- 11] Cathodoluminescent Microscopy offers a great deal of new information for sedimentological researchers. CL can be used for routine mineral identification and is especially useful for determining the extent of quartz cement and the diagenetic history of carbonates. CL is relatively inexpensive, safe and easy to use, and requires no special sample preparation outside of the normal thin section preparation. Its only drawback is the gradual destruction of thin sections under the high energy electron beam.
- 12] The Whirlpool Sandstone within the study area has

had a maximum depth of burial between 900 and 1400 m. Assuming that the geothermal gradient of 2.58 °C/100 m, calculated by Judge and Beck [1973] has remained constant in the geologic past, then the maximum diagenetic temperature that the Whirlpool has experienced is 36 °C.

13] During eodiagenesis, mechanical compaction reduced the initial porosity of the Whirlpool Sandstone by 10%. Later, during mesodiagenesis, the remaining initial porosity [30%] was occluded by chemical compaction, specifically, the formation of quartz and calcite cements.

14] Eodiagenetic quartz cement was formed in response to minor amounts of pressure solution, brought about by mechanical compaction. The formation of eodiagenetic calcite cement may have been due to increased levels of  $\text{Ca}^{+2}$  that were introduced into the Whirlpool by pore fluids migrating up-dip from deep within the depositional basin to the southeast. These fluids could have had elevated levels of  $\text{Ca}^{+2}$  due to the conversion of smectite to illite.

15] Pyrite has been precipitated in response to the early migration of  $\text{H}_2\text{S}$  bearing pore solutions up-dip, from deep within the depositional basin. These fluids would contain substantial levels of reduced sulphur due to the maturation of hydrocarbons. These reducing fluids

may have also formed the reduced zone found at the top of the Queenston Formation.

16]           The Whirlpool Sandstone has roughly 20% quartz cement. It has been demonstrated that pressure solution has been minimal, thus, there has been an external source of silica. Since the local diagenetic temperatures were too low to promote any reactions that might produce free silica, e.g., the conversion of smectite to illite in shales, the silica must have been carried into the study area via the migration of silica saturated pore fluids up-dip from areas deep within the depositional basin the southeast. The silica in these fluids was probably derived from the conversion of smectite to illite in shales within the depositional basin. In order to produce the volume of silica cement observed in the Whirlpool, great volumes of water have been flushed through the unit. The origin of this water could be the dewatering of shales within the depositional basin and/or the circulation of groundwater in an aquifer system. Since the Whirlpool Sandstone is the only permeable layer in large accumulations of shale, it would act as the channel for any water that was formed in these shales during diagenesis, or for any ground water that had circulated down into the basin.

17]           Calcite cement is more abundant in the upper marine units of the Whirlpool Sandstone. Since the amount of

calcite cement is not constant throughout the unit it is unlikely that the source of the cement was the up-dip migrating pore fluids. Rather, it seems more reasonable to suggest that the calcite cement was derived from local detrital carbonate deposited in the upper marine beds. The fluids that formed the silica cement were acidic in nature. They dissolved the local detrital carbonate, but the reduced porosity did not allow the  $\text{Ca}^{+2}$  rich fluid to mix with the bulk pore water. Quartz cementation ceased when the porosity had been reduced sufficiently to inhibit the passage of the migrating pore fluids. Thus, the calcite cement precipitated from static pore fluids. The pH of these fluids was fixed in the range 6.3 to 9.3 by mineral reactions like the alteration of feldspar and/or the alteration of detrital and early authigenic clays to illite. At this pH  $\text{HCO}_3^-$  is the dominant carbonate species in solution. The addition of  $\text{CO}_2$  from the decay of organic detritus in the upper marine beds increased the amount of  $\text{HCO}_3^-$  via the dissociation of  $\text{H}_2\text{CO}_3$ , which led to the precipitation of calcite cement. Nonferroan calcite has been precipitated close to where it dissolved, i.e., there has not been much mixing of fluids.

18]        The major proportion of secondary porosity was formed during the mesodiagenetic regime due to the dissolution of calcite. Decarbonitization has occurred due to the dilution



affect caused by the release of intershale water into the pore fluids, creating a mixture that was undersaturated with respect to  $\text{CaCO}_3$ .

19]           The formation of dolomite cement in the Whirlpool was in response to a decrease in the amount of available iron relative to magnesium due to the precipitation of ferroan calcite. The zonation in the dolomite reflects rapid changes in porewater composition.

20]           The only clay mineral present in the Whirlpool Sandstone in the study area is authigenic illite. It occurs in four morphologies, listed below in order of decreasing abundance: pore lining, wispy, laths growing from the surface of quartz overgrowths; pore lining, short digitate flakes, with wispy, lath like terminations; "spaghetti like" laths bridging pore space; and, "mudcrack" illite on the surfaces of detrital grains. It is possible that the "mudcrack" illite represents detrital illite, or illite that has been mechanically infiltrated down into the unit after deposition. The digitate illite may represent a mixed layer assemblage. The first two morphologies probably represent illite that has directly precipitated from alkaline,  $\text{K}^+$  rich pore solutions. Since the majority of the illite is highly crystalline, direct precipitation is favoured. However, it is also possible that the pore fluids have been alkaline and  $\text{K}^+$  rich long enough to promote

the complete recrystallization of all earlier clays.

21]           The oil and gas reserves found in the Whirlpool Sandstone in the Lake Erie area have probably migrated up-dip from source areas deep within the depositional basin to the southeast.

## B I B L I O G R A P H Y

- Alling, H.L., 1936, Petrography of the Niagara Gorge Sediments, Proc. of the Rochester Academic Soc., v. 7, No. 7, p. 189-207.
- Amieux, P., 1982, La Cathodoluminescent: Methods D'etude Sedimentologique des Carbonates, Bull. Des Centres de Recherches Elf Aquitaine, v. 6, No. 2, p. 437-483.
- Candy, 1963, The Geochemistry of Some Ordovician and Silurian Shales From Southwestern Ontario, unpublished MSC, Thesis, McMaster University.
- Basu, A., Young, S.W., Suttner, L.J., James, W.C. and Mack, G.H., 1975, Re-evaluation of the use of undulatory extinction and polycrystallinity in detrital quartz for provenance interpretation, Jour. Sed. Petrol., v. 45, p. 873-882.
- Berner, R.A. [ed.], 1971, Principles of Chemical Sedimentology, McGraw-Hill Book Co., New York, 239 p.
- Blatt, H., 1979, Diagenetic Processes in Sandstones, S.E. P.M. Spec. Pub. No. 26, p. 141-157.
- Blatt, H., Middleton, G.V. and Murray, R. [eds.], 1980, The Origin of Sedimentary Rocks, 2nd ed., Prentice-Hall Inc., 782 p.

- Bjorlykke, K., 1979, Discussion: Cementation of Sandstones, Jour. Sed. Atrol., v. 49, p. 1358-1359
- Boles, J.R. and Franks, S.G., 1979, Clay diagenesis in the Wilcox Sandstones of southeast Texas, Jour. Sed. Petrol., v. 49, p. 55-70.
- Bolton, T.E., 1957, Silurian stratigraphy and paleontology of the Niagara Escarpment in Ontario, Geo. Survey of Can., Memoir 289, 145 p.
- Borg, I.Y. and Smith, D.K., 1969, Calculated X-ray Powder Patterns for Silicate Minerals, Geol. Soc. Amer. Memoir 122.
- Carrol, D., 1970, Clay Minerals: A guide to their X-ray Identification, Geol. Soc. Amer. Spec. Paper 126, 80 p..
- Choquette, P.W. and Pray, L.C., 1970, Geologic Nomenclature and Classification of Porosity in Sedimentary Carbonates, Amer. Assoc. Petrol. Geol. Bull., v. 54, p. 207-250.
- Collins, A.G. [ed.], 1975, Geochemistry of oil field waters Developments in Petrol. Science 1, Elsevier Sci. Publ. Co., New York, 496 p..
- Cramer, F.H. and Diez de Cramer, M., 1972, North American Silurian palynofacies and their spatial arrangements: Acritarchs, Palaeontographica, v. 138, p. 107-180.

- Dickenson, W.R. and Suczek, C.A., 1979, Plate tectonics and sandstone composition, Amer. Assoc. of Petrol. Geol. Bull., v. 63, No. 12, p. 2164-2182.
- Drever, J.I., 1982, The Geochemistry of Natural Waters, Prentice-Hall Inc., New Jersey, 388 p..
- Fisher, D.W., 1954, Stratigraphy of the Medina Group, New York and Ontario, Amer. Assoc. of Petrol. Geol. Bull., v. 38, p. 1979-1996.
- Folk, R.L. [ed.], 1974, Petrology of Sedimentary Rocks, Hemphill Publ. Co., Austin Texas, 182 p..
- Fuchtbauer, H. [ed.], 1974, Sediments and Sedimentary Rocks I, John Wiley and Sons Inc., 464 p..
- Gaither, A., 1953, A study of porosity and grain relationships in experimental sands, Jour. Sed. Petrol., v. 23, p. 180-195.
- Galloway, W.E., 1974, Deposition and diagenetic alteration of sandstone in northeast Pacific arc-related basins: implications for greywacke genesis, Geol. Soc. Amer. Bull., v. 85, p. 379-390.
- Gardiner, S., 1982, Depositional Environment, Petrology, Diagenesis and Reservoir aspects of the Notkewin Member, Fort St. John Group, West-Central Alberta, unpublished B.Sc. Thesis, McMaster University.
- Geitz, O., 1952, The Whirlpool Sandstone, unpublished M.S.c. Thesis, McMaster University.

- Grabau, A.W., 1913a, Early Paleozoic delta deposits of North America, Geol. Soc. of Amer. Bull., v. 24, p. 399-528.
- Grabau, A.W., 1913b, Principles of Stratigraphy, Sciler and Co., New York.
- Gray, J. and Boucott, A.J., 1971, Early Silurian spore tetrads from New York: Earliest new world evidence for vascular plants?, Science, v. 173, p. 918-921.
- Guyen, N., Hower, V.F. and Davies, D.K., 1980, Nature of authigenic illite in sandstone reservoirs, Jour. Sed. Petrol., v. 50, No. 3, p. 761-766.
- Helgeson, H.C., Brown, T.H. and Leeper, R.H., 1969, Handbook of Theoretical Activity Diagrams Depicting Chemical Equilibrium in Geologic Systems Involving and Aqueous Phase at One Atmosphere and 0° to 300° C, Freeman, Cooper and Co., San Francisco, 253 p..
- Hancock, N.J. and Taylor, A.M., 1978, Clay Mineral diagenesis and oil migration in the Middle Jurassic Brent Sand Formation, Jour. Geol. Soc. London, v. 135, p. 69-71.
- Hewitt, M.D., 1982, A subsurface study of the Middle-Lower Silurian Thorold Sandstone from Consumer's Gas Silver Creek, 004 Grimsby Pool, North-Central Lake

- Erie, unpubl. B.Sc. Thesis, McMaster University.
- Hill, P.J., 1974, Stratigraphic palynology of acritarchs from the type area of the Llandovery and Welsh Borderland, *Rev. Palaeobot. Palynol.*, v. 18, p. 11-23.
- Hoffman, J. and Hower, J., 1979, Clay mineral assemblages as low grade metamorphic geothermometers: application to the thrust faulted tectonic belt of Montana, U.S.A., In *Aspects of Diagenesis*, S.E.P.M. Spec. Publ., v. 26, p. 55-80.
- Holstein, A., 1936, Heavy minerals of the Silurian rocks of the Niagara Escarpment, unpublished Ph. D. Thesis, University of Toronto.
- Houghton, H.F., 1980, Refined techniques for staining plagioclase and alkali feldspars in thin section, *Jour. Sed. Petrol.*, v. 50, p. 629-631.
- Hurst, A. and Irwin, H., 1981, Modeling of clay diagenesis in sandstones, *Clay Minerals*, v. 17, p. 69-77.
- Hutcheon, I., 1982, Aspects of the diagenesis of coarse grained siliciclastic rocks, *Geoscience Canada*, v. 10, No. 1, p. 57-75.
- Judge, A.J. and Beck, A.E., 1973, Analysis of heat-flow data: several boreholes in a sedimentary basin, *Can. Jour. of Earth Sci*, v. 10, No. 10, p. 1494-1507.

- Kopp, O.C., 1981, Cathodoluminescence Petrography: A valuable tool for teaching and research, *Jour. of Geol. Educ.*, v. 29, p. 108-113.
- Land, L.S., Dutton, S.P., 1978, Cementation of a Pennsylvanian Deltaic Sandstone: Isotoxic Data, *Jour. Sed. Petrol.*, v. 48, No. 4, p. 1167-1176.
- Legall, F.D., 1980, Organic metamorphism and thermal maturation history of Paleozoic strata, Southern Ontario, unpubl. M.Sc. Thesis, University of Waterloo.
- Liberty, B.A. and Bolton, T.E., 1971, Paleozoic Geology of the Bruce Peninsula Area, Ontario, Ont. Geol. Surv., Memoir 360, 136 p..
- Lindholm, R.C. and Finkelman, R.B., 1971, Calcite staining: semi-quantitative determination of ferrous iron, *Jour. Sed. Petrol.*, v. 42, p. 239-242.
- Lister, T.R., 1970, A monograph of the acritarchs and Chitinozoa from the Wenlock and Ludlow Series of Ludlow and Millishope areas, Shropshire, *Palaeont. Soc. [Monogr.]*, [1]-1-100.
- Magara, K., 1978, Composition and fluid migration, practical petroleum geology, Elsevier Sci. Publ. Co., New York, 319 p..



- Marshal, D.J., 1978, Suggested standards for the reporting of Cathodoluminescent results, *Jour. Sed. Petrol.*, v. 48, p. 651-653.
- Martini, I.P., 1965, The sedimentology of the Medina Formation outcropping along the Niagara Escarpment [Ontario and New York State], unpubl. Ph. D. Thesis, McMaster University, 420 p..
- Middleton, G.V., 1982, A Brief Guide to the Sedimentology of the Hamilton Area, Dept. of Geol., McMaster University, unpubl. Tech. Memo, 82-1.
- Miller, M.A. and Eames, L.E., 1982, Palynormorphs from the Silurian Medina Group [Lower Llandoverly] of the Niagara Gorge, Lewiston, New York, U.S.A., *Palynology*, v. 6, p. 221-254.
- Nickel, E., 1978, The present status of Cathodoluminescence as a tool in Sedimentology, *Minerals Sci. Eng.*, v. 10 No. 2, p. 73-100.
- Pittman, E.D., 1972, Diagenesis of quartz in sandstones as revealed by scanning electron microscopy, *Jour. Sed. Petrol.*, v. 42, p. 507-519.
- Potocki, D.J., 1981, A Study of the Lower Cretaceous Niton Basal Quartz Sandstone of Western Alberta; with specific reference to Porosity and Permeability modification, unpubl. B.Sc. Thesis, McMaster University.

- Rexroad, C.B. and Rickard, L.V., 1965, Zonal conodonts from the Silurian strata of the Niagara Gorge, *Jour. Paleontology*, v. 39, p. 1217-1220.
- Rhoten, F.E. and Smeck, N.E., 1981, Equilibration of clays in natural and simulated bottom sediment environments, *Clays and Clay Minerals*, v. 29, No. 1, p. 17-22.
- Rickard, L.V., 1975, Correlation of the Silurian and Devonian rocks in New York State, New York State Mus. and Sci. Serv., Map and Chart Ser., No. 24.
- Robin, P., 1978, Pressure solution at grain-to-grain contacts, *Geochimica Cosmochimica ACTA*, v. 42, p. 1383-1389.
- Salas, C.J., 1983,  
  
unpubl. B.Sc. Thesis, McMaster University.
- Sandford, D.V., 1969, Silurian of Southwestern Ontario, *Ont. Petrol. Inst.*, 8th Ann. Conf., Session 5, 44 p..
- Schmidt, V. and McDonald, D.A., 1979, Secondary Reservoir Porosity in the Course of Sandstone Diagenesis, A.A.P.G. Short Course, April 1980.
- Scholle, P.A. [ed.], 1979, A colour illustrated Guide to Constituents, Textures, Cements and Porosities of Sandstones

- and Associated Rocks, A.A.P.G., Memoir 28.
- Seyler, B., 1981, The Whirlpool Sandstone [Medina Group] in outcrop and the subsurface: a description and interpretation of the environment of deposition, unpubl. M.Sc. Thesis, SUNY College at Fredonia.
- Sippel, R.F., 1968, Sandstone petrology, evidence from Luminescence Petrography, Jour. Sed. Petrol., v. 38, No. 2, p. 530-554.
- Stanton, G.D., 1977, Secondary porosity in sandstones of the Lower Wilcox [Eocene], Karnes County Texas, Trans. of the Gulf Coast Assoc. of Geol. Socs., v. XXVII.
- Taylor, S.M., 1950, Pore space reduction in sandstones, A.A.P.G. Bull., v. 34, p. 701-716.
- Thorez, J., 1975, Phyllosilicates and Clay Minerals-A laboratory handbook for their X-ray diffraction analysis, G. Lelotte [ed.], p..
- Towe, K.M., 1962, Clay mineral diagenesis as a possible source of silica cement in sedimentary rocks, Jour. Sed. Petrol., v. 78, p. 353-368.
- Walker, T.R., 1974, Formation of Red Beds in moist tropical climates: A Hypothesis, Geol. Soc. of Amer. Bull., v. 85, p. 633-638.
- Weaver, C.E., 1960, Possible uses of clay minerals in the search of oil, A.A.P.G. Bull., v. 44, p. 1505-1518.

Williams, M.Y., 1919, The Silurian geology and faunas  
of the Ontario peninsula and Manitoulin and  
adjacent islands, Geol. Surv. of Can., Memoir  
111.

## APPENDIX 1

# CATHODOLUMINESCENT MICROSCOPY

### Instrumentation:

The standard reporting method suggested by Marshall [1977] has been adopted to report all parameters associated with the CL instrumentation:

Beam Energy: 12 kv D.C.

Beam Current: 15 microamp

Spot Diameter: Focus set to 6

Gun Type: Cold Cathode

Ambient Gas: Air

Instrument Type: Nuclide Luminoscope with  
a Leitz petrographic  
microscope.

For operating instructions read the accompanying operators manual supplied by Nuclide Corporation.

### Sample Preparation:

The thin sections were prepared slightly thicker and were lightly polished on the bottom and highly polished on the top. They were left uncovered and were washed in acetone before use on the Luminoscope.

## Photography

Kodac 400 speed colour print film was used with the following exposure times:

Plain Light:	0.5 seconds
CL	: 30.0 seconds
XN	: 10.0 seconds.

Unfortunately, due to the fact that minerals from different sources will have varying CL light intensities the above exposure times for CL can serve only as a general guide. Thus, the correct CL exposure time for each new mineral assemblage must be determined by experimentation.

The camera used was fitted with an eye corrective lens to ensure proper focusing of the image. Initially the image was focused under plain light and this position was used for both CL and plain light photos. The image was then refocused under cross nichols.

The transmitted light was turned to maximum intensity and the room was darkened for all pictures. For the CL pictures the beam current was adjusted until a stable reading of 15 microamps was obtained.

### Suggestions:

The use of purified N<sub>2</sub> gas did not produce any noticeable effects and since it is expensive its use is not recommended. Initially the beam current will be very unstable due to the "boiling off" of mounting medium and moisture in the

slide. The beam will stabilize after a few minutes as the gas production ceases.

The beam should not be left on the slide for any length of time, i.e. during start-up, as it will badly burn the slide.

## APPENDIX 2

### S T A I N I N G T E C H N I Q U E S

#### Calcite and Dolomite:

A method developed by Lindholm and Finkelman [1971] was used to identify ferroan/non-ferroan calcite and dolomite. The method proved to be very effective, allowing routine identification on the basis of stain colour and the degree of etching.

Calcite tends to etch to a great deal and readily stains. Dolomite resists etching and does not usually stain. Thus, dolomite rhombs will stand out from surrounding calcite after the staining procedure.

Nonferroan calcite stains a pinkish-red to red colour while calcite containing FeO stains blue. Table 2A-1 shows the range of colours that occurs with increasing FeO content in calcite [after Lindholm and Finkelman, 1971].

#### Method:

- 1] A 2% etching solution of HCl was prepared by adding 2 mL of concentrated HCl [12 normal] to 98 mL of distilled water [always add acid to water].
- 2] A 0.2% solution of HCl was prepared by adding



2 mL of concentrated HCl to 998 mL of distilled water.

- 3] 0.5 g of alizarin red-S and 2.5 g of potassium ferricyanide were dissolved in 500 mL of the 0.2% HCl solution.
- 4] Uncovered thin sections were placed in the 2% HCl etching solution for no more than 20 seconds.
- 5] After 20 seconds of etching the sections were immersed in the staining solution, at room temperature, for 4 minutes.
- 6] After 4 minutes in the staining solution the sections were removed and rinsed in distilled water and allowed to air dry.

Since the colour of the stain can be affected by factors like acidity and temperature it is important that the procedure outlined above is followed. Also, the solutions will decompose after a few days, thus, fresh solutions should be used in order to ensure proper stain colouration.

#### Feldspars:

A staining method reported by Houghton [1980] was used to identify plagioclase and K-feldspar. However, the method proved to be ineffective even after repeated treatments. It is not known for sure why the staining procedure did not

work, but one possible explanation could be the weathered nature of the feldspar grains.

Method:

- 1] A saturated solution of Na-cobaltinitrite was prepared by dissolving 50 g of the compound in 100 mL of distilled water.
- 2] A 5% solution of BaCl was prepared by dissolving 5 g of BaCl in 100 mL of distilled water.
- 3] A solution consisting of 0.01 g of K-rhodizonate dissolved in 30 mL of distilled water was prepared.
- 4] An etch bath of concentrated HF acid [55%] was prepared by pouring about 30 mL of the acid into a plastic, open dish. NOTE: the fumes and the liquid can cause severe burns with no warning. It is recommended that double gloves be used when working with HF.
- 5] An uncovered thin section was held "rock down" over the HF, at room temperature, for 30 seconds. Flat tweezers were used to grip the slide.
- 6] The slide was then immersed in the Na-cobaltinitrite solution for 45 seconds.

- 7] The slide was then rinsed with distilled water and the excess water was shook off.
- 8] The slide was then dipped in and out of the BaCl solution. The slide should not be in contact with the solution for more than 2 seconds.
- 9] The slide was then rinsed in distilled water.
- 10] The wet surface of the slide was then treated with several drops of the rhodizonate solution. Spreading of the solution over the slide was achieved by tilting the section.
- 11] The rhodizonate was allowed to sit on the slide for 10 seconds and then the slide was rinsed with distilled water and allowed to dry.

The bariumrhodizonate stains plagioclase a pinkish-red, while the cobaltinitrite stains K-feldspar yellow.

The thin sections should be cut a little thicker than usual and left uncovered. The cobaltinitrite and BaCl solutions have long shelf lives and thus can be prepared in advance, but the rhodizonate solution must be prepared fresh before each staining attempt.

## APPENDIX 3

### X R D A N A L Y S I S O F C L A Y S

#### Sample Preparation:

Samples weighing 15 grams were reduced to fine powder using a mortar and pestle. To the powder was added 10 grams of a deflocculating agent, Calgon Water Softener, and 200 mL of distilled water. This mixture was then placed in an ultrasonic bath for twelve hours. The ultrasonic bath serves to disperse the fine, clay, fraction. The suspension was then transferred to a one litre cylinder, previously filled with 800 mL of distilled water. After 225 minutes the top 200 mL was removed using a pipette. According to Stoke's Law this volume would contain only particles 2 microns in size, or the fine clay fraction. The 200 mL of clay rich suspension was then vacuum filtered through a 0.45 micron millipore filter. The resulting clay residue, while still wet, was then mounted equally, on two glass slides, by pressing the filtered material onto the slides. As the slide dries from the outside in, the surface tension of the water will basally orient the clay particles.

#### Analysis:

One slide from each sample was scanned from  $5^{\circ}$  to  $45^{\circ} 2 \theta$ , at a scanning speed of  $1^{\circ} 2 \theta$  per minute, using CuK radiation at 16 Ma and 45 Kv. The second slide was kept in an atmosphere of ethylene glycol for two hours at  $60^{\circ} \text{C}$  and then scanned as above. The first sample was then heated for two hours at  $550^{\circ} \text{C}$  and then scanned as above. This procedure was completed only for those samples that gave good initial peaks.

#### Analysis of Diffraction Traces:

In order to fit the untreated, glycolated and heated diffraction traces together, the originals were cut into three and then reduced by 65% on a photocopier. This put the traces on heavy paper and did not destroy the originals. The completed diffractogram was then photo-reduced to 8 1/2 by 11 inches. It is best to use a medium, black, permanent marker on the chart recorder as this will give clear lines after reduction.